

AD-A052 536

OREGON GRADUATE CENTER BEAVERTON
MECHANISM OF ENHANCED TOUGHNESS IN MARTENSITIC ALLOYS. (U)
FEB 78 W E WOOD

F/G 11/6

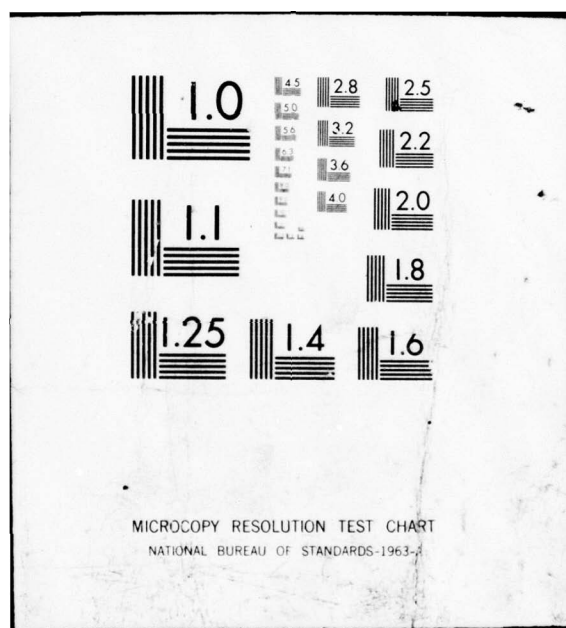
N00019-77-C-0135

NL

UNCLASSIFIED

1 OF 2
AD
A052536





ADA052536

8
4

Department of the Navy
Naval Air Systems Command
Washington, D.C. 20361

AD No. 100-100000
FILE COPY

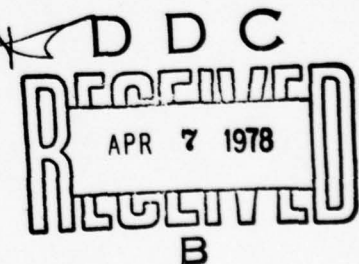
MECHANISM OF ENHANCED TOUGHNESS IN MARTENSITIC ALLOYS

Final Technical Report N00019-77-C-0135

February 1978

Approved for public release, distribution unlimited.

W. E. Wood
Oregon Graduate Center
19600 N.W. Walker Road
Beaverton, OR 97005



Unclassified

SECURITY CLASSIFICATION OF THIS PAGE (When Data Entered)

REPORT DOCUMENTATION PAGE		READ INSTRUCTIONS BEFORE COMPLETING FORM
1. REPORT NUMBER	2. GOVT ACQUISITION NO.	3. RECIPIENT'S CATALOG NUMBER
(9) Final Rept. 1 Oct 76-30 Sep 77		77
4. TITLE (and Subtitle)	5. TYPE OF REPORT & PERIOD COVERED	
Mechanism of Enhanced Toughness in Martensitic Alloys	Final Report 10-1-76 to 9-30-77	
6. AUTHOR(s)	7. PERFORMING ORG. REPORT NUMBER	
(10) W. E. Wood	(15) N00019-77-135 new	
8. PERFORMING ORGANIZATION NAME AND ADDRESS	9. PROGRAM ELEMENT, PROJECT, TASK AREA & WORK UNIT NUMBERS	
Oregon Graduate Center 19600 NW Walker Rd. Beaverton, OR 97005	(11)	
10. CONTROLLING OFFICE NAME AND ADDRESS	12. REPORT DATE	
Naval Air Systems Command	2-14-78 14 Feb 78	
14. MONITORING AGENCY NAME & ADDRESS (if different from Controlling Office)	13. NUMBER OF PAGES	
	(12) 149 P.	
16. DISTRIBUTION STATEMENT (of this Report)	15. SECURITY CLASS. (of this report)	
Approved for public release, distribution unlimited	Unclassified	
17. DISTRIBUTION STATEMENT (of the abstract entered in Block 20, if different from Report)	15a. DECLASSIFICATION/DOWNGRADING SCHEDULE	
18. SUPPLEMENTARY NOTES		
19. KEY WORDS (Continue on reverse side if necessary and identify by block number)		
Fracture toughness, microstructure, 4340 steel, 300M steel, heat treatment, retained austenite, twinning, segregation		
20. ABSTRACT (Continue on reverse side if necessary and identify by block number)		
The objective of this program was to establish the role of heat treatment parameters on the fracture toughness of ultrahigh strength steels. Microstructural examination, plane strain fracture toughness, Charpy and tensile tests were conducted on alloys 4340 and silicon modified 4340. Heat treatments included both direct as well as step quench schedules. Austenitizing temperatures ranged from 870°C to 1200°C, and step quenching temperatures (see reverse side)		

Unclassified

SECURITY CLASSIFICATION OF THIS PAGE(When Data Entered)

ranged from 250°C to 1100°C. Holding times at these temperatures varied from a few seconds to 2 hours. Tempering temperatures ranged from the as quenched condition to 400°C. Valid plane strain fracture toughness results of over 90,000 psi-in^{1/2} were achieved for alloy 4340 and values of 85,000 psi-in^{1/2} were achieved for silicon modified 4340 at ultimate strength levels of over 300,000 psi for both alloys. A consistent drop in the fracture toughness values was observed as the intermediate step-quenching temperature decreased or the holding time at this temperature increased. A concurrent increase in the amount of twinning was seen without any change in the amount and/or distribution of retained austenite. Auger electron data suggest that segregation effects do occur during austenitizing treatments and that this segregation is dependent on the initial as well as the intermediate step quench temperature. The existence of segregation variations is consistent with the changes in the observed twin characteristics.

The program utilized optical metallography, scanning and transmission electron microscopy, and Auger electron spectroscopy.

Unclassified

SECURITY CLASSIFICATION OF THIS PAGE(When Data Entered)

CONTENTS

	<u>PAGE</u>
I. ABSTRACT	1
II. INTRODUCTION	2
III. EXPERIMENTAL PROCEDURE	4
A. Material	4
B. Heat Treatment	5
C. Mechanical Testing	6
D. Microstructural Analysis	6
E. Auger Electron Spectroscopy	8
F. Acoustic Emission Analysis	8
IV. RESULTS	9
A. Mechanical Properties	9
1. Tensile Properties	9
2. Fracture Toughness	10
3. Charpy-V-Notch Tests	15
B. Microstructure	16
C. Fracture Morphology	21
D. Auger Electron Spectroscopy	23
V. DISCUSSION	27
CONCLUSIONS	33

Acknowledgements
References
Tables
Figure Captions
Figures

ACCESSION for		
NTIS	White Section <input checked="" type="checkbox"/>	
DDC	Buff Section <input type="checkbox"/>	
UNANNOUNCED <input type="checkbox"/>		
JUSTIFICATION _____		
BY _____		
DISTRIBUTION/AVAILABILITY CODES		
Dist.	AVAIL. and/or SPECIAL	
A		

I. ABSTRACT

The objective of this program was to establish the role of heat treatment parameters on the fracture toughness of ultrahigh strength steels. Microstructural examination, plane strain fracture toughness, Charpy and tensile tests were conducted on alloys 4340 and silicon modified 4340. Heat treatments included both direct as well as step quench schedules. Austenitizing temperatures ranged from 870°C to 1200°C, and step quenching temperatures ranged from 250°C to 1100°C. Holding times at these temperatures varied from a few seconds to 2 hours. Tempering temperatures ranged from the as quenched condition to 400°C. Valid plane strain fracture toughness results of over 90,000 $\text{psi-in}^{1/2}$ were achieved for alloy 4340 and values of 85,000 $\text{psi-in}^{1/2}$ were achieved for silicon modified 4340 at ultimate strength levels of over 300,000 psi for both alloys. A consistent drop in the fracture toughness values was observed as the intermediate step-quenching temperature decreased or the holding time at this temperature increased. A concurrent increase in the amount of twinning was seen without any change in the amount and/or distribution of retained austenite. Auger electron data suggest that segregation effects do occur during austenitizing treatments and that this segregation is dependent on the initial as well as the intermediate step quench temperature. The existence of segregation variations is consistent with the changes in the observed twin characteristics.

The program utilized optical metallography, scanning and transmission electron microscopy, and Auger electron spectroscopy.

II. INTRODUCTION

The emergence of fracture mechanics and the concept of plane strain fracture toughness, K_{IC} , as a quantitative means of a material's tendency to fail in a brittle manner is playing an increasingly important role in the selection and use of high strength alloys.⁽¹⁾ Such steels are often chosen according to their relative fracture toughness at different strength levels, and the use of these materials is limited by their low fracture toughness at high strength levels. Hence there is a great need to develop an understanding of the mechanisms involved in the fracture of these alloys, and an understanding of the variables which control the fracture toughness. It is the recognition and utilization of these factors which will provide the basis for the design of new high strength alloys with superior properties.

Maraging steels, as a class of alloys, exhibit one of the best combinations of strength and toughness available, better than conventionally treated low alloy steels such as 4140 and 4340⁽²⁾. However, cost limits their use except where absolutely necessary. Results have indicated that the long associated poor fracture toughness of these very high strength low alloy steels can be significantly improved, approaching the values obtained for the maraging steels, without the high cost. This has been accomplished by

altering only the heat treatment procedures. Furthermore the fracture toughness levels have been achieved without a reduction in strength. (3-6)

An excellent review of the current understanding of the interrelationships of composition, transformation kinetics, morphology and mechanical properties of alloy steels has recently been prepared by Parker⁽⁷⁾. Investigations of the structure-properties relationship of steel have been carried out for fifty years and many investigators have examined the martensitic transformation as well as the kinetics of formation of bainite. However, satisfactory explanations are in many cases still lacking.

Almost all of these investigations, as recently as 1972, concentrated on heat treatments to produce a structure with a fine prior austenite grain size to provide strength, as high a ductile-brittle transition temperature as possible, and high total ductility. However, several studies, (3-7) in the last few years have shown that, quite unexpectedly, very high levels of fracture toughness could be achieved by using very high austenitizing temperatures which produced a very coarse prior austenite grain size.

Much of the recent work aimed at establishing the mechanism of the enhanced toughness of these coarse prior austenite grained materials has dealt with differences between the conventional 870°C solution treatment and a modified 1200°C → 870°C step quench solution treatment, as well as those structures produced by isothermally transforming to either bainite or bainite and tempered martensite. The latter three treatments all result in

retained austenite compared to the standard 870°C treatment. The effect of transformation temperatures, times, and composition on various properties have all been summarized by Parker⁽⁷⁾.

One area however has received little attention, and that is the fact that step quenching from 1200 → 870°C does not result in as high a toughness as does direct quenching from 1200°C. The primary objective of this program has been to establish the critical role of heat treatment parameters, in particular the effect of solution treatment temperature and step quenching, on the fracture toughness of two well studied and commercially important alloys, AISI 4340 and 300M. In order to understand the role of heat treatment parameters, and hence microstructure, it is necessary to characterize the microstructure in detail. This investigation has utilized optical microscopy, scanning and transmission electron microscopy, acoustic emission analysis and Auger electron spectroscopy in conjunction with tensile, plane strain fracture toughness and Charpy-V notch tests.

III. EXPERIMENTAL PROCEDURE

A. Material

Two alloys, aircraft quality 4340, mil spec AM 56359 and 300M, a vacuum remelted silicon modified 4340, were used in this program. The alloys had the following compositions:

	C	Mn	Si	Cr	Ni	Mo	Cu	S	P	V
4340	.4	.69	.32	.69	1.87	.20	.16	.015	.010	-
300M	.42	.79	1.64	.79	1.84	.36	.05	.006	.010	.08

B. Heat Treatment

A controlled atmosphere tube furnace was utilized for all high temperature austenitization treatments. This furnace maintained a temperature within $\pm 5^{\circ}\text{C}$. Test specimens were either quenched directly from the solution temperature into an agitated oil bath or step quenched into a salt bath prior to oil quenching. All tempering was carried out for an hour. Step quench holding times varied from a few seconds to 2 hours before oil quenching. These specimens were stepped into salt baths to insure rapid thermal equilibrium for the short hold times. All tests were carried out on standard ASTM compact tension fracture toughness specimens. Sections for optical and transmission electron microscopy were taken from mid-thickness areas adjacent to the fracture path.

For the isothermal transformation to bainite and retained austenite, 4340 and 300M were again used. By varying the isothermal holding time and temperature the amount of retained austenite was controlled. Electron microscopy was employed to determine the distribution and morphology of retained austenite. The approximate percentage of retained austenite was estimated from recently published data⁽⁷⁾.

C. Mechanical Testing

All fracture toughness tests were carried out using ASTM specified compact tension test specimens according to specification E399-72. Testing was carried out at room temperature. Specimens were 5/8" thick and were tested in the longitudinal direction. All specimens were machined to final dimensions prior to heat treating except for the starter slot. This was added after heat treating by using a .008" thick grinding wheel. A 22,000 lb Instron Lawrence dynamic test system was used for all testing, including fatigue precracking at 6 Hz. Fracture toughness testing was carried out at a cross head speed of 0.1 cm/min.

Room temperature longitudinal impact properties were determined using standard ASTM Charpy-V-notch specimens as well as precracked Charpy specimens. Testing was carried out on a Tinius Olson machine adjusted to a 60 ft-lb capacity, and utilized a Dynatup instrumented test system.

Standard ASTM .250 in. diameter tensile bars were machined and heat treated. Testing was carried out at a crosshead speed of 0.1 cm/min. Strain was measured with a strain gage extensometer.

D. Microstructural Analysis

Sections for optical and transmission electron microscopy were taken from the midsection of the K_{Ic} specimens. For optical metallography polished specimens were etched in a combination picral and

nital etch. Thin foil preparation was carried out using both the window technique and the jet polishing technique, (Fischione unit). Two electrolytes, glacial acetic acid + perchloric acid and glacial acetic acid + chromium trioxide, were used. The best results were obtained from the latter in conjunction with the window technique. The exact composition of the electrolyte and the polishing conditions are given below:

Electrolyte:

Glacial Acetic Acid	135 ml
Chromium Trioxide	25 gms
Water	7 ml

Polishing Conditions:

Temperature	10-15° C
Voltage	25 volts
Current density	0.1-0.2 Amp/cm ²

The starting material was obtained in 10-15 mil thick sections by cutting heat treated specimens with a 1/32" abrasive wheel. Sections were cut while flooded with water. A very low cutting rate was employed. These 10-15 mil sections were then carefully ground to about 5 mils thickness. From this thickness final polishing by either the window or the jet polishing technique was carried out.

Secondary electron scanning microscopy was carried out at 25 KV. For each specimen the region adjacent to the fatigue precrack was examined, since this is the region of crack initiation during the K_{Ic} test. This region typically extends about .020" from the fatigue crack.

E. Auger Electron Spectroscopy

A cylindrical-Auger electron system (P.H.I. Model 10-155) was used. Measurements were carried out at 1.5×10^{-9} Torr. Primary beam current was $4\mu A$, except for monitoring sputter-profiles when a $50\mu A$ beam current was used in order to insure a large beam diameter.

A P.H.I. Model 04161 sputter gun was used with Argon ions. The ion gun was set to provide a 30mA ion current at 2 KV. The ion beam was positioned with a Faraday cup.

The samples fractured at -90°C were cooled by positioning them against the sample breaker, (PHI Model 10-520), cooled by flowing liquid nitrogen through a feedthrough. A thermocouple was spot welded onto the specimen to record the temperature.

F. Acoustic Emission Analysis

An Acoustic Emission Technology (AET) Model 201 test system was employed. This system consisted of a variable bandpass filter, a 60 dB preamplifier, a Model AC 175-L piezoelectric transducer, and a main amplifier with variable gain of 0-40 dB. Both total counts and RMS value were monitored. The system had a variable threshold level and was operated in

the floating mode. The transducer was mounted on the CTS fracture specimen. A modified Sony video recorder was utilized to record the test for subsequent data analysis. In order to eliminate the hydraulic noise so that it would not interfere with the emission generated from the test system, a 'composite' grip assembly was designed and used. This allowed a total system gain of 90 dB to be utilized while maintaining a threshold setting of less than 0.7 volt.

IV. RESULTS

A. Mechanical Properties

1. Tensile Properties

Tensile results are given in Tables I and II and in Figures 1-8, for both 4340 and 300M, as a function of solution treatment and tempering temperature. Solution treatment at either 870°C, 1100°C or 1200°C resulted in similar yield and ultimate strengths. However, in many of the as quenched and lightly tempered specimens failure occurred near or at the ultimate strength level. This made absolute values difficult to measure in some cases. Hardness tests for CTS fracture specimens, however, confirmed the predicted ultimate strengths based on published conversion tables for low-alloy steels.

Step quenching for 5, 30, or 60 minutes produced a uniformly reduced yield and ultimate strength as shown in Figure 2. Iso-thermal transformation at 350°C for alloy 4340 should result in about 75% upper bainite. However, a 2 minute hold time allows only a small amount

of bainite to transform before final quenching to form martensite. Hence, as indicated in Figure 3, the strength remains high. Longer holding times resulted in consistently lower strength levels. As the isothermal transformation temperature decreased the strength increased. This behavior was expected since the bainite formed at higher temperatures has a coarse microstructure and shows inferior mechanical properties.

The same results were obtained for alloy 300M with the exception that the presence of added silicon retards the tempering kinetics so that the maximum yield strength is not obtained until a tempering temperature of over 300°C is reached.

2. Fracture Toughness

A summary of the heat treatment conditions for which the resulting fracture toughness has been evaluated is given in Tables III and IV. Plane strain fracture-toughness data are presented in Tables V-VIII and Figures 9-29. All values were valid fracture toughness values except those marked by an asterisk, where P_m/P_Q exceeded 1.10. The effect of increasing the austenitizing temperature from 870 to 1200°C is apparent in Figure 9 for the as quenched test condition. Increasing the temperature from 870 to 1100°C resulted in only a small increase from about $35 \text{ ksi-in}^{1/2}$ to $43 \text{ ksi-in}^{1/2}$. Not shown in this figure, but included in the tables is data for a 1150°C treatment. This heat treatment resulted in a toughness of about

52 ksi-in^{1/2}. Further increases in the solution temperature to 1200°C and direct quenching produced the highest toughness in the as quenched condition, 66 ksi-in^{1/2}.

Aside from the increased toughness due to raising the solution temperature, Figure 9 also reveals the effect of step quenching to 870°C for successively longer holding times. Stepping to 870°C for 30 seconds did not reduce the toughness, but 30 seconds in a salt bath was not sufficient to reduce the specimen temperature to 870°C. Hence, little change was expected. Five minutes is sufficient, however, to reduce the specimen temperature to 870°C and figure 9 demonstrates the negative effect of this treatment on the fracture toughness. Holding for 30 minutes and one hour reduced the toughness even further. Not shown in the figures, but included in the tables are the results of short time 15 minute holds at 1200°C. The results demonstrated that holding for 1 hour was not necessary. The trends shown in Fig. 9 are representative of the effect of heat treatment on fracture toughness of both 4340 and 300M. The same trends were seen for the quenched and tempered samples as long as the tempering temperatures were below about 175°C. These effects can be summarized as follows:

- (1) Direct quenching from 1200°C produced the highest toughness.
- (2) Direct quenching from lower temperatures produced successively lower toughnesses.

(3) Step quenching to 870°C reduced the toughness with the extent of the toughness reduction dependent on the holding time at 870°C.

The effects of tempering on 4340 are shown in Figures 10-18.

There are several important features on these curves. First, for low tempering temperatures, below 175°C, the 1200°C clearly has superior toughness while the 1100°C treatment provides little benefit over that of the 870°C treatment.

Figures 15-17 illustrate the results of isothermal transformation above and below the Ms temperature. Clearly as the amount of bainite at any transformation is increased, the toughness decreases. On the other hand as the transformation temperature decreases, the toughness increases.

Under all circumstances the maximum toughness was obtained with a tempered martensitic microstructure rather than a bainitic microstructure.

Alloy 300M showed essentially the same behavior as 4340 for the direct and step quenched and tempered conditions. In some cases, however, isothermal transformation produced results different from 4340 (see fig. 22). One has to keep in mind, though, that isothermal transformation results in larger amounts of retained austenite in 300M as compared to 4340 upon quenching to room temperature. The strength levels thus vary widely. Figs. 24 and 25 compare the tempering response of the two alloys for two different austenitizing temperatures.

A more meaningful analysis of the fracture toughness data is one based on strength level rather than tempering temperature, Figures 26-29. Based on this analysis, for ultimate strengths at 280,000 psi and above, the 1200°C/1 hr. treatment was the best. Raising the solution treatment temperature from 870 → 1100 → 1150 → 1200°C resulted in a progressive increase in fracture toughness for tensile strengths above 280 ksi. Lower strength levels achieved by tempering resulted in a temper embrittlement and a drop in toughness for specimens with a coarse prior austenite grain size. Similarly step quenching to either 1100 or 870°C, Figure 27, did not result in as high a value of fracture toughness as direct quenching from 1200°C.

Overall toughness levels as a function of ultimate strength are shown for both alloys in Figures 28-29. The numbers refer to various heat treatments shown in Tables IX and X respectively. In both these figures, each specific heat treatment identified by a code number occurs several times due to different tempering temperatures. These figures reveal the large variation in fracture toughness which can be produced by various heat treatments.

It is clear that a 1200°C direct quench or a short step quench, which does not allow large amounts of bainite formation or considerable segregation to occur, is required in order to achieve the maximum level of toughness at the maximum tensile strength. This is also true for 300M except that the added silicon allows a slightly longer hold time (3 min) at low

isothermal transformation temperatures before the strength and toughness start decreasing.

The effect of tempering and the effect of increasing the solution treatment temperatures on the actual load vs displacement curve obtained from a C.O.D. gage is shown in Figures 30 and 31. These figures illustrate the wide variation in load to failure. In all cases shown valid K_{Ic} test data was obtained and the maximum load to failure is associated with the specimen exhibiting the maximum fracture toughness.

Acoustic emission analysis was carried out on a limited number of specimens in order to attempt to establish a relationship between K_{Ic} and the amount of acoustic emission from the test specimens. Figure 32 is a block diagram of the experimental setup used during these tests.

Examples of actual test results are shown in Figures 33-35. These curves are traces of both the load vs COD gage, i.e. the typical fracture toughness load curve, and the total counts or total number of acoustic emission events recorded using a ringdown counting type of analysis. Figures 33-35 represent three different characteristic A.E. curves. For a specimen which exhibited little or no crack growth as indicated by the load curve, there was a corresponding low level of emission. However, when the specimen exhibited stable crack growth prior to unstable catastrophic failure, the acoustic emission technique immediately detected crack growth. Hence the A.E. system acted as a sensitive means of detecting crack growth. The

relationship of total counts and fracture toughness may be seen in Figures 36-37. In almost all cases as the fracture toughness increased, total A.E. decreased. In other words, as defined, the fracture toughness of a material is a measure of the material's resistance to crack initiation.

3. Charpy-V-Notch Tests

Both standard Charpy and precracked Charpy tests were carried out on a limited number of specimens. The results are shown in Figures 38-40 for 3 different heat treatments. The curves show the load in pounds obtained by the Dynatup instrumented test system. While not in terms of ft-lbs or joules, the data do show relative changes which occur due to various heat treatments. A comparison of just the standard V-notched specimens indicates little difference when tempered between 150-200°C. Above this tempering range, the coarse grained material was embrittled relative to the 870°C treatment. This is consistent with K_{Ic} results. The precracked Charpy data are not conclusive since in most cases only single data points were obtained. This was due to the difficulty experienced in pre-cracking the Charpy bars without premature failure. Also, it was not possible to be sure in every case if the sample was precracked to the same length. Hence, a large scatter was expected. Difficulty in precracking was due to a malfunctioning precracking assembly.

The precracked Charpy data do show, however, the effect of temper embrittlement on impact toughness, as did the K_{Ic} tests, much more clearly than the standard specimens. Thus, it can be concluded

that the very sharp notch is more sensitive to microstructure than the standard Charpy radius.

Note that for the conventional heat treatment the standard Charpy test failed to detect a loss in toughness whereas the pre-cracked specimen did, Figure 38.

B. Microstructure

The microstructure of each alloy was examined by both optical and electron microscopy. Both replica and thin foil techniques were utilized. Grain size calculations were carried out for various austenitizing treatments. The results are summarized as follows:

<u>Solution Treatment</u>	<u>Grain Size, ASTM</u>	
	<u>4340</u>	<u>300M</u>
As received	9	6.5
870°C/1 hr	9	6.5
1000°C/1 hr	9	4
1100°C/1 hr	5.5	2
1100°C/2 hr	-	2
1150°C/1 hr	3	2
1200°C/15 min	1	-
1200°C/30 min	1	-
1200°C/1 hr	1	2
1200°C/1 hr → 1100°C/15 min	-	2
1200°C/1 hr → 1100°C/1 hr	-	2

Clearly 4340, a rolled plate material had a finer grain size initially. However, after solutioning at 1200°C, both alloys have ASTM grain size of about 1-2. Step quenching does not result in a further increase in grain size. Since the grain size is very large after the 1100°C/1 hr. treatment but the

fracture toughness is unchanged and since step quenching did not result in as high a fracture toughness as the direct quench, then grain size per se cannot be controlling the fracture toughness of these alloys.

The fracture toughness is essentially dependent on the micro-structure which is itself established by the heat treatment procedure. Both these alloys are normally used in either the quenched and tempered or isothermally transformed condition. Hence the structures are normally either tempered martensite or bainite or duplex martenite and bainite. The high hardenability of these alloys normally prevents the formation of pearlite. The detail and substructure present in both martensite and bainite cannot be resolved optically and require high resolution electron microscopy. Even with these techniques satisfactory explanations are not always possible due to the extremely complex nature of these structures. One objective of this program has been to examine the structures produced as a result of various heat treatments in order to relate the importance of these structures in terms of fracture toughness.

Using optical microscopy the as received condition of the material can be examined, Figure 41. Alloy 4340, received as rolled plate, has an initially banded structure which is still present after solution treatment at 870°C. 300M contains many residual carbides in the as received condition. Solution treatment at 870°C does not eliminate all these carbides. Solution temperatures of 1800°F (982°C) are required.

Large dark etching plates are visible in Figure 42b. These are martensitic plates which have been autotempered during the quench. In some of these dark etching plates a parallel series of subunits are visible, when viewed under very high magnifications, i.e. 2000X. Unfortunately, it is impossible to uniquely identify these optically, and electron microscopy is required. These large plates are present in both alloys and are large enough to be observed optically in the coarse grained material, Fig. 43a.

Examples of alloy 4340 heat treated to produce a partially or nearly fully bainitic structure are shown via optical metallography in Figures 43b-c. A three minute hold at 335°C after an initial 1200°C solution treatment resulted in a duplex martensitic, light etching constituent, and bainitic dark etching constituent, in Figure 43b. About 1 minute is required in order to quench a 5/8" thick specimen to 335°C in a salt bath. Hence the specimen was held at temperature for about 2 minutes. Holding for 60 minutes at 335°C results in nearly a fully bainitic structure for 4340, at least when viewed optically. A similar condition exists if the prior solution treatment is 870°C, although it is more difficult to optically resolve the structure due to the fine grain size.

Representative optical micrographs of alloy 300M heat treated to produce triplex, bainitic-martensitic-retained austenite, structures are shown in Figure 44. For alloy 300M, a 3 min. hold at 315°C or 350°C should only produce about 2-5% bainite for a $1\frac{1}{2}\%$ silicon content. The remaining

austenite has evidently transformed to martensite for the case of an initial 870°C solution treatment. Retained austenite is found, however, within the bainitic ferrite laths as will be shown in thin foil transmission electron micrographs.

By holding 300M for 1 hour at 315°C about 75% transformation to bainite occurs according to the TTT curve after an initial 900°C solutioning. (8) This is in good agreement with Figure 44b which shows large white regions which are probably untempered martensite formed during the quench to room temperature. Similar micrographs for a prior 1200°C solution treatment are shown in Figures 44c and 44d for 300M. Again transmission electron micrographs shown in the following figures are necessary in order to reveal subtle differences in these structures.

Transmission electron micrographs of alloy 4340 and 300M are presented in Figures 45-50 and 51-54 respectively for several heat treatment conditions. The first major difference between the conventional 870°C treatment and the 1200°C, or any other coarse prior austenite grain size producing heat treatment, is the presence of retained austenite in the latter. This is shown in Figure 45, which contains a bright field and a corresponding dark field micrograph showing the presence and very fine distribution of retained austenite. Figure 45c is a SAD pattern from this region and Figure 45d is the indexed pattern revealing both austenite and ferrite diffraction spots. In 870°C specimens only trace amounts of austenite could be found. Step

quenching from 1200°C to 1100°C did not produce any observable change in the distribution of retained austenite, as shown in Figure 46b and c. The 1200°C and the step quenched specimens both consisted of blocky as well as lath martensite as shown in Figure 47a-b. The lath martensite is labelled A and the blocky or plate as B. There is however one important difference between the 1200°C direct quench and the step quench. Step quenching resulted in more twinning, the amount of twinning increasing with the increasing hold time at 1100°C, as compared to the direct quench. The presence of twins is confirmed in Figs. 47-50 for alloy 4340 step quenched to any of the following temperatures: 1100°C, 870°C, or 275°C. In all cases the martensite formed was extensively twinned. Figures 47c-e are dark field micrographs of region B in Figure 47b. Figure 47g is a dark field of the large plate shown in 47f. The nature of the network of plates formed along prior austenite grain boundaries is evident in Figure 47h.

Step quenching to 870°C/30 min resulted in a similar twin pattern as shown in Figure 48. Clearly the structure is heavily twinned, unlike that directly quenched from 1200°C.

In a similar fashion solution treatment at 1100°C resulted in extensive twinning, again unlike that of the 1200°C directly quenched specimen.

Isothermal transformation to lower bainite and martensite by quenching to 275°C for 1 hr. produced the expected lower bainitic structure shown in Fig. 50a. with the typical carbide distribution. A SAD pattern of a

nearby martensitic region clearly reveals the twinned structure present in the martensite.

Alloy 300M was similar to 4340 with a few exceptions. The 870°C/1 hr. treatment produced a martensitic structure containing twins, as the SAD pattern indicates in Fig. 51b. 300M with the benefit of added silicon retained more austenite after a 1200°C/1 hr. treatment than did 4340. This is evident from Figure 52b, a dark field revealing the distribution of retained austenite in Fig. 52a. Again the structure contained both lath and blocky martensite, Fig. 52c, and the blocky martensite was again strongly twinned as the SAD pattern in Fig. 52d indicates.

Step quenching 300M from 1200°C to 870°C prior to oil quenching produces a structure similar to 4340 in that both twins and retained austenite were present, Fig. 53 a-e. Finally, isothermal transformation for one hour at 350°C resulted in a duplex structure comprising an upper bainite structure consisting of ferrite and retained austenite, rather than ferrite and carbide, and martensite, both blocky and lath, Fig. 54 a-b.

In summary, variations in twins and retained austenite have been observed. Table XI summarizes the distinguishing features associated with several heat treatments.

C. Fracture Morphology

The fracture morphology of both alloy 4340 and 300M were extensively examined. Mixed structures were present for nearly all heat

treatment conditions. Figure 55a clearly shows one such mixed ductile and cleavage mode. Tempering reduces the amount of cleavage, Figure 55b. Only regions adjacent to the fatigue crack were examined. The 1200°C/1 hr heat treated specimens exhibited the fracture morphology shown in Figure 56. High magnification micrographs indicated both shallow dimpled morphologies and quasicleavage. Step quenching to 1100°C or 870°C resulted in a somewhat more clearly defined intergranular fracture mode, Figure 57. Micrographs for the 1200 → 335°C step quench to form a duplex martensitic-bainitic structure are included in Figure 58. The transition from a ductile to a brittle fracture is obvious as the holding time at 335°C is increased from 1 minute to 1 hr.

Step quenching to 250°C for 1 hour from 1200°C or 870°C resulted in a quasicleavage failure mode, transgranular regardless of prior austenite grain size. Step quenching to 315°C for 1 hour from 870°C resulted in a mixed ductile and quasicleavage failure mode, again transgranular.

Alloy 300M did not exhibit intergranular features, even for the large grained specimens, Figure 60 b,c. However, tempering at 200°C produced a much more ductile fracture surface compared to the fracture surface of a quenched test specimen. For this case increased ductility can be associated with improved toughness. However, a comparison of Figure 60a and 60b demonstrates that it is very difficult to evaluate the relative toughness of specimens by just examining the fracture appearance. For this case both specimens exhibit a ductile failure mode. Again, as for 4340, isothermal

transformation to a basically bainitic structure resulted in an entirely quasicleavage fracture mode, Figure 61.

A limited amount of work was carried out in order to characterize fracture surface profiles by chromium plating and sectioning perpendicular to the fracture surface and to the direction of crack propagation. Figure 62 illustrates two cases which exhibited a significantly different fracture profile, intergranular in one case and transgranular in the other, and yet the toughness levels were comparable.

D. Auger Electron Spectroscopy

The test conditions studied under this program are shown in Table XII. Only alloy 4340 was analyzed in the time available. It was not thought possible to produce an intergranular failure in 300M as evidenced in K_{IC} test specimen results. Tests were initially conducted at room temperature, and then in an effort to produce a more highly intergranular failure, specimens were ice brine quenched and broken at -90°C . This however produced an opposite effect in some cases. Namely, fracturing at -90°C resulted in a transgranular failure. Since the failure mode is very important in interpreting the Auger electron data, the fracture morphology will be considered first.

Scanning electron micrographs of the fracture surfaces are shown in Figures 72-75. For the $870^{\circ}\text{C}/1\text{ hr}$ treatment the failure mode was basically intergranular but ductile tearing and some transgranular fracture

was present, Fig. 72 a-b. Fracture at -90°C however produced a more uniformly intergranular failure mode, which was the objective.

A low magnification micrograph of a fractured pin heat treated at 1200°C/1 hr, water quenched, and broken at room temperature is shown in Figure 73a. Figure 73b-c are higher magnification micrographs showing the 'intergranular' failure mode. Again extreme tearing along grain boundaries was observed. However, unlike the 870°C treatment, ice brine quenching and fracturing at -90°C did not produce a more uniformly intergranular failure, but rather resulted in a completely transgranular failure. Step quenching from 1200°C → 870°C (Fig. 74) or 1200°C → 1100°C (Fig. 75) produced similar results. Also, Fig. 75a, is an example of two distinctly different failure modes in different areas of the same fracture surface. These nonuniform failure modes prevented a more clearly defined segregation analysis from being obtained. Further work requires the use of a high resolution scanning Auger electron system.

A typical Auger analysis provides data as shown in Figure 63. Individual peaks are labelled. However, due to the varying sensitivities of each element, scale changes, etc., it is difficult to draw conclusions directly from such a curve. Rather, all the data for this study was entered into a computer which was programed to adjust for the varying sensitivities and to calculate the atomic percent of each element detected. For all the data shown in Figs. 64-71, at least three separate analyses were averaged. Typical output from the computer analysis is shown in Table XIII.

The average atomic percent of the elements detected on the fracture surface of specimens heat treated at 870°C/1 hr, 1200°C/1 hr → 1100°C/1 hr, or 1200°C/1 hr fractured at -90°C are shown in Figs. 64-66 respectively as a function of argon ion sputtering time. In all cases sputtering was continued until a nonchanging level was reached representing a nominal bulk level. Of course, it is important to realize that the accuracy of Auger data in absolute values is perhaps only \pm 30%. However, the technique is very sensitive to relative changes. Hence, absolute values are not necessarily meaningful, but relative changes are indicative of real compositional variations.

The results in Figure 64-66 show, for example, that as the argon level increases during sputtering, both the carbon and oxygen levels decrease indicating some surface contamination even though the specimen was broken in situ. Again this is to be expected. In an attempt to establish the effect of various solution treatments on grain boundary composition, the average atomic percent of several elements found on the fracture surface has been plotted in Figs. 67-71 as a function of heat treatment. While the results do show some interesting variations, it is important to realize that in some cases the failure was transgranular and in others basically intergranular.

The average atomic percent of each element in specimens broken at room temperature vs at -90°C before sputtering is shown in Figs. 67-68. Keeping in mind that the 1200°C → 870°C shifted from an

intergranular to transgranular failure mode and referring to the curves for sulfur, phosphorus, and chlorine, it appears that each of these elements has a higher concentration on the grain boundary than in the bulk. With the exception of chlorine, there is little difference for the 870°C treatment. However, this can be due to the fact that for the 870°C treatment, both the room temperature and the -90°C case were basically intergranular. Hence little change was expected. A better comparison in this case would be before and after sputtering since it was intergranular initially. This would enable a comparison of the grain boundary versus bulk level. The comparison can be seen in Fig. 70 for the 870°C treatment. It is evident that at least for sulfur, little grain boundary segregation was observed. No change is observed for the 1200 → 870 or 1200°C direct treatment either. However, this is not surprising since when fractured at -90°C failure was transgranular initially. Hence, sputtering would not provide a grain boundary profile.

One final point is illustrated in Fig. 71. Wide variations in what appears to be chlorine were observed. This was not due to any contamination in the system since dummy specimens did not show any chlorine. The chlorine is unexpected and large variations were experienced. However, no consistent pattern was observed based on either sputtering conditions, fracture mode considerations, or heat treatment. Spark source mass spectrographic analysis did confirm the presence of some chlorine, <.001 wt. percent in the bulk level. Further work would be required, including scanning Auger data to indeed verify the presence of chlorine and its distribution on the surface.

V. DISCUSSION

While various studies have examined the effects of compositional variations, isothermal transformations, continuous cooling, and tempering,⁽⁷⁾ there has been no published work carried out to explain the effects of step quenching versus direct quenching on these alloys. Studies in the past have been limited to comparisons between fine grained specimens, 870°C/1 hr type treatments, and step quenched coarse grain specimens, 1200 → 870°C type treatments, and usually only for 30 minute hold periods at 870°C. The work that has been done on elevated solution treatment temperatures has been aimed at the effects of residual carbides, and is usually limited to about 1000°C.

A major objective of this program has been to explore the effects of direct quenching rather than step quenching from a fracture toughness-microstructure viewpoint, since the highest level of fracture toughness under this program was obtained by direct quenching from 1200°C.

From a fracture toughness viewpoint, the two treatments below represent the optimum heat treatment used in this program to achieve the highest levels of fracture toughness at tensile strengths of 280,000 psi and above for alloy 4340:

1200°C/1 hr.

1200°C/1 hr → 1100°C/10 min *

*about 3 minutes required to reach 1100°C.

Alloy 300M behaved in the same manner except that for the very highest strength levels, 300-320,000 psi, a short step quench to 315°C or 275°C for 3 minutes apparently resulted in some improvement over the direct quench from 1200°C. However even the 1200°C/1 hr treatment was far better as compared to the 870°C treatment. Again, for step quenched specimens, it required about 1-1 1/2 minutes to reach the lower temperature so that the actual time at 260°C or 315°C was really on the order of only 1 $\frac{1}{2}$ minutes. This implies that for the 300M with the added silicon, only about 5% bainite would be present. More likely however is the retention of additional austenite during final oil quenching to room temperature, since the intermediate holding time would allow time for carbon enrichment of the austenite which would in turn lead to an enhanced stabilization relative to the directly quenched from 1200°C case. This difference is only apparent when in the as quenched or lightly tempered condition (below 200°C temper).

This fact in conjunction with the fact that there is a definite increase in retained austenite due to 1200°C solution treatment as opposed to an 870°C treatment suggests that retained austenite may be responsible for improved properties. This would be further supported by evidence (7) that the retained austenite apparently does transform under strain, at least as tested in .050 in. thick tensile specimens. If this is so then the effect of retained austenite would depend on its stability which would be affected by composition, tempering treatment and solution treatment procedures.

As shown in this study, isothermal transformation to bainite and retained austenite in alloy 300M, (as much as 25% retained austenite) does not necessarily combine to provide improved toughness. In fact, the strength level for an $870^{\circ}\text{C} \rightarrow 315^{\circ}\text{C}/1\text{ hr}$ treatment was just above 200 ksi. Hence, in the case of duplex bainite and retained austenite, even though the amount of austenite retained was high for 300M, the toughness and strength level were both relatively low. Again austenite stability may be dominant when large amounts of retained austenite are present.

The presence of retained austenite may be used to explain the improved toughness when comparing an 870°C treatment, which does not contain retained austenite, except in trace amounts, to the direct 1200°C treatment. However, this program has shown that step quenching treatments result in a drop in toughness compared to a direct 1200°C treatment. A major effort of this program has been to find an explanation for this behavior which is not restricted just to 4340 and 300M alloys but can include the entire class of low alloy steels.

From the mechanical property data and the microscopy results, it is clear that the presence of twins may be associated with a drop in the fracture properties of the material under study. As shown in this study, the amount and/or distribution of retained austenite does not change by step quenching the specimens to an intermediate temperature prior to oil quenching. Although no micrographs are presented here to show the presence of retained austenite in $1200^{\circ}\text{C} \rightarrow 870^{\circ}\text{C}$ step quenched sample, Lai et al.⁽⁴⁾ have shown that this

treatment also gives extensive network of interlath retained austenite films as compared to the specimens quenched directly from 870°C, and have also pointed out that the conventional austenitizing temperature of 870°C resulted in more twinning as compared to the 1200°C treatment. Summarizing then, the amount and distribution of retained austenite is not affected by the step-quench treatment after prior solutioning at 1200°C while the twin density of the specimens tested in this program increases dramatically as the holding times increase at intermediate temperatures or as the holding temperature is lowered.

The distribution and partitioning of alloying elements during austenitization at high temperatures can account for these observations. Ritchie et al.⁽⁹⁾ have proposed that austenitizing above 1100°C followed by fast quenching prevents segregation of impurities (trace elements like Sb, S, P) to prior austenite grain boundaries. The resultant homogeneous dispersion of impurities changes the mode of fracture and hence the toughness of low alloy steels. In another paper, Clark et al. (10) suggested the existence of a particular temperature, independent of grain size, above which the thermodynamic driving force for segregation to grain boundaries will be minimal and a lower temperature below which segregation would be essentially complete. They also showed 1100°C to be the temperature above which the thermodynamic driving force for segregation is too small to drive the embrittling species to the grain boundaries and below which substantial segregation to austenite grain boundaries

takes place. In their opinion, a two-step quench could be beneficial in improving fracture toughness properties as long as the holding times at intermediate temperatures do not allow damaging segregation to occur. Regarding segregation of different elements to austenite grain boundaries, not only impurity or trace elements like Sb, S, P, but also alloying elements like Mn, Cr, Ni, Mo, etc. should be considered. Andrew and Weston (11) have shown the temperature range for the dissolution of MnS inclusions to be above 1200°C and although the SEM analysis of these specimens has not shown dissolution of MnS inclusions, it can be argued that at high soaking temperatures these inclusions provide a source of high local concentrations of Mn and S and any dissolution occurring will enrich the surrounding austenite in these two elements. Apart from this, there is also some manganese present which is not associated with inclusions. A recent paper by Ray and Seal ⁽¹²⁾ has shown the dramatic effect of an increase in the manganese content on the amount of twinning in low carbon steels. Similarly, Wirth and Bickerstaffe ⁽¹³⁾ have demonstrated a relationship between the chromium content and the amount of twinning in maraging steels.

In the light of these observations, it is thus suggested that at high austenitizing temperatures, diffusion rates are high enough and the thermodynamic driving force for segregation so small that any segregation to austenite grain boundaries or other preferred sites is prevented. If the steel is quenched directly from this temperature (1200°C in our case) in this homogeneous condition, predominantly dislocated lath martensite is formed.

On the other hand, if the steel is stepped to a lower temperature (1100°C or lower in our case), the thermodynamic driving force for segregation increases and segregation may occur producing enrichment of elements such as Mn, Cr, Ni, etc. at preferred sites in the austenite. Partitioning and redistribution of alloying elements in austenite may produce local changes in stacking fault energy which has been shown to exert a strong influence on the transformation characteristics of quenched iron base alloys, especially on the amount of twinning. (14-16)

In order to attempt to confirm this, Auger electron spectroscopy analysis was carried out as described earlier. The results obtained under this program do suggest segregation of sulfur to grain boundaries in some cases. Furthermore unexpected large variations in chlorine were detected, although spark source mass spectrographic analysis revealed a total bulk content only 70 atomic parts per million. In order to conclusively demonstrate whether segregation does occur preferentially along prior austenite grain boundaries during solution treatment, or alternately, if fracture is transgranular, does segregation provide a preferential crack path, a detailed program probably of doping alloys in order to aid detection would be necessary. Also, a scanning O.J. system would be necessary in order to take into consideration mixed mode fracture profiles.

The results of the Charpy tests do confirm a difference depending on whether the standard root radius is used or a precracked sharp root radius

which would approach that of a fracture toughness specimen. The pre-cracked Charpy was very sensitive to temper embrittlement while the standard Charpy was not.

In summary the results of this program have shown that for commercially available 4340 and 300M, the 1200°C solution treatment produced the maximum toughness at strength levels of 280,000 psi or higher. Step quenching normally resulted in a loss in toughness concomitant with the presence of twins. The overall increase in fracture toughness is evidently related to all three parameters, retained austenite, twins, and segregation, in a complex interrelated manner. This program has shown that retained austenite is not the only factor. However, further work is required in order to better establish the presence and extent of segregation. The presence of twins has often been suggested as reducing fracture toughness. However, in those cases, as now, it is impossible to alter the twin density without altering other parameters. In the present program it has not been established whether the presence of twins per se caused a drop in toughness or whether the factor(s) which induced twinning, i.e. segregation, is also responsible for reducing the toughness.

CONCLUSIONS

1. For maximum toughness, initial austenitization at 1200°C was required.

2. Maximum toughness was obtained using several different heat treatment schedules. In addition to the direct quench from 1200°C, step quench treatments to 1100, 870°C or 315°C all produced high toughness levels if the holding time was short.
3. Valid plane strain fracture toughness results of over 90,000 $\text{psi-in}^{1/2}$ were achieved for alloy 4340 combined with tensile strengths of 300,000 psi. K_{Ic} values of over 85,000 $\text{psi-in}^{1/2}$ have been obtained for alloy 300M at equivalent strength levels.
4. The amount of twinning depends upon the intermediate temperature and the holding time at this temperature during step-quenching operations going up with lower temperatures and longer holding times.
5. The change in twin density can be explained by a segregation model giving rise to local changes in the stacking fault energy of austenite at intermediate temperatures.
6. The fracture toughness properties of AISI 4340 steel are affected not only by the amount and distribution of retained austenite but also by the extent of segregation during austenitization and the resultant twinning.

ACKNOWLEDGEMENTS

The author gratefully acknowledges the assistance of Dr. K. Khan for electron microscopy analysis and J. Biskey for assistance with heat treating, mechanical testing and metallography. The assistance of S. Shankar, K. Datta, D. Kumar and S. Srivathsan during the testing and analysis of the data is also acknowledged.

This research was performed under the Department of the Navy, Naval Air Systems Command and Office of Naval Research, Washington, D.C., Contract Nos. N00019-76-C-0149 and N00019-77-0135.

REFERENCES

1. Fracture toughness of high strength materials: Theory and Practice, Iron and Steel Inst. Special Publication No. 120, London, 1970.
2. Metal Progress Data Book, American Society for Metals, Metals Park, Ohio, 1975.
3. V.F. Zackay, E.R. Parker, and W.E. Wood, Influence of some microstructural features on the fracture toughness of high strength steels. Third Int. Conf. on Strength of Metals and Alloys, Cambridge, England, Inst. of Metals, London, 1973, pp. 175-179.
4. G.Y. Lai, W.E. Wood, R.A. Clark, V.F. Zackay and E.R. Parker, Met. Trans. 1974, Vol. 5, pp. 1663-1670.
5. R.D. Goolsby, W.E. Wood, E.R. Parker, V.F. Zackay, Electron Microscopy and Structure of Materials (Eds. G. Thomas, R.M. Fulrath, and R.M. Fisher - Univ. of California Press), 1972, pp. 798-807.
6. G.Y. Lai, Mat. Sci. and Eng. 1975, Vol. 19, pp. 153-156.
7. E.R. Parker, Met. Trans. 1977, Vol. 8A, pp. 1025-1042.
8. B.N.P. Babu, D. Eng. Thesis, Department of Materials Science and Engineering, University of California, Berkeley, Aug. 1974, LBL #2772.
9. R.O. Ritchie, J.F. Knott, and L.C.E. Gniets: The Microstructure and Design of Alloys Proc. 3rd Intl. Conf. on Strength of Metals and Alloys, Inst. of Metals and Iron and Steel Inst., London, 1973, p.124.
10. G. Clark, R.O. Ritchie, and J.F. Knott: Nat. Phys. Sci., 1972, Vol. 239, p.104.
11. R.C. Andrew and G.M. Weston: Met. Sci. April 1977, p.142.
12. R.K. Ray and A.K. Seal: Met. Trans. 1977, Vol.8A, p.793.
13. A. Wirth and J. Bickerstaffe: Met. Trans. 1974, Vol 5, p.799.
14. G.B. Olson and M. Cohen: Met. Trans. 1976, Vol. 7A, p. 1905.
15. G.V. Kurdjumov and A.G. Khachaturyan: Acta. Met. 1975, Vol.23, p.1077.

REFERENCES (cont'd)

16. F. Lecroisey and A. Pineau: Met. Trans. 1972, Vol.3, p.387.

Table I Room Temperature Longitudinal Tensile Data for Alloy 4340

I.D.	Heat Treatment		σ_{ys} ksi	σ_{ult} ksi	Elong %	R.A. %
	Solution Treat.	Tempering Temp. °C				
C86	870/1 hr	AQ**	224	302*	1.1	1.6
C87		AQ	223	293*	1.0	3.1
C88		175++	238	288	13.6	45.4
C89		175	234	284	13.6	35.1
C92		200	225	274	12.7	46.4
C90		280	219	236	14.6	48.8
C91		280	219	241	12.8	55.7
C93		350	186	208	12.6	51.8
C94	1100/1 hr	AQ	214	321	6.5	9.3
C95		AQ	213	322	4.9	7.8
C96		280	195	228	9.1	37.4
C1	1200/1 hr	AQ	213	241*	1.2	3.2
C2		AQ	225	245*	1.2	3.1
C3		175	225	278*	3.4	4.7
C4		175	216	268	5.5	8.6
C5		200	217	267	3.6	8.6
C6		280	202	228	1.1	3.2
C7		280	202	226	1.3	5.5
C8		350	185	208	4.8	12.4
C9	1200/1hr + 1100/10 min	AQ	191	269*	1.2	4.0
C10		AQ	269	293*	1.3	4.0
C11		175	208	265	4.3	7.9
C12		175	208	267	4.1	6.3
C13		280	195	222*	1.5	3.2

Table I (cont'd) Room Temperature Longitudinal Tensile Data for Alloy 4340

I.D.	Heat Treatment		σ_{ys} ksi	σ_{ult} ksi	Elong %	R.A. %
	Solution Treat.	Tempering Temp. °C				
C56	1200/1 hr → 335/5 min	AQ	127	169	9.3	24.4
C57		AQ	126	170	9.3	25.2
C58	175	121	164	10.3	33.3	
C59	175	129	168	7.8	28.6	
C60	280	131	166	12.3	33.9	
C61	1200/1 hr → 335/30 min	AQ	122	156	12.7	35.7
C62		AQ	113	150	8.7	37.0
C63	175	120	156	10.3	33.9	
C64	175	120	152	13.1	43.2	
C65	280	120	154	7.1	32.6	
C66	1200/1 hr → 335/60 min	AQ	121	153	13.3	39.7
C67		AQ	121	154	11.9	32.6
C68	175	124	156	13.6	37.6	
C69	175	117	153	14.3	36.0	
C70	280	127	153	12.5	38.1	
C34	1200/1 hr → 300/5 min	AQ	142	200	3.9	14.9
C35		AQ	146	194	4.4	21.1
C36	175	150	186	7.5	38.4	
C37	175	136	185	10.3	41.8	
C38	280	163	189	8.0	36.6	
C39	1200/1 hr → 300/30 min	AQ	146	182	12.9	55.6
C40		AQ	146	182	12.8	44.3
C41	175	143	183	13.9	39.9	
C42	175	147	180	11.4	52.9	
C43	280	146	183	12.5	46.0	

Table I (cont'd) Room Temperature Longitudinal Tensile Data for Alloy 4340

I.D.	Heat Treatment		Solution Treat. Temp. °C	σ_{ys} ksi	σ_{ult} ksi	Elong %	R.A. %
	1200/1 hr → 300/60 min	AQ					
C44	1200/1 hr → 300/60 min	AQ		144	168	15.6	44.9
C45		AQ		147	180	16.6	47.3
C46		175		143	178	14.7	50.2
C47		175		147	179	11.9	44.6
C48		280		148	180	12.6	40.9
C29	1200/1 hr → 280/5 min	AQ		178	251	3.9	8.6
C20		AQ		154	249	4.0	7.9
C21		175		174	234	8.3	22.3
C22		175		188	237	7.6	27.0
C23		280		188	219	6.8	26.3
C24	1200/1 hr → 280/30 min	AQ		162	201	13.4	50.6
C25		AQ		159	199	13.5	53.2
C26		175		158	198	11.6	45.5
C27		175		160	198	14.2	49.0
C28		280		161	198	13.1	53.2
C29	1200/1 hr → 280/1 hr	AQ		160	197	14.1	46.6
C30		AQ		158	197	14.6	44.0
C31		175		157	190	19.5	48.8
C32		175		157	199	10.8	45.9
C33		280		156	196	11.7	46.8

* Premature failure

** As quenched

++ All tempering times are for 1 hr. unless otherwise noted

Table I (cont'd) Room Temperature Longitudinal Tensile Data for Alloy 4340

I. D.	Heat Treatment		Solution Treat. Temp. °C	σ_{ys} ksi	σ_{ult} ksi	Elong %	R. A. %
	1200/1 hr → 1100/1 hr	AQ					
C14	1200/1 hr → 1100/1 hr	AQ		208	304*	4.8	4.8
C15		AQ		186	275*	3.8	5.5
C16		175		198	253	6.8	14.6
C17		175		238	249*	4.9	13.1
C18		280		190	222	5.1	13.8
C71	1200/1 hr → 350/5 min	AQ		115	149	4.8	18.3
C72		AQ		125	162	6.4	18.9
C73		175		121	160	7.5	27.5
C74		175		122	155	5.9	29.9
C75		280		127	152	8.0	30.0
C76	1200/1 hr → 350/30 min	AQ		110	142	10.1	30.5
C77		AQ		114	146	9.2	31.2
C78		175		108	148	11.9	35.7
C79		175		114	147	11.1	35.9
C80		280		110	145	10.8	38.5
C81	1200/1 hr → 350/1 hr	AQ		117	147	10.6	30.0
C82		AQ		112	146	9.2	30.6
C83		175		112	147	11.8	34.7
C84		175		113	146	11.9	35.9
C85		280		116	146	10.9	36.4
C49	1200/1 hr → 335/2 min	AQ		195	294	2.5	5.4
C50		AQ		204	297	2.4	4.7
C51		175		195	265	6.3	10.8
C52		175		212	265	6.3	7.8
C53		200		209	258	6.3	13.0
C54		280		194	228	5.3	12.3
C55		350		178	201	4.7	12.5

Table II Room Temperature Longitudinal Tensile Data for Alloy 300M

I. D.	Heat Treatment ^a	Solution Treat. Tempering Temp. °C	σ_{ys} ksi	σ_{ult} ksi	Elong %	R.A. %
D1	1200/1 hr	AQ	197	-	-	-
D2		AQ	194	305	3.8	3.9
D3		175	220	284	5.4	15.2
D4		175	217	284	6.3	14.5
D5		200	225	281	6.3	9.3
D6		200	207	271	3.5	12.3
D7		280	230	277	3.9	17.5
D8		280	226	263	5.2	11.7
D9		350	199	241	6.7	13.1
D10		350	198	235	2.9	12.3
C11	200/5 hrs		230	283	6.3	15.2
D12	200/5 hrs		229	280	3.5	15.2
D13	1200/15 min	200	228	287	4.3	9.4
D14		200	233	288	3.7	7.1
D15	200/5 hrs		228	285*	3.9	9.4
D16		200/5 hrs	219	219*	0.2	4.0
D17	1200/30 min	200	230	293	5.1	9.3
D18		200	229	295*	5.5	10.1
D19	200/5 hrs		237	245*	0.4	4.0
D20	200/5 hrs		236	291	4.3	8.6
D21	1200/1 hr → 315/1 hr	AQ	96	201	10.7	13.2
D22		175	133	166	13.0	41.3
D23		175	96	201	15.0	12.5
D70		175	112	183	13.3	25.6
D24		280	132	166	12.5	43.6

Table II (cont'd) Room Temperature Longitudinal Tensile Data for Alloy 300M

I.D.	Heat Treatment	Solution Treat. Tempering Temp. °C	σ_{ys} ksi	σ_{ult} ksi	Elong %	R.A. %
D44	870/1 hr	AQ	190	325	8.6	23.1
D45		AQ	195	328	6.6	19.5
D46		175	222	283	5.8	35.0
D47		175	218	282	10.6	39.4
D48		200	221	279	11.1	39.9
D49		280	228	270	7.4	41.5
D50		280	229	271	9.3	37.1
D51		350	205	243	12.0	34.0
D52	870/1 hr → 315/2 min	AQ	180	331	8.1	21.0
D53		175	221	281	12.7	29.2
D54		175	221	284	10.4	38.3
D55		280	229	268	6.4	42.6
D56	870/1 hr → 315/5 min	AQ	196	327	6.3	11.8
D57		175	219	280	9.6	35.7
D58		175	216	278	10.0	35.4
D59		280	221	261	6.8	39.2
D60	870/1 hr → 315/1 hr	AQ	102	220	16.9	12.0
D61		175	111	215	18.0	31.4
D62		175	113	212	17.0	28.9
D63		280	133	192	24.0	40.8
D64	870.1 hr → 350.1 hr	AQ	211	—	—	—
D65		175	235	295	6.3	16.7
D66		175	226	296	6.7	9.3
D67		280	235	280	7.0	25.5

*Failed prematurely

Table II (cont'd) Room Temperature Longitudinal Tensile Data for Alloy 300M

I.D.	Heat Treatment	Solution Treat.	°C	σ _{ys} ksi	σ _{ult} ksi	Elong. %	R.A. %
D25	1200/1 hr → 315/5 min	AQ		203	228*	0.5	0.8
D26		175		-	-	-	-
D27		175		228	295	4.8	9.3
D28		280					
D29	1200/1 hr → 315/2 min	AQ		175	-	-	-
D30		175		230	301	4.4	7.2
D31		175		-	-	-	-
D32		280		238	278	1.9	3.2
D33	1200/1 hr → 350/1 hr	AQ		161	-	0.5	0.8
D34		175		196	261	2.8	5.5
D35		175		181	256	2.7	4.0
D36		280		204	255	2.1	4.0
D37	1100/1 hr	AQ		212	-	0.6	0.8
D38		AQ		220	-	0.4	1.6
D39		175		232	303	5.9	13.1
D40		175		230	299	7.8	13.9
D41		200		227	296	6.9	15.3
D42		280		241	285	6.3	18.6
D43		350		210	248	2.8	5.5

Table III
SUMMARY OF
4340 HEAT TREATMENTS STUDIED IN THIS PROGRAM

Solution Treatment °C/hr (oil quenched)	AQ	Tempering Temperature °C				
		125	175	200	280	350
870/1 hr	x	x		x	x	
1100/1 hr	x	x	x	x	x	
1150/1 hr	x		x	x		
1200/15 min	x		x			
1200/1 hr	x	x	x	x	x	x
1200/1→1100/1 min			x	x		
1200/1→1100/10 min	x	x	x	x		x
1200/1→ 1100/30 min			x			
1200/1→ 1100/1 hr			x	x	x	x
1200/1→ 1000/30 min	x		x	x		
1200/1→870/30 sec	x					
1200/1→ 870/5 min	x					
1200/1→ 870/30 min	x		x	x	x	x
1200/1→ 870/1 hr	x					
870/1→ 250/1 hr	x		x	x		x
870/1→ 315/3 min	x		x			
870/1→ 350/10 min	x		x	x		x
870/1→ 315/1 hr	x		x	x		
1200/1→ 250/1 hr	x		x	x	x	x
1200/1→ 250/5 min 335/1 hr	x		x	x		
1200/1→ 275/5 min			x			
1200/1→ 257/30 min			x			
1200/1→ 275/1 hr	x		x	x		x
1200/1→ 300/3 min				x		
1200/1→ 300/5 min	x					
1200/1→ 300/1 hr	x		x	x		

Table III (cont'd)

SUMMARY OF

4340 HEAT TREATMENTS STUDIED IN THIS PROGRAM

Solution Treatment °C/hr (oil quenched)	AQ	Tempering Temperature °C				350
		125	175	200	280	
1200/1 → 315/10 sec			x	x		
1200/1 → 335/1 min				x		
1200/1 → 335/3 min	x		x	x	x	
1200/1 → 335/5 min	x					
1200/1 → 335/10 min			x	x		
1200/1 → 335/30 min			x			
1200/1 → 335/1 hr	x			x		
1200/1 → 350/1 min	x		x	x	x	
1200/1 → 350/5 min	x		x			
1200/1 → 350/30 min			x			

Table IV
SUMMARY OF
300M HEAT TREATMENTS STUDIED IN THIS PROGRAM

Solution Treatment °C/hr (oil quenched)	AQ	125	150	175	200	280	350	400
870/1 hr	x	x	x	x	x	x	x	x
1100/1 hr	x		x	x	x	x	x	x
1200/15 min	x				x			x
1200/30 min					x			
1200/1 hr	x	x	x	x	x	x	x	x
1200/1 hr → 1100/10 min	x				x			
1200/1 hr → 1100/1 hr	x				x			
1200/1 hr → 870/1/2 hr	x				x	x	x	x
1200/1 hr → 315/3 min	x			x	x			x
1200/1 hr → 315/10 min					x	x	x	
1200/1 hr → 315/1 hr	x				x	x	x	x
1200/1 hr → 260/3 min	x				x	x		
1200/1 hr → 260/30 min	x				x	x	x	x
1200/1 hr → 200/3 min	x				x	x	x	x
1200/1 hr → 200/1 hr	x				x	x	x	x
870/1 hr → 315/3 min					x			
870/1 hr → 315/60 min	x				x			

Table V

Room Temperature Longitudinal Fracture Toughness
Data for Alloy 4340

Specimen I.D.	Austenitizing** Treatment °C/hr	Tempering Temperature °C(1 hr)	K _{Ic} ksi-in ^{1/2}	K _{max} ksi-in ^{1/2}	Pm/PQ
AC 2	870/1 hr	AQ	38.6	38.6	1.00
AC 14		AQ	34.4	34.4	1.00
AC 18		AQ	33.5	37.7	1.02
AC 19		125	42.2	42.2	1.00
AC 98		180	59.8	66.4	1.04
AC 3		200	61.5	67.9	1.04
AC 5		200	64.6	64.6	1.00
AC 6		280	77.5	88.2	1.03
AC 7		280	75.1	80.6	1.03
AC 8		350	92.6	113.3	1.12*
AC 9	↓	350	103.3	117.8	1.05
AC 12	1100/1 hr	AQ	43.0	43.0	1.00
AC 13		AQ	43.1	43.1	1.00
AC 53		125	45.6	50.8	1.07
AC 27		175	58.2	62.0	1.01
AC 26		175	61.1	63.7	1.01
AC 28		200	61.4	61.4	1.00
AC 117	↓	280	70.5	83.5	1.04
AC 76	1150/1 hr	AQ	50.7	53.1	1.01
AC 77		AQ	53.7	57.3	1.04
AC 78		175	70.1	76.4	1.04
AC 116		175	72.9	87.6	1.04
AC 114		200	70.1	76.0	1.04
AC 115	↓	200	67.3	73.6	1.04

Table V (cont'd) Room Temperature Longitudinal Fracture Toughness Data for Alloy 4340

Specimen I.D.	Austenitizing** Treatment °C/hr	Tempering Temperature °C(1 hr)	K _{Ic} ksi-in ^{1/2}	K _{max} ksi-in ^{1/2}	Pm/PQ
AC 178	1200/15 min	AQ	65.1	74.0	1.08
AC 179		AQ	52.8	81.1	1.18*
AC 180		175	78.8	93.8	1.11*
AC 181	↓	175	79.9	96.3	1.12*
<hr/>					
AC 15	1200/1 hr	AQ	67.3	79.6	1.11*
AC 22		AQ	46.8	62.9	1.18*
AC 30		AQ	65.9	76.4	1.07
AC 24		125	83.1	89.7	1.04
AC 25		125	84.0	84.0	1.00
AC 110		175	87.1	96.8	1.05
AC 29		175	85.4	98.4	1.08
AC 111		200	92.2	103.6	1.06
AC 112		200	85.9	98.1	1.06
AC 23		225	66.4	85.1	1.17*
AC 113		280	64.6	90.6	1.19*
AC 31		280	59.6	70.1	1.08
AC 54		350	72.6	91.5	1.11*
AC 55	↓	350	80.8	81.9	1.01*
AC 86	1200/1 hr→1100/1 min	175	91.4	101.0	1.05
AC 88	↓	200	85.7	100.0	1.06
<hr/>					
AC 126	1200/1 hr→1100/10 min	AQ	80.5	88.3	1.05
AC 127		AQ	78.3	100.8	1.13*
AC 125		125	71.3	93.1	1.10
AC 89		175	93.5	107.6	1.05
AC 123	↓	175	85.4	98.3	1.08

Table V (cont'd) Room Temperature Longitudinal Fracture Toughness
Data for Alloy 4340

Specimen I.D.	Austenitizing** Treatment °C/hr	Tempering Temperature °C(1 hr)	K _{Ic} ksi-in ^{1/2}	K _{max} ksi-in ^{1/2}	Pm/PQ
AC 124	1200/1 hr → 1100/10 min	200	85.9	98.9	1.09
AC 34		200	67.9	77.4	1.05
AC 128		350	84.2	88.6	1.04
AC 129		350	85.7	104.8	1.06
AC 32		200	72.0	76.5	1.02
AC 33	↓	200	63.0	70.0	1.03
AC 182	1200/1 hr → 1100/60 min	AQ	60.8	82.4	1.12*
AC 183		175	83.9	109.6	1.10
AC 35		200	66.3	72.2	1.05
AC 36		200	67.5	72.3	1.03
AC 184		280	63.6	64.5	1.04
AC 118		350	82.7	99.8	1.09
AC 119	↓	350	86.0	112.1	1.08
AC 185	1200/1 hr → 1000/3 min	AQ	67.3	67.3	1.00
AC 186		175	80.9	97.9	1.10
AC 187		200	82.5	97.9	1.07
AC 188	↓	200	80.8	89.9	1.05
AC 120	1200/1 hr → 1000/30 min	AQ	78.1	98.5	1.09
AC 121		175	83.1	99.7	1.09
AC 122	↓	175	91.4	110.2	1.08
AC 39	1200/1 → 870/30 sec	AQ	62.6	75.4	1.11*
AC 40	↓	AQ	65.0	74.2	1.10
AC 50	1200/1 → 870/5 min	AQ	60.2	70.4	1.09
AC 52	↓	AQ	56.7	67.2	1.11*

Table V (cont'd) Room Temperature Longitudinal Fracture Toughness
Data for Alloy 4340

Specimen I.D.	Austenitizing** Treatment °C/hr	Tempering Temperature °C(1 hr)	K_{Ic} Ksi-in ^{1/2}	K_{max} Ksi-in ^{1/2}	Pm/PQ
AC 47 1200/1 →	870/30 min	AQ	51.7	53.6	1.01
AC 51		AQ	53.0	63.4	1.10
AC 43		150	59.4	68.8	1.06
AC 48		175	65.5	70.7	1.01
AC 49		175	61.0	72.4	1.12*
AC 37		200	60.7	82.8	1.13*
AC 38		200	61.0	70.6	1.08*
AC 41		280	52.3	58.1	1.06
AC 42		280	53.0	59.1	1.06
AC 44		350	85.6	96.1	1.01
AC 45	↓	350	84.7	96.3	1.06
AC 1200/1 →	870/60 min	AQ	52.9	56.1	1.03
AC 56 870/1 →	315/3 min	AQ	40.3	48.1	1.10
AC 57		AQ	39.4	45.5	1.07
AC 58		200	51.4	54.5	1.03
AC 59	↓	200	53.0	59.0	1.03
AC 196 870/1 →	315/10 min	AQ	60.4	61.7	1.01
AC 197		AQ	55.5	81.8	1.27*
AC 198		175	72.3	82.8	1.06
AC 199		200	71.1	79.2	1.04
AC 200		200	66.1	73.7	1.08
AC 201	↓	280	71.5	71.5	1.00
AC 66 870/1 →	315/60 min	AQ	49.5	59.6	1.04
AC 61	↓	AQ	52.5	63.1	1.06

Table V (cont'd) Room Temperature Longitudinal Fracture Toughness Data for Alloy 4340

Specimen I.D.	Austenitizing** Treatment °C/hr	Tempering Temperature °C(1 hr)	K _{Ic} Ksi-in ^{1/2}	K _{max} Ksi-in ^{1/2}	Pm/PQ
AC 62	870/1 → 315/60 min	200	57.2	66.8	1.09
AC 63		200	58.6	62.4	1.02
AC 195	↓	280	63.5	63.5	1.00
AC 189	870/1 → 250/1 hr	AQ	76.2	76.2	1.00
AC 190		AQ	81.6	81.6	1.00
AC 191		175	83.3	83.3	1.00
AC 192		175	79.7	83.5	1.04
AC 193		200	70.9	73.7	1.15*
AC 194	↓	280	81.6	81.6	1.00
AC 156	1200/1 → 350/1 min	AQ	70.4	84.3	1.15*
AC 160		AQ	63.8	82.2	1.17*
AC 132		175	90.55	91.8	1.01
AC 133		175	78.8	87.5	1.04
AC 134		200	81.4	88.7	1.06
AC 135	↓	200	80.0	98.8	1.08
AC 216	1200/1 → 350/5 min	AQ	53.2	75.9	1.2*
AC 217		AQ	60.7	-	1.03
AC 218		175	87.2	-	1.02
AC 219		175	79.6	-	1.03
AC 136	↓	280	77.0	94.2	1.06
AC 220	1200/1 → 350/30 min	175	60.0	61.5	1.09
AC 221	↓	175	58.8	59.4	1.01

Table V (cont'd) Room Temperature Longitudinal Fracture Toughness Data for Alloy 4340

Specimen I.D.	Austenitizing** Treatment °C/hr	Tempering Temperature °C(1 hr)	K _{Ic} ksi-in ^{1/2}	K _{max} ksi-in ^{1/2}	Pm/PQ
AC 64	1200/1 → 335/3 min	AQ	58.2	66.3	1.06
AC 65		AQ	60.5	66.8	1.03
AC 73		175	80.2	82.1	1.01
AC 70		200	74.5	82.7	1.03
AC 71		200	78.2	79.7	1.00
AC 74		280	68.5	81.4	1.06
AC 222	1200/1 → 335/5 min	AQ	62.8	69.7	1.09
AC 137		175	69.4	89.1	1.14*
AC 157		175	70.7	93.8	1.17*
AC 75		200	82.7	88.7	1.01
AC 210	1200/1 → 335/10 min	AQ	53.8	66.4	1.09
AC 211		AQ	52.7	63.7	1.08
AC 212		175	62.2	74.7	1.13*
AC 213		200	66.0	83.6	1.06
AC 214		200	63.3	77.9	1.12
AC 215		280	80.9	80.9	1.00
AC 223	1200/1 → 335/30 min	175	54.5	55.1	1.04
AC 66	1200/1 → 335/60 min	AQ	43.5	50.7	1.08
AC 67		AQ	45.9	45.9	1.00
AC 68		200	53.9	58.1	1.01
AC 69		200	47.2	57.4	1.10
AC 79		200	50.5	58.4	1.04

Table V (cont'd) Room Temperature Longitudinal Fracture Toughness Data for Alloy 4340

Specimen I.D.	Austenitizing ^{**} Treatment °C/hr	Tempering Temperature °C(1 hr)	K _{Ic} ksi-in ^{1/2}	K _{max} ksi-in ^{1/2}	Pm/PQ
AC 87	1200/1 → 315/10 sec	175	90.2	100.8	1.04
AC 84		200	88.4	93.4	1.02
AC 85		200	88.2	99.9	1.08
AC 72		200	89.7	94.6	1.02
AC 139	1200/1 → 315/3 min	200	80.0	88.2	1.08
AC 140	↓	200	76.8	90.3	1.02
AC 82	1200/1 → 300/3 min	200	79.2	88.8	1.05
AC 83	↓	200	80.4	84.7	1.03
AC 224	1200/1 → 300/5 min	AQ	73.01	83.05	1.11*
AC 225	↓	AQ	67.1	80.8	1.15*
AC 141	1200/1 → 300/60 min	AQ	59.7	59.7	1.00
AC 158	↓	AQ	48.2	72.0	1.38*
AC 142		175	67.3	67.3	1.00
AC 143		175	55.8	55.8	1.00
AC 159		175	60.9	60.9	1.00
AC 80		200	62.5	62.5	1.00
AC 81	↓	200	65.4	65.4	1.00
AC 226	1200/1 → 275/5 min	175	75.9	-	1.03
AC 227	↓	175	95.6	-	1.02
AC 228	1200/1 → 275/30 min	175	82.7	82.7	1.00
AC 229	↓	175	73.1	73.1	1.00
AC 144	1200/1 → 275/60 min	AQ	81.7	81.7	1.00
AC 145	↓	175	81.7	81.7	1.00
AC 146	↓	175	81.5	81.5	1.00
AC 207	↓	175	85.6	85.6	1.00

Table V (cont'd) Room Temperature Longitudinal Fracture Toughness Data for Alloy 4340

Specimen I.D.	Austenitizing** °C/hr	Tempering Temperature °C(1 hr)	K _{Ic} ksi-in ^{1/2}	K _{max} ksi-in ^{1/2}	Pm/PQ
AC 208	1200/1 → 275/60 min	200	69.3	70.0	1.03
AC 163		200	-	-	-
AC 209		280	107.1	107.1	1.00
AC 148	1200/1 → 250/1 hr	AQ	73.7	112.0	1.18*
AC 164		AQ	94.8	94.8	1.00
AC 202		AQ	84.7	84.7	1.00*
AC 203		AQ	72.3	81.5	1.13
AC 149		175	72.3	112.8	1.28*
AC 150		200	82.3	-	1.04
AC 151		200	62.4	62.4	1.00
AC 230		280	68.1	71.2	1.19*
AC 231		350	81.9	95.7	1.12*
AC 152	1200/1 → 250/5 min	AQ	84.1	84.1	1.00
AC 153		175	83.8	103.1	1.04*
AC 154		175	74.4	103.2	1.12
AC 161		175	75.2	86.2	1.08
AC 155		200	76.4	76.4	1.05
AC 162		200	73.0	73.0	1.00

* exceeds maximum allowable value, 1.10 for valid K_{Ic} test

** 870/1 hr. refers to a one hour hold at 870°C followed by oil quenching
 1200/1 hr → 1100/10 min. refers to a one hour hold at 1200°C followed by
 step quenching to 1100°C for 10 minutes followed by oil quenching.

Table VI.

Room Temperature Longitudinal Fracture Toughness
Data for Alloy 300M

Specimen I.D.	Austenitizing** Treatment °C/hr	Tempering Temperature °C(1 hr)	K _{Ic} Ksi-in ^{1/2}	K _{max} Ksi-in ^{1/2}	Pm/PQ
BC 7	870/1	AQ	36.5	54.1	1.13*
BC 7		AQ	36.5	55.5	1.11
BC 38		125	45.9	62.4	1.03
BC 27		150	44.6	58.2	1.05
BC 39		175	68.5	80.9	1.01
BC 10		200	68.0	78.9	1.02
BC 28		200	65.5	76.9	1.02
BC 11		280	63.9	65.4	1.03
BC 29		280	66.6	73.9	1.02
BC 30		350	68.0	65.3	1.03
BC 100		400	36.5	36.5	1.00
BC 101	↓	400	55.1	55.1	1.00
BC 14	1100/1	AQ	39.8	60.6	1.18*
BC 13		AQ	42.8	61.8	1.13
BC 45		175	76.5	93.1	1.05
BC 31		200	76.3	93.5	1.05
BC 32		280	72.3	95.3	1.06
BC 33		350	72.6	87.9	1.08
BC 102	↓	400	57.0	63.4	1.00
BC 103	1200/15 min	AQ	23.5	23.5	1.00
BC 104		AQ	-	-	-
BC 47	↓	200	89.0	95.1	1.03

Table VI (cont'd) Room Temperature Longitudinal Fracture Toughness
Data for Alloy 300 M

Specimen I.D.	Austenitizing** Treatment °C/hr	Tempering Temperature °C(1 hr)	K _{Ic} Ksi-in ^{1/2}	K _{max} Ksi-in ^{1/2}	Pm/PQ
BC 43	1200/15 min	200/5 hr	89.0	97.1	1.04
BC 44	↓	200/5 hr	85.7	104.0	1.07
BC 41	1200/30 min	200/5	79.4	96.9	1.07
BC 42	↓	200/5	79.1	96.8	1.05
BC 105	↓	400	58.9	63.0	1.0
BC 15	1200/1	AQ	43.7	55.3	1.02
BC 16	↓	AQ	39.7	65.3	1.22*
BC 37		125	53.0	75.2	1.07
BC 48		125	53.4	76.3	1.08
BC 49		150	59.5	81.3	1.08
BC 40		175	89.5	107.4	1.05*
BC 46		175	77.7	106.1	1.13*
BC 17		200	80.1	100.5	1.04
BC 18		200	85.5	98.3	1.02
BC 35		200	82.8	101.4	1.08
BC 19		280	78.1	95.5	1.04
BC 36		280	83.6	98.0	1.08
BC 20		350	73.9	94.5	1.04
BC 106		400	59.9	60.0	1.00
BC 107	↓	400	54.3	57.1	1.10
BC 21	1200/1→870/30 min	AQ	42.6	42.6	1.00
BC 22	↓	AQ	41.7	59.0	1.07
BC 23		200	75.7	84.4	1.03
BC 24		200	79.0	93.2	1.01
BC 25		280	72.4	83.6	1.04
BC 26		350	66.0	83.4	1.08
BC 108		400	63.0	75.5	1.03
BC 109	↓	400	55.7	63.4	1.05

Table VI (cont'd) Room Temperature Longitudinal Fracture Toughness
Data for Alloy 300 M

Specimen I.D.	Austenitizing Treatment °C/hr	Tempering Temperature °C(1 hr)	K_{Ic} ksi-in ^{1/2}	K_{max} ksi-in ^{1/2}	Pm/PQ
BC 56	1200/1→315/3 min	AQ	49.6	68.7	1.06
BC 110		175	64.3	73.5	1.00
BC 111		200	82.2	82.4	1.04
BC 34		200	84.0	98.0	1.09
BC 112		400	57.3	64.8	1.00
BC 113	↓	400	54.0	61.1	1.06
BC 71	1200/1→315/10 min	280	62.8	62.8	1.00
BC 72	↓	280	59.1	59.1	1.00
BC 54	1200/1→315/60 min	AQ	46.7	67.8	1.15*
BC 55		200	61.6	82.5	1.12*
BC 73		280	66.0	68.4	1.14*
BC 74		350	54.7	-	1.09
BC 75		400	-	-	-
BC 76	↓	400	39.5	39.5	1.00
BC 77	1200/1→260/3 min	AQ	-	-	-
BC 78		200	63.7	64.2	1.03
BC 79		200	61.6	61.6	1.03
BC 80	↓	280	73.6	74.8	1.06
BC 81	1200/1→260/30 min	AQ	64.2	65.0	1.05
BC 82		200	82.0	82.4	1.02
BC 83		200	84.3	85.3	1.04
BC 84		280	78.6	-	1.10
BC 85		350	51.1	51.1	1.00

Table VI (cont'd) Room Temperature Longitudinal Fracture Toughness Data for Alloy 300 M

Specimen I.D.	Austenitizing** Treatment °C/hr	Tempering Temperature °C(1 hr)	K_{Ic} ksi-in $^{1/2}$	K_{max} ksi-in $^{1/2}$	Pm/PQ
BC 86	1200/1 → 260/30 min	400	40.7	40.7	1.00
BC 87	1200/1 → 200/30 min	AQ	-	-	-
BC 88		200			
BC 89		200			
BC 90		280			
BC 91		350			
BC 92		400			
BC 93	1200/1 → 200/60 min	AQ	44.5	46.3	1.03
BC 94		200	56.5	62.6	1.02
BC 95	200	59.3	61.4	1.02	
BC 96		280	72.1	103.1	1.07
BC 97		350	45.7	45.7	1.00
BC 98		400	42.1	42.1	1.00
BC 99		400	40.8	40.8	1.00
BC 53	870/1 → 315/3 min	200	67.3	74.2	1.01
BC 50	870/1 → 315/60 min	AQ	43.2	50.9	1.07
BC 51		200	60.7	73.2	1.07

* exceeds maximum allowable value, 1.10, for valid K_{Ic} test

** 870/1 hr. refers to a one hour hold at 870°C followed by oil quenching
 1200/1 hr → 1100/10 min. refers to a one hour hold at 1200°C followed by step quenching to 1100°C for 10 minutes followed by oil quenching.

Table VIII Fracture Toughness versus Heat Treatment for Alloy 300M

Austenitizing Temperature °C (for 1 hour)	Intermediate Holding Temperature °C	Final Tempering Temperature °C (for 1 hour)	Plane Strain Fracture Toughness K_{Ic} (Average Values)			
			Hold Time at Intermediate Temperatures			
315	As quenched	45,570				53,740*
		175	64,300			
		200	83,120			69,000*
		280	60,970			75,300
		350				54,730
	As quenched	400	57,340			39,500
						64,250
		200	62,650			83,190
		280	73,630			78,550
		350				51,130
6 1200	As quenched	400				40,710
						44,540
		200	62,850			57,900
		280	65,570			72,080
		350	50,130			45,720
200	As quenched	400	64,840			41,440
						43,200
		315	200	67,260		60,730
870	As quenched					

*Possible error in heat treatment process, additional samples to be tested.

Table VIII (cont'd) Fracture Toughness versus Heat Treatment for Alloy 300M

Austenitizing Temperature °C (for 1 hour)	Intermediate Holding Temperature °C (for 1 hour)	Final Tempering Temperature °C (for 1 hour)	Plane Strain Fracture Toughness K_{Ic} (Average Values)					
			1 min	3 min.	10 min.	30 min.	60 min.	
As quenched								
1100	125			80,170			65,000*	
	175	91,370		71,330				
	200	85,710		89,410			83,890	
1200	280			85,890				
	350	84,900		63,600				
As quenched								
1000	175		67,310		78,000			
	200	80,900		87,250				
		81,670						
As quenched								
870	315	39,890	39,890	60,370				
	175	52,180	52,180	72,290	51,010			
	200			71,130		57,880		
	280			71,530		63,460		

TABLE IX. Heat Treatment Code for Figure 28, Alloy 4340

<u>Heat Treatment</u>	<u>Code #</u>
870/1	1
1100/1	2
1150/1	3
1200/1	4
1200/1 → 1100/10 min	5
1200/1 → 1100/60 min	6
1200/1 → 1000/30 min	7
1200/1 → 870/30 min	8
1200/1 → 350/1 min	9
1200/1 → 335/3 min	10
1200/1 → 335/5 min	11
1200/1 → 335/10 min	12
1200/1 → 335/30 min	13
1200/1 → 335/60 min	14
1200/1 → 315/3 min	15
1200/1 → 300/5 min	16
1200/1 → 300/60 min	17
1200/1 → 275/30 min	18
1200/1 → 275/60 min	19
1200/1 → 250/60 min	20

Table X Heat Treatment Code for Figure 29, Alloy 300M

<u>Heat Treatment</u>	<u>Code #</u>
870/1 hr	1
1100/1 hr	2
1200/15 min	3
1200/30 min	4
1200/1 hr	5
1200/1 → 870/1/2 hr.	6
1200/1 → 315/3 min	7
1200/1 → 315/1 hr.	8
1200/1 → 260/3 min	9
1200/1 → 260/30 min	10
1200/1 → 200/3 min	11
1200/1 → 200/1 hr.	12
870/1 → 315/3 min	13
870/1 → 315/1 hr	14

TABLE XI Heat Treatment and Distinguishing Microstructural Parameters

<u>Solution Treatment</u>	<u>Characteristic Substructures</u>
<u>4340</u>	
1. 870°C/1 hr	Lath martensite and twinned plate martensite
2. 1200°C/1 hr	Predominant lath martensite and inter lath retained austenite.
3. 1200°C/1 hr → 1100°C/1 hr	Lath martensite + twinned plate martensite + blocky martensite + retained austenite
4. 1200°C/1 hr → 870°C/1 hr	Lath martensite + extensively twinned plate martensite and blocky martensite + retained austenite
5. 1200°C/1 hr → 275°C/1 hr	Lower bainite + lath martensite + twinned plate martensite + blocky martensite + retained austenite
<u>300M</u>	
6. 870°C/1 hr	Extensive twinning, lath and blocky martensite little retained austenite
7. 1200°C/1 hr	Lath martensite + blocky twinned martensite + interlath retained austenite
8. 1200°C/1 hr → 870°C/30 min	Lath + twinned martensite and retained austenite

Table XII Auger Electron Spectroscopy Test Specimen Conditions

Spec #	Heat Treatment		Quench	Fracture Temperature
	Soln.	Treatment		
A1	870°C/1 hr		H ₂ O	R.T.
A2	870°C/1 hr		IBQ	-90°C
B1	1200°C/1 hr		H ₂ O	R.T.
B2	1200°C/1 hr.		IBQ	-90°C
C1	1200°C/1 hr. → 870°C/1/2 hr		H ₂ O	R.T.
C2	1200°C/1 hr. → 870°C/1/2 hr		IBQ	-90°C
D1	1200°C/1 hr. → 870°C/1 hr.		H ₂ O	R.T.
E1	1200°C/1 hr → 1100°C/1 hr.		H ₂ O	R.T.
E2	1200°C/1 hr → 1100°C/1 hr.		IBQ	-90°C

Table XIII

HEAT TREAT 1200C 1HR H2O QUENCH 7/8/77, SAMPLE #1 SPUTTER #1 RUN#1

HEAT TREAT 1200C 1HR H2O QUENCH 7/8/77, SAMPLE #1 SPUTTER #1 RUN#1				
ELEMENT	PEAK EV	PEAK HEIGHT	%OF ELEMENT	SENSITIVITY
P	120	0.10	0.07	0.4730
S	152	3.10	0.80	1.2981
CL	181	1.60	1.01	0.5350
C	272	6.00	20.67	0.1106
N	301	1.40	1.29	0.3645
O	510	16.00	5.37	1.0204
FE	703	47.00	69.60	0.2270
NI	848	0.90	1.19	0.2550

HEAT TREAT 1200C 1HR H2O QUENCH 7/8/77, SAMPLE #1 SPUTTER #1 RUN#2

HEAT TREAT 1200C 1HR H2O QUENCH 7/8/77, SAMPLE #1 SPUTTER #1 RUN#2				
ELEMENT	PEAK EV	PEAK HEIGHT	%OF ELEMENT	SENSITIVITY
P	120	0.10	0.08	0.4730
S	152	2.40	0.72	1.2981
CL	181	1.10	0.80	0.5350
C	272	6.60	23.14	0.1106
N	301	1.10	1.17	0.3645
O	510	12.00	4.56	1.0204
FE	703	40.00	68.32	0.2270
NI	848	0.80	1.22	0.2550

HEAT TREAT 1200C 1HR H2O QUENCH 7/8/77, SAMPLE #1 SPUTTER #1 RUN#3

HEAT TREAT 1200C 1HR H2O QUENCH 7/8/77, SAMPLE #1 SPUTTER #1 RUN#3				
ELEMENT	PEAK EV	PEAK HEIGHT	%OF ELEMENT	SENSITIVITY
P	120	0.80	0.80	0.4730
S	152	1.80	0.58	1.2981
CL	181	0.80	0.63	0.5350
C	272	6.20	23.57	0.1106
N	301	1.00	1.15	0.3645
O	510	10.60	4.37	1.0204
FE	703	37.00	68.54	0.2270
NI	848	0.70	1.15	0.2550

HEAT TREAT 1200C 1HR H2O QUENCH 7/8/77, SAMPLE #1 SPUTTER #1 RUN#4

HEAT TREAT 1200C 1HR H2O QUENCH 7/8/77, SAMPLE #1 SPUTTER #1 RUN#4				
ELEMENT	PEAK EV	PEAK HEIGHT	%OF ELEMENT	SENSITIVITY
P	120	0.10	0.09	0.4730
S	152	1.70	0.58	1.2981
CL	181	0.80	0.66	0.5350
C	272	6.10	24.26	0.1106
N	301	0.90	1.09	0.3645
O	510	10.00	4.31	1.0204
FE	703	35.00	67.81	0.2270
NI	848	0.70	1.21	0.2550

BEST AVAILABLE COPY

Figure

- 1 Tensile properties of 4340 vs. heat treatment
- 2 " " " " "
- 3 " " " " "
- 4 " " " " "
- 5 " " " " "
- 6 Tensile properties of 300M vs. heat treatments
- 7 " " " " "
- 8 " " " " "
- 9-18 Plane strain fracture toughness vs. heat treatment for alloy 4340
- 19-23 " " " " " " " " " " 300M
- 24 Plane strain fracture toughness of 4340 vs 300M after a solution treatment of $870^{\circ}\text{C}/1\text{ hr.}$
- 25 Plane strain fracture toughness of 4340 and 300M after a solution treatment of $1200^{\circ}\text{C}/1\text{ hr.}$
- 26-27 Plane strain fracture toughness of 4340 vs ultimate strength for several solution treatments.
- 28 Plane strain fracture toughness of 4340 vs ultimate strength and heat treatment.
- 29 Plane strain fracture toughness of 300M vs ultimate strength and heat treatment.
- 30 Effect of tempering on the load vs COD gage curve for alloy 4340 solution treated at 1200°C.
- 31 Effect of solution treatment temperature on the load vs COD gage curve for alloy 4340 tempered at 200°C.
- 32 Acoustic emission test system
- 33-35 Acoustic emission vs COD gage opening for 3 different heat treatments.

Figure

36-37 Acoustic emission vs applied stress intensity for several heat treatments.

38 Charpy-V-Notch toughness vs tempering temperature for an 870°C/1 hr treatment.

39 " " " " " " " " " " " " " " 1200°C/1 hr treatment.

40 " " " " " " " " " " " " " " 1200°C/1 hr - 1100°C/1 hr treatment.

41 Optical Micrographs
(a) - as received 4340
(b) - as received 300M

42 Optical Micrographs
300M (a) - 870°C/1 hr, as quenched
(b) - 1200°C/1 hr, as quenched

43 Optical Micrographs
4340 (a) 1200/1 hr → 870/30 min, A.Q.
(b) 1200/1 hr → 335/3 min., A.Q.
(c) 1200/1 hr → 335/60 min, A.Q.

44 Optical Micrographs
300M (a) 870/1 hr → 315/3 min, A.Q.
(b) 870/1 hr → 315/60 min, A.Q.
(c,d) 1200/1 hr → 315/60 min, A.Q.

45 Transmission electron micrographs, 4340, 1200°C/1 hr + 200°C temper
(a) Bright field micrograph
(b) Dark field of area shown in (a) showing distribution of retained austenite
(c) SAD pattern from (a)
(d) Analysis of SAD shown in (c)

46 Transmission electron micrographs; 4340
1200°C/1 hr → 1100°C/30 min. + 200°C temper
(a) bright field

Figure

46(cont'd)

1200°C/1 hr → 1100°C/60 min + 200°C temper

(b) bright field

(c) dark field of area shown in (b) showing distribution of retained austenite

47 Transmission electron micrographs; 4340; 1200°C/1 hr → 1100°C/60 min + 200°C temper.

(a) Bright field showing lath, A, and blocky, B, martensite

(b) Bright field showing lath, A, and blocky, B, martensite; arrows show a pocket of laths inside the blocky martensite

(c-d-e) Dark field micrographs showing fine twins within the blocky martensite labelled B in (b)

(f) Bright field showing martensite plates with carbides and twins

(g) Dark field of twins within the plates shown in (f)

(h) Composite showing blocky martensite along prior austenite grain boundary.

48 Transmission electron micrographs; 4340 1200°C/1 hr → 870°C/30 min. 200°C temper

(a) Bright field

(b) Dark field showing the presence of twins

(c-d) Dark fields demonstrating the extensive twins present throughout the structure

(e) Bright field composite of twins

49 Transmission electron micrograph; 4340; 1100°C/1 hr + 200°C temper
Bright field showing presence of twins

50 Transmission electron micrograph; 4340; 1200°C/1 hr → 275°C/60 min

(a) Bright field showing lower bainitic structure containing carbides within bainitic plates.

(b) SAD pattern from martensitic region revealing the presence of twins

51 Transmission electron micrograph; 300M; 870°C/1 hr.

(a) Bright field showing twins

(b) SAD pattern from (a)

52 Transmission electron micrographs; 300M; 1200°C/1 hr + 200°C temper

(a) Bright field

(b) Dark field of (a) showing the presence of retained austenite

(c) Bright field showing blocky martensite

(d) SAD of blocky martensite in (c) and indicating the presence of twins

Figure

53 Transmission electron micrographs; 300M; $1200^{\circ}\text{C}/1\text{ hr} \rightarrow 870^{\circ}\text{C}/30\text{ min}$

- (a) Bright field showing both lath and plate martensite
- (b) Bright field with apparent twins
- (c) Bright field showing lath martensite
- (d) SAD of region (c)
- (e) Dark field of region shown in (c) revealing the presence of retained austenite.

54 Transmission Electron micrographs, 300M; $870^{\circ}\text{C}/1\text{ hr} \rightarrow 350^{\circ}\text{C}/60\text{ min.}$

- (a) Bright field revealing upper bainite structure with extensive retained austenite present
- (b) Blocky and lath type martensite also present in this specimen

55 Scanning electron micrographs, 4340, $870^{\circ}\text{C}/1\text{ hr}$

- (a) As quenched
- (b) 200°C temper

56 Scanning electron micrographs, 4340, $1200^{\circ}\text{C}/1\text{ hr.}$

- (a-b) 175°C temper
- (c-d) 200°C temper

57 Scanning electron micrographs, 4340

- (a) $1200^{\circ}\text{C}/1\text{ hr} \rightarrow 1100^{\circ}\text{C}/60\text{ min}$
- (b) $1200^{\circ}\text{C}/1\text{ hr} \rightarrow 870^{\circ}\text{C}/30\text{ min}$

58 Scanning electron micrographs, 4340

- (a) $1200^{\circ}\text{C}/1\text{ hr} \rightarrow 335/1\text{ min} + 200^{\circ}\text{C}$ temper
- (b) $1200^{\circ}\text{C}/1\text{ hr} \rightarrow 335/3\text{ min} + 200^{\circ}\text{C}$ temper
- (c) $1200^{\circ}\text{C}/1\text{ hr} \rightarrow 335/60\text{ min} + 200^{\circ}\text{C}$ temper

59 Scanning electron micrographs, 4340

- (a) $1200^{\circ}\text{C}/1\text{ hr} \rightarrow 250/1\text{ hr}$
- (b) $870^{\circ}\text{C}/1\text{ hr} \rightarrow 225/1\text{ hr}$
- (c) $870^{\circ}\text{C}/1\text{ hr} \rightarrow 315/1\text{ hr}$

60 Scanning electron micrographs, 300M

- (a) $870^{\circ}\text{C}/1\text{ hr} + 200^{\circ}\text{C}$ temper
- (b-c) $1200^{\circ}\text{C}/1\text{ hr} + 200^{\circ}\text{C}$ temper

Figure

61 Scanning electron micrograph, 300M,
1200°C/1 hr → 315/1 hr + 200°C temper

62 Optical micrograph of nickel coated and sectioned fracture paths
(a) AC 72:1200°C/1 hr → 335/1 min + 200°C temper
(b) AC 75:1200°C/1 hr → 335/5 min + 200°C temper

63 Representative Auger electron spectroscopy analysis revealing the presence of P, S, Cl, as well as C, N, O, Fe, Ni. Specimen was broken in air and hence C and O contamination was present.

64 Average atomic percent of elements present on fracture surface of alloy 4340 after solution treating at 870°C followed by ice brine quenching.

65 Average atomic percent of elements present on fracture surface of alloy 4340 after a 1200°C/1 hr → 1100°C/1 hr solution treatment followed by ice brine quenching.

66 Average atomic percent of elements present on fracture surface of alloy 4340 after a 1200°C/1 hr solution treatment followed by ice brine quenching.

67 Average atomic percent of elements present on the fracture surface of specimens broken at room temperature, before sputtering, as a function of solution treatment.

68 Average atomic percent of elements present on the fracture surface of specimens broken at -90°C, before sputtering as a function of solution treatment.

69 Average atomic percent of elements present on the fracture surface of specimens broken at -90°C, after sputtering, as a function of solution treatment.

70 Average atomic percent of nickel and sulfur present on the fracture surface of specimens broken at -90°C before and after sputtering as a function of solution treatment.

71 Average atomic percent of chlorine present on the fracture surface of specimens broken at -90°C before and after sputtering, as a function of solution treatment.

Figure

72 Scanning electron micrographs of 4340 specimens solution treated at 870°C/1 hr.

- (a-b) Fractured at room temperature
- (c) Fractured at -90°C

73 Scanning electron micrographs of 4340 specimens solution treated at 1200°C/1 hr.

- (a-c) Fractured at room temperature
- (d-e) Fractured at -90°C

74 Scanning electron micrographs of 4340 specimens solution treated at 1200°C/1 hr → 870°C/30 min.

- (a) Fractured at room temperature
- (b-c) Fractured at -90°C

75 Scanning electron micrographs of 4340 specimens solution treated at 1200°C/1 hr → 1100°C/1 hr.

- (a) Fractured at room temperature
- (b) Fractured at -90°C

76 Plane strain fracture toughness of several alloys as a function of tensile strength

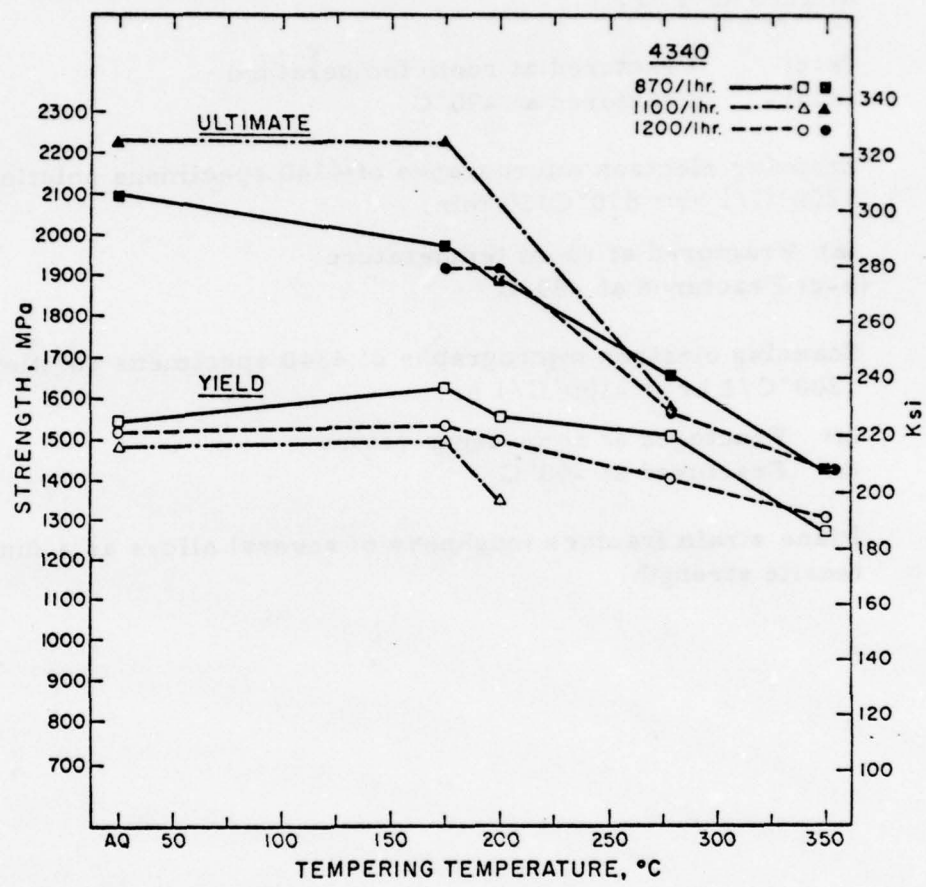


Figure 1

74

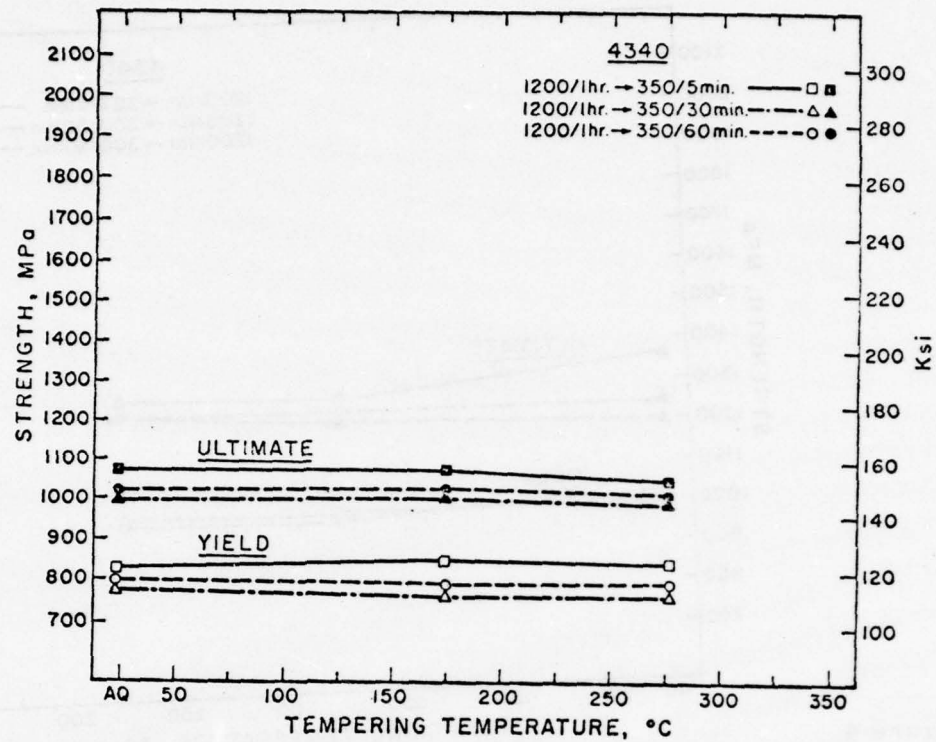


Figure 2

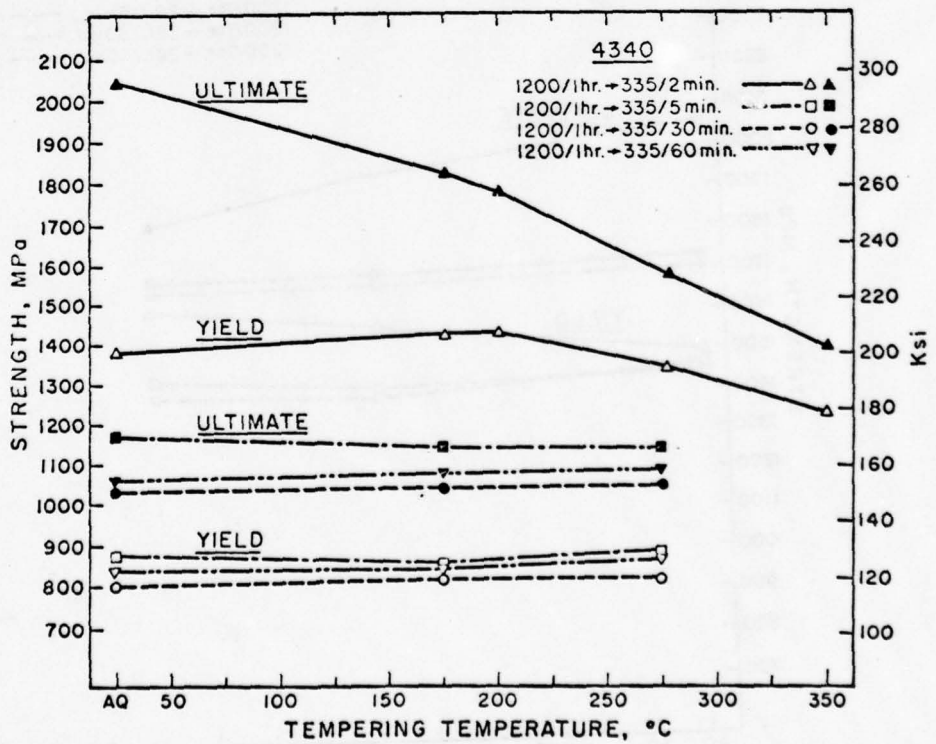


Figure 3

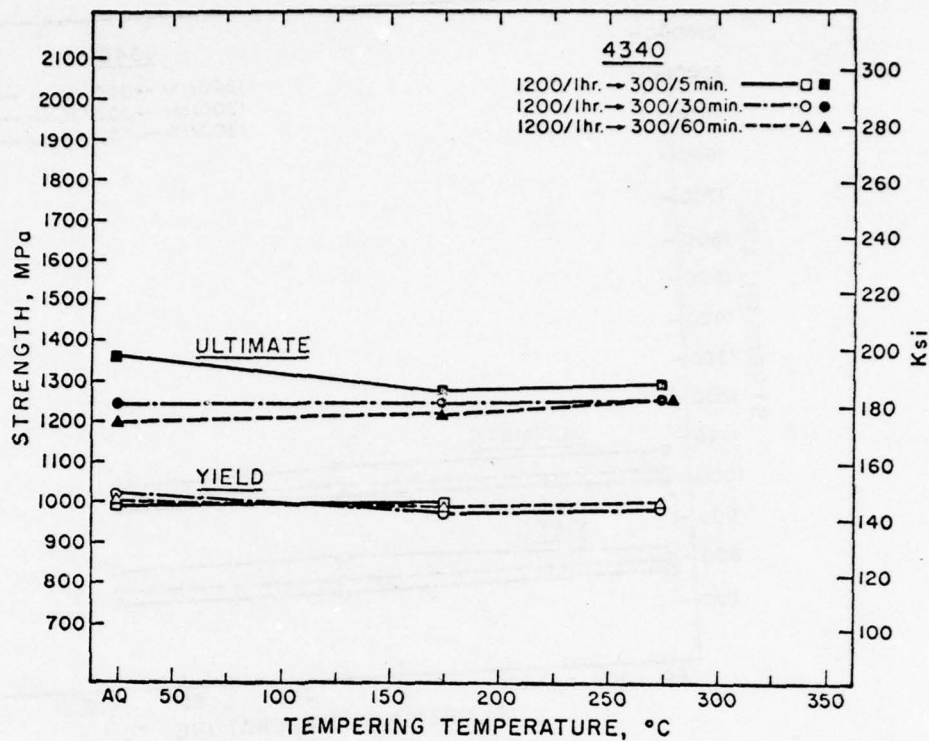


Figure 4

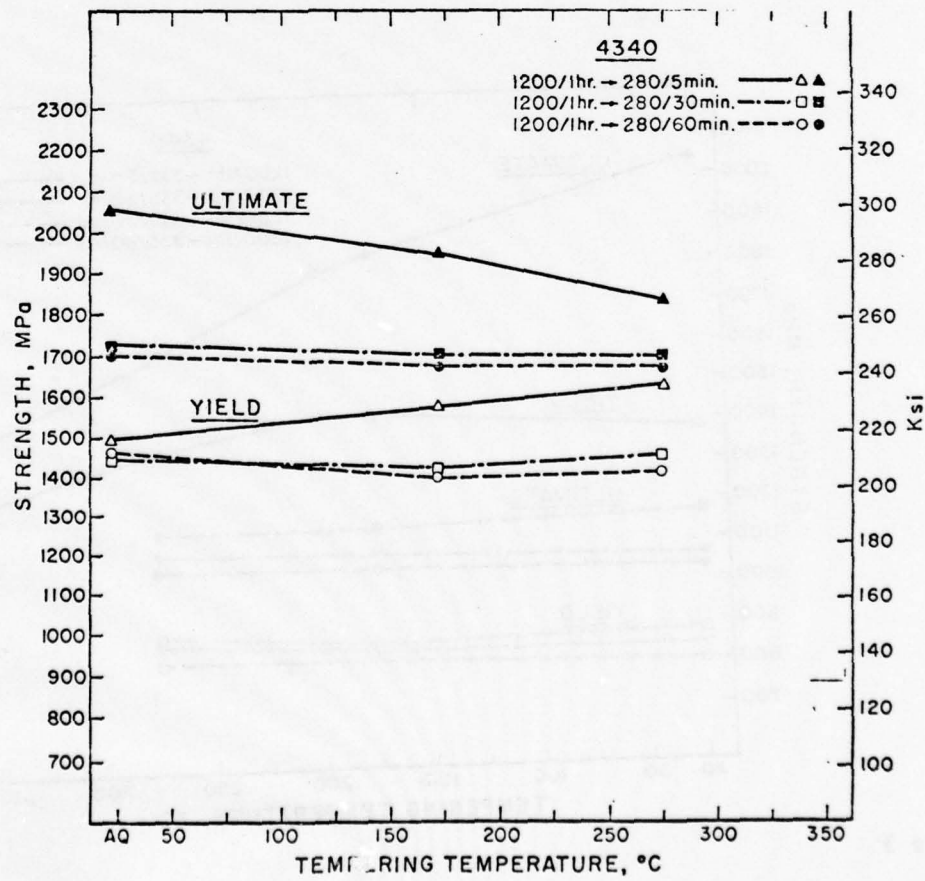


Figure 5

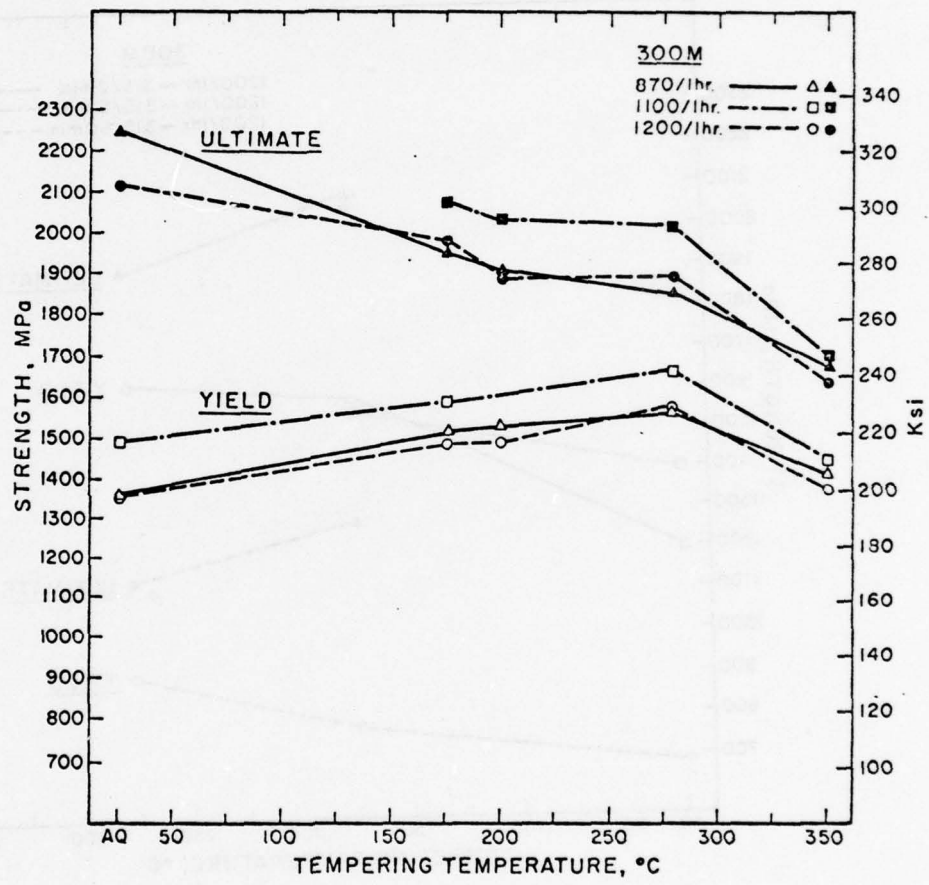


Figure 6

77

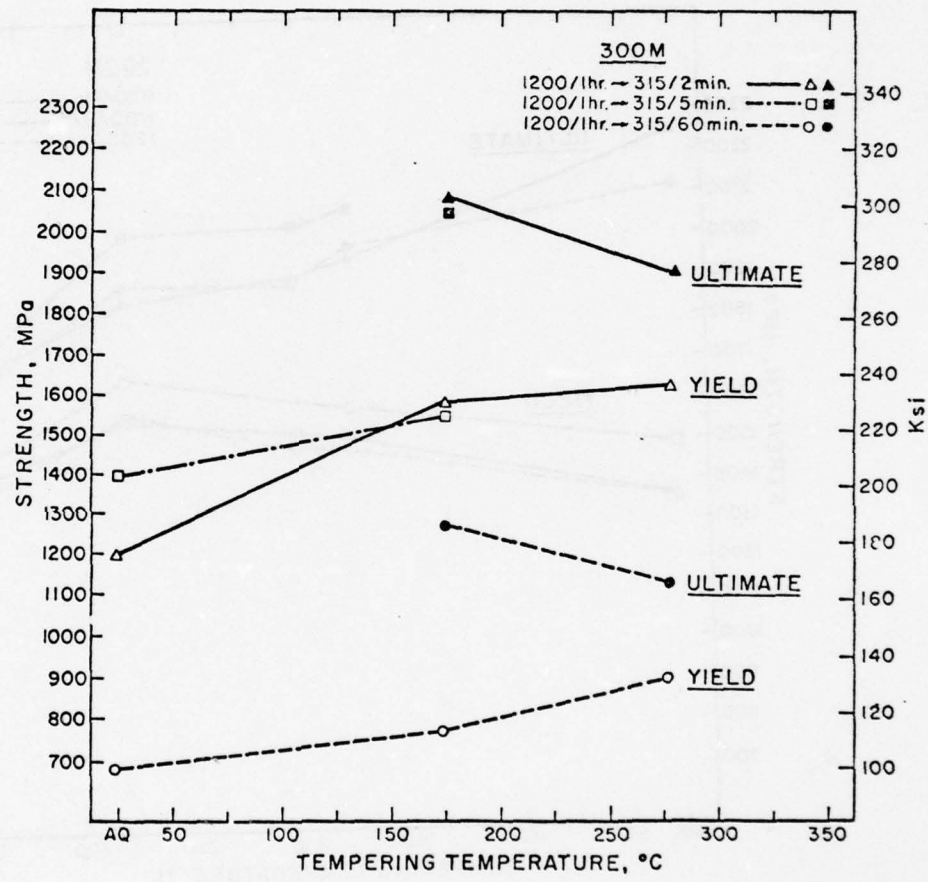


Figure 7

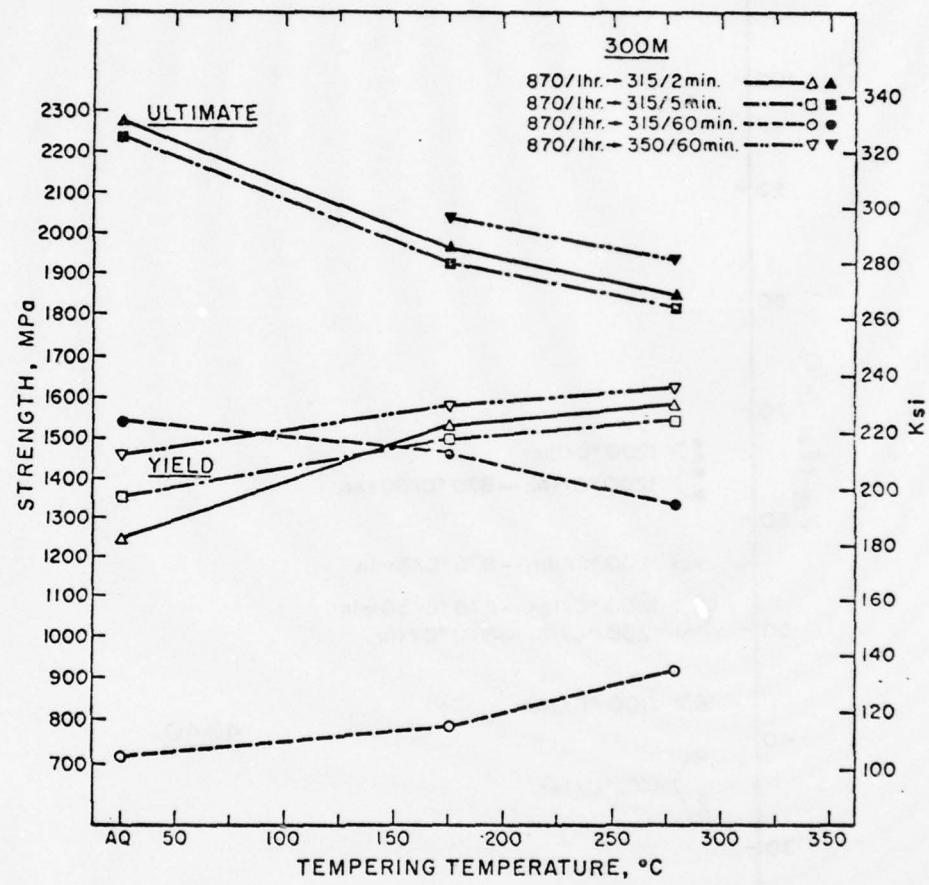


Figure 8

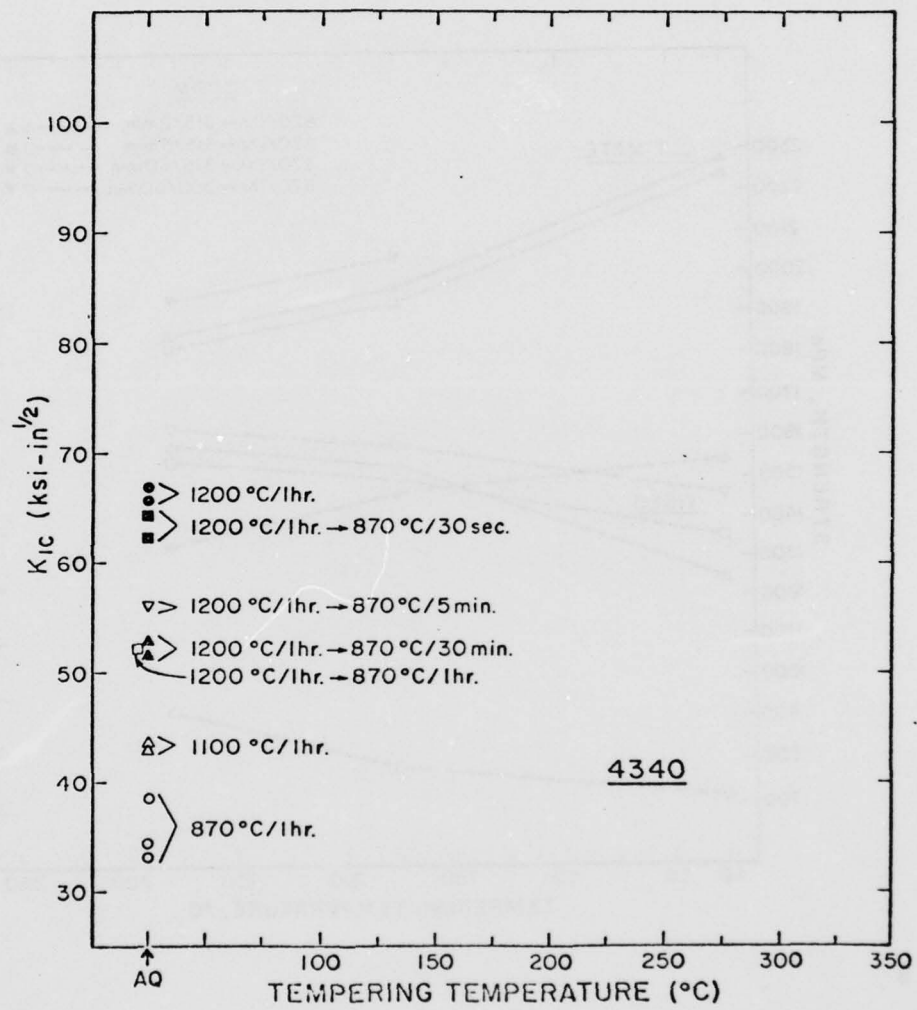


Figure 9

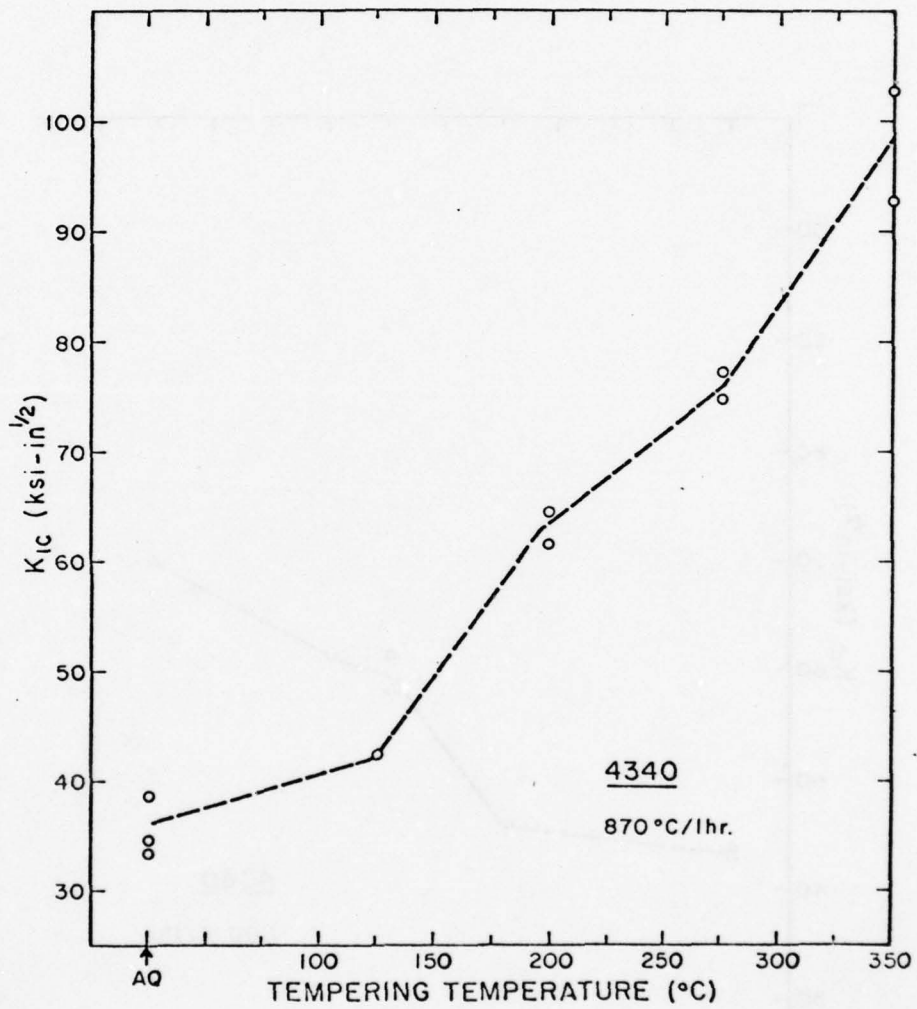


Figure 10

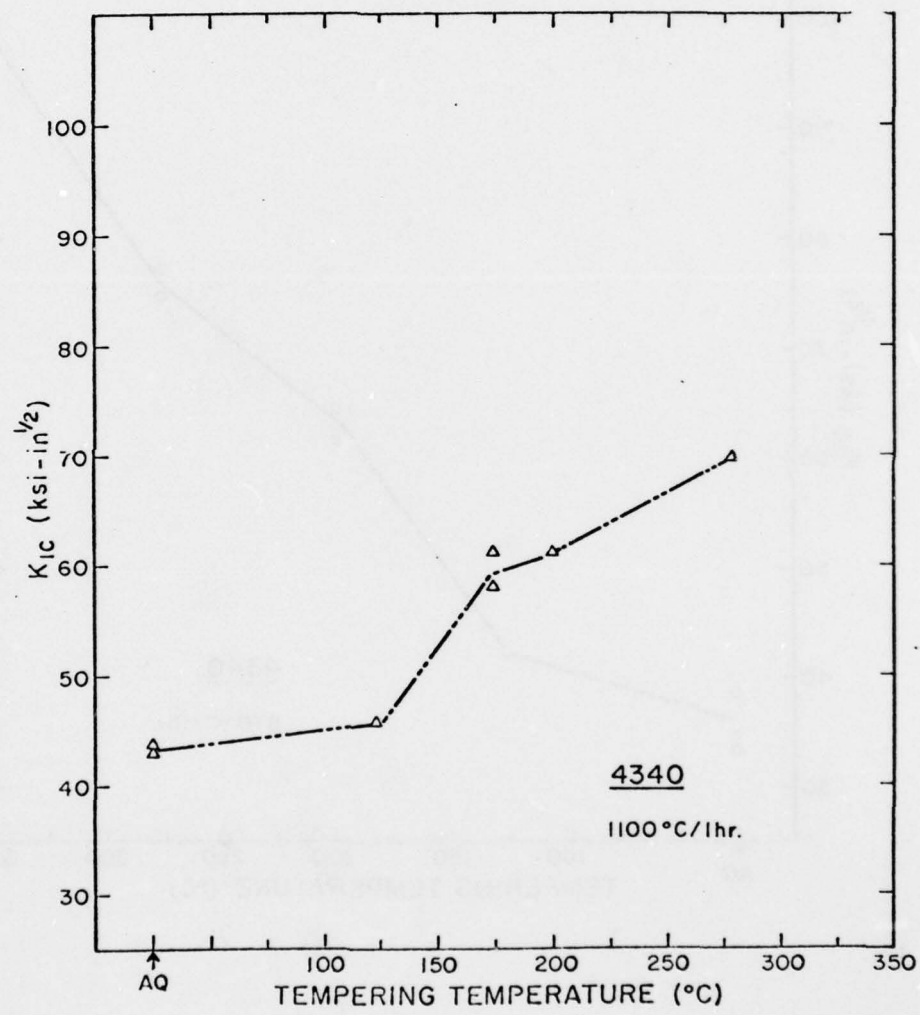


Figure 11

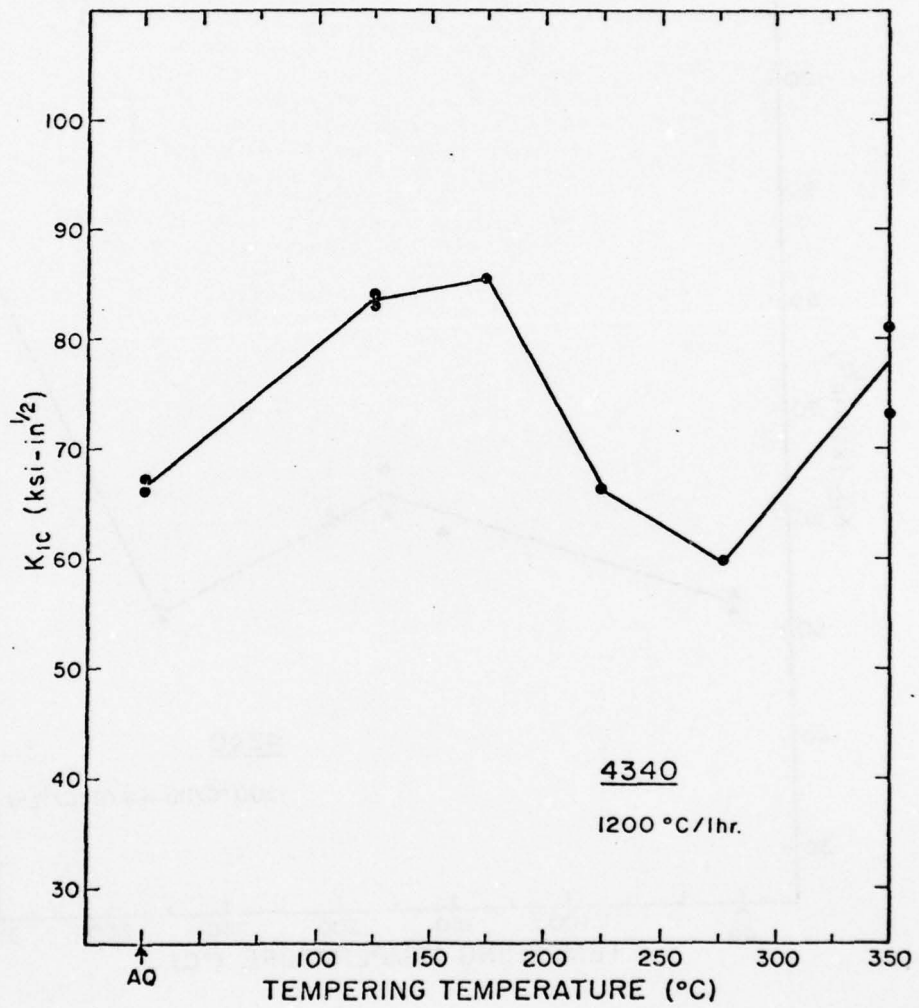


Figure 12

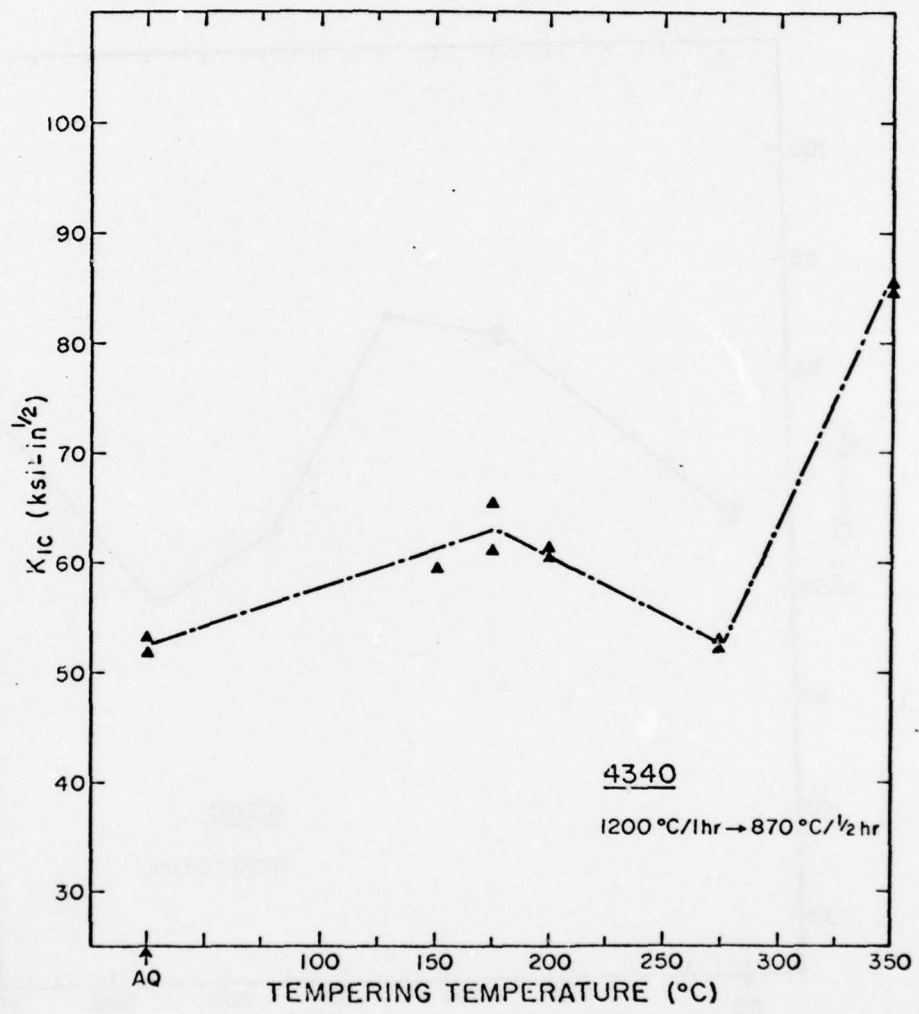


Figure 13

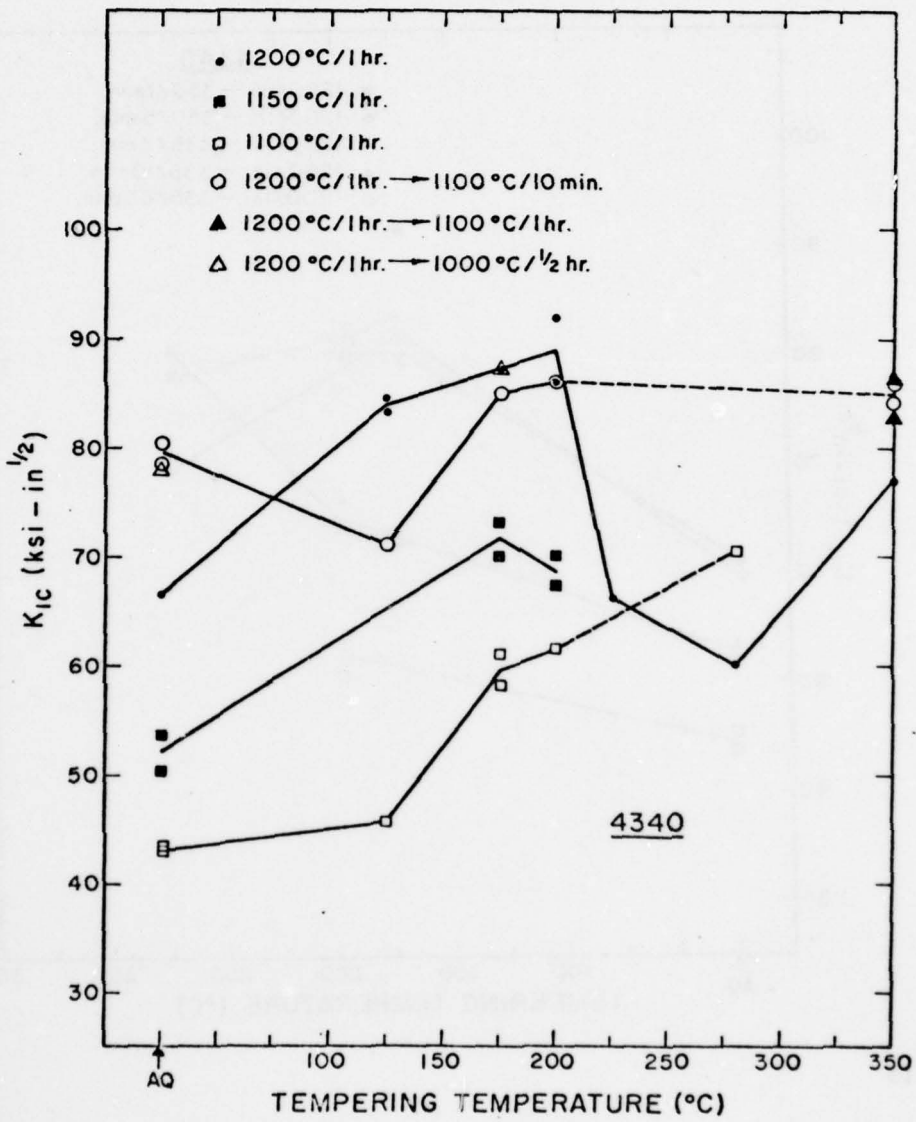


Figure 14

85

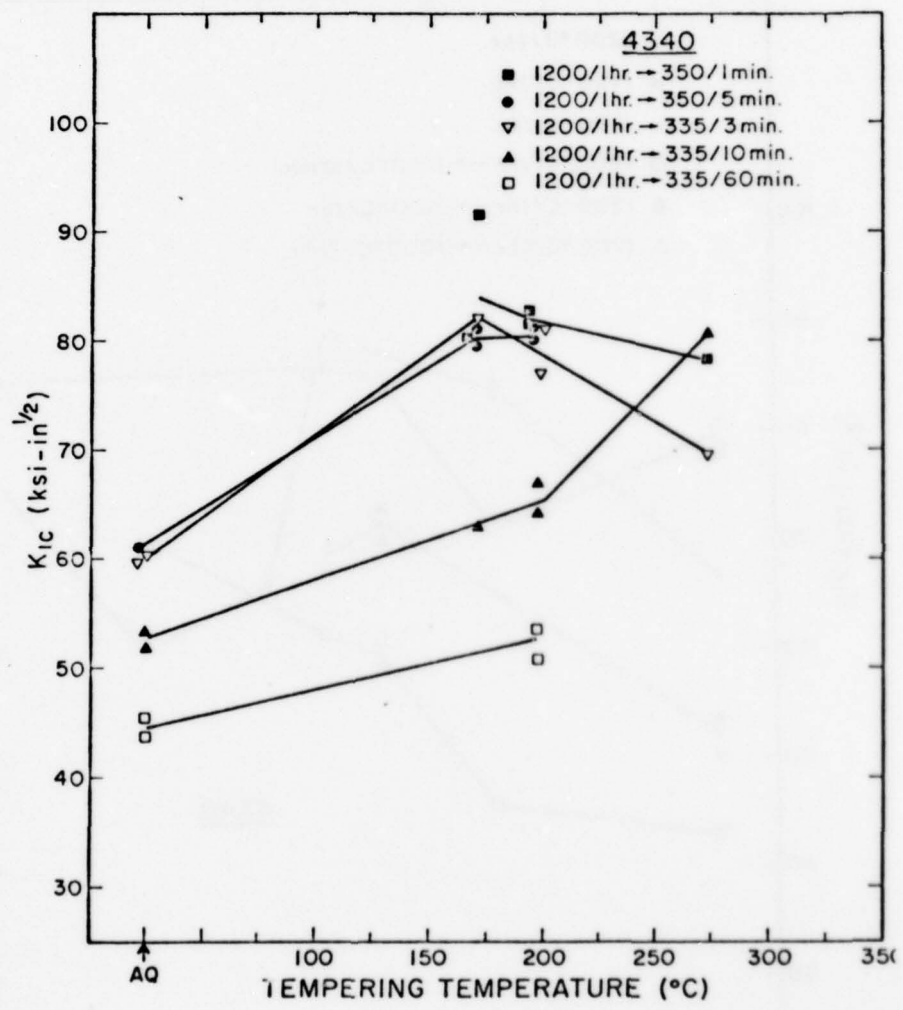


Figure 15

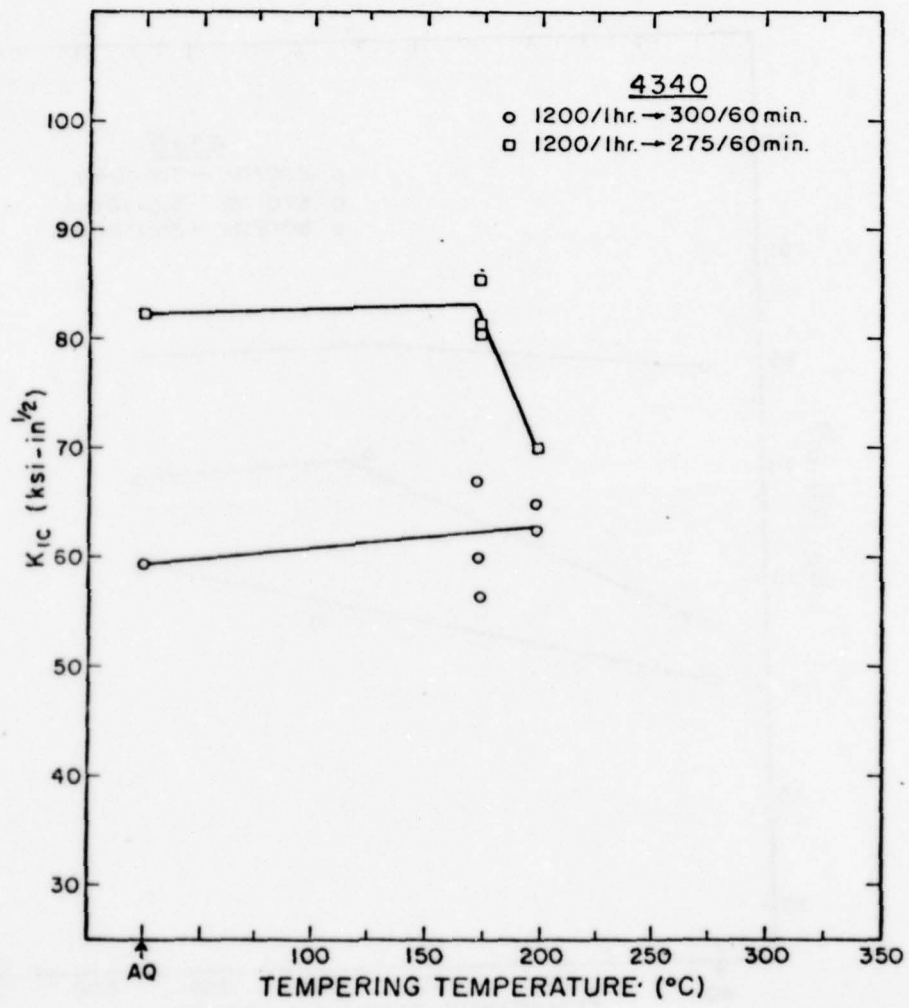


Figure 16

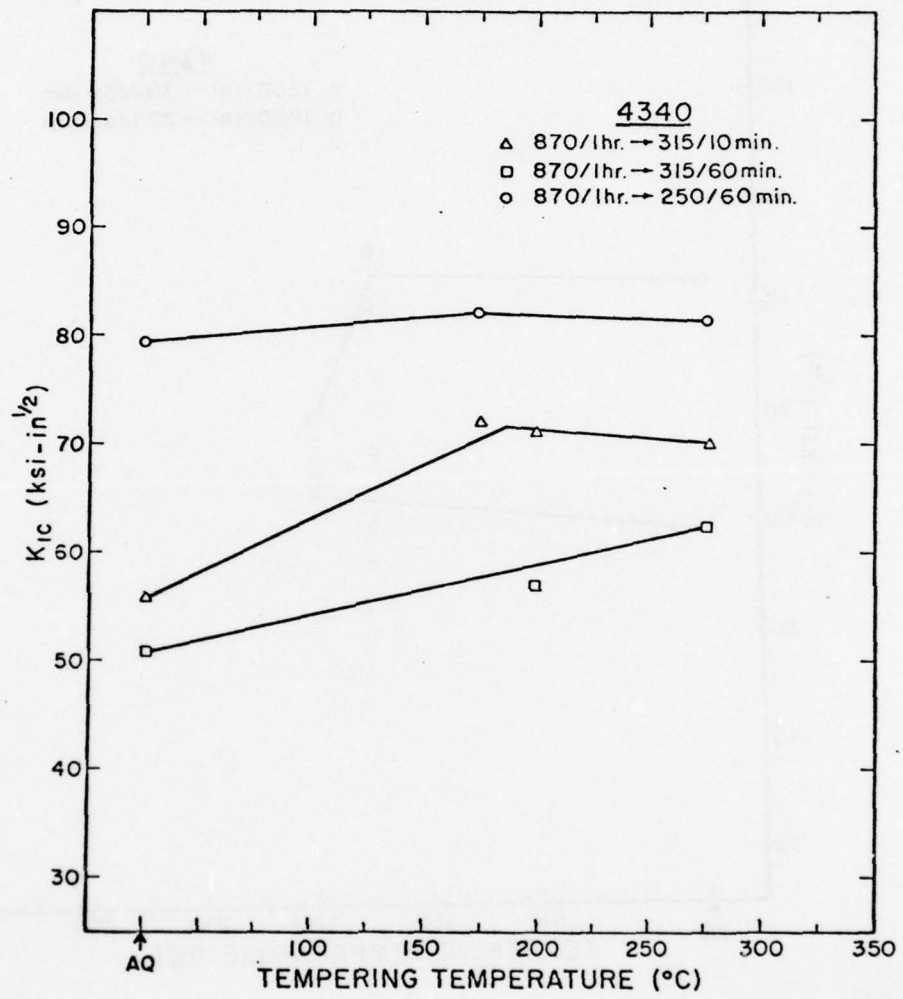


Figure 17

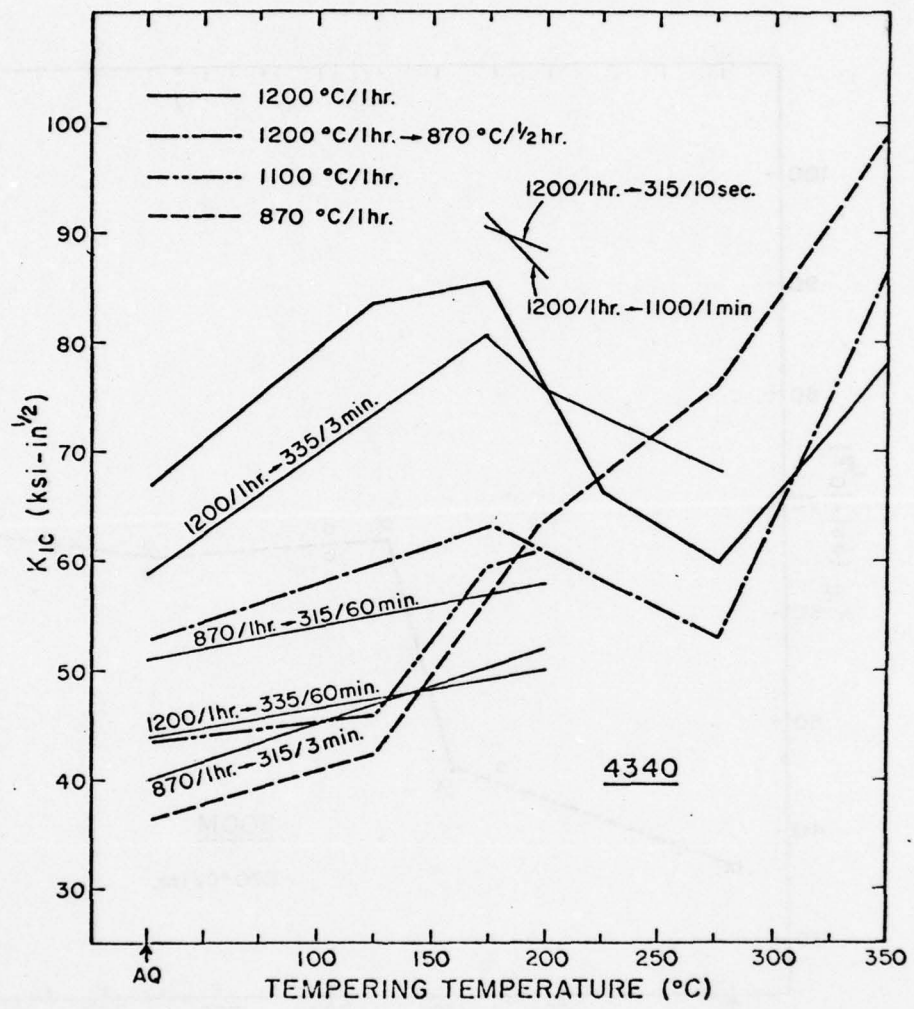


Figure 18

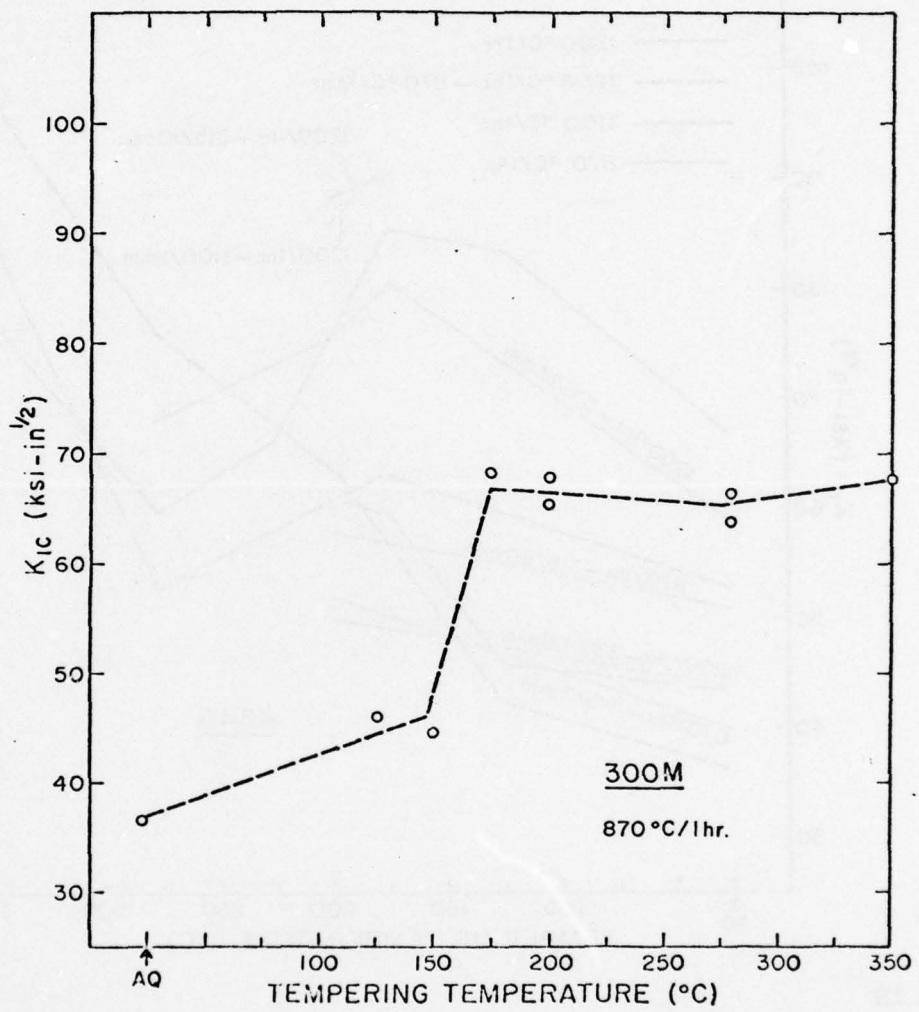


Figure 19

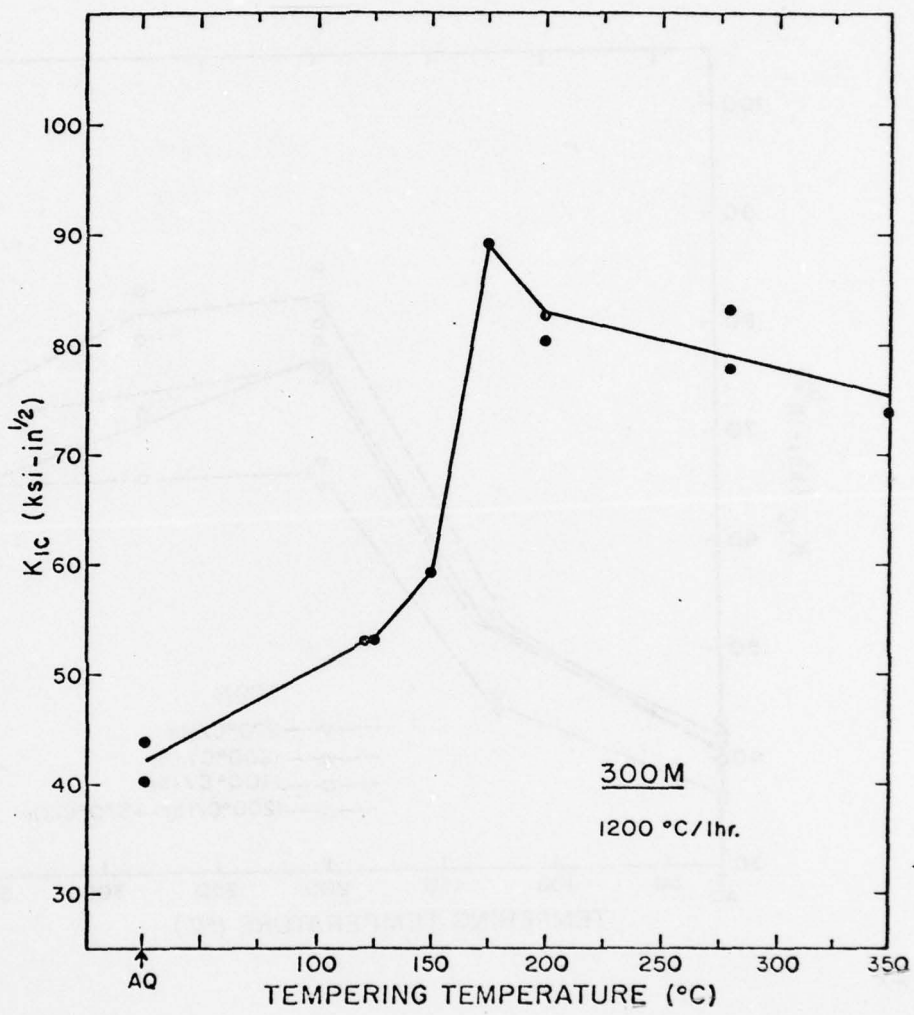


Figure 20

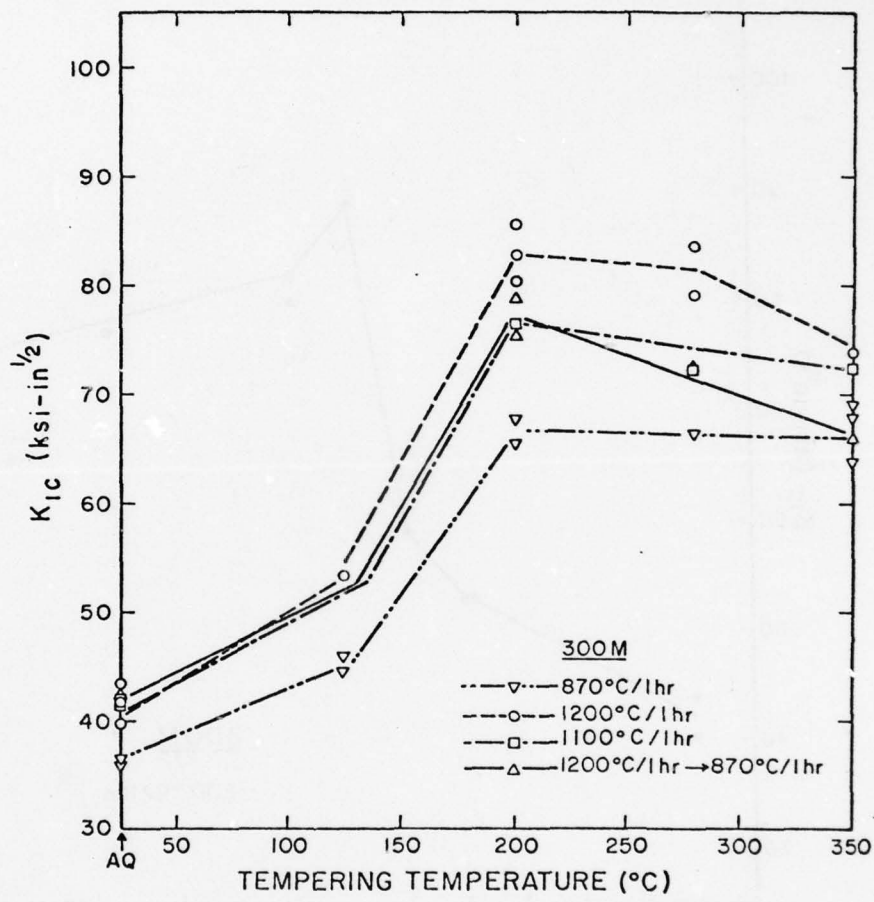


Figure 21

92

AD-A052 536

OREGON GRADUATE CENTER BEAVERTON
MECHANISM OF ENHANCED TOUGHNESS IN MARTENSITIC ALLOYS. (U)
FEB 78 W E WOOD

F/G 11/6

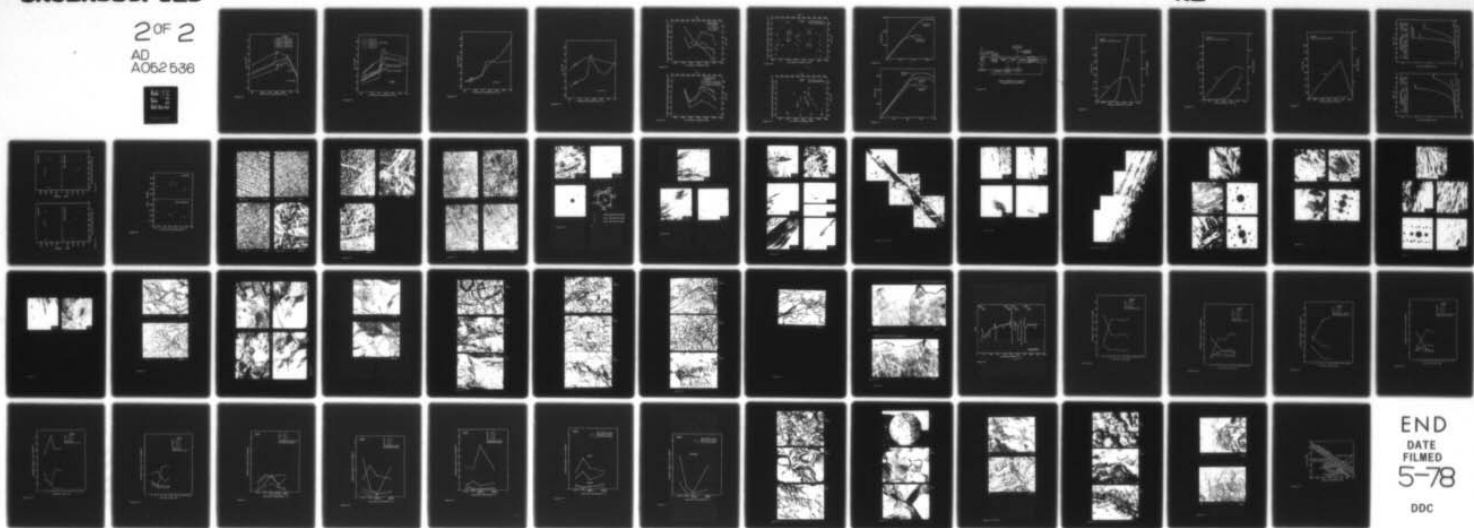
N00019-77-C-0135

NL

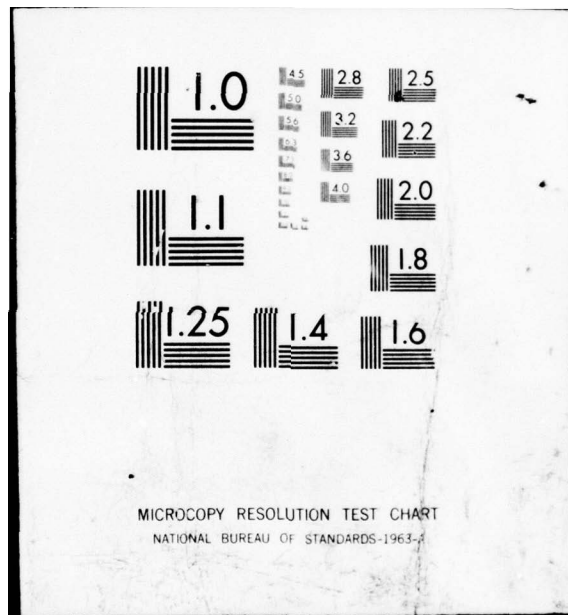
UNCLASSIFIED

2 OF 2
AD
A052 536

FFP



END
DATE
FILMED
5-78
DDC



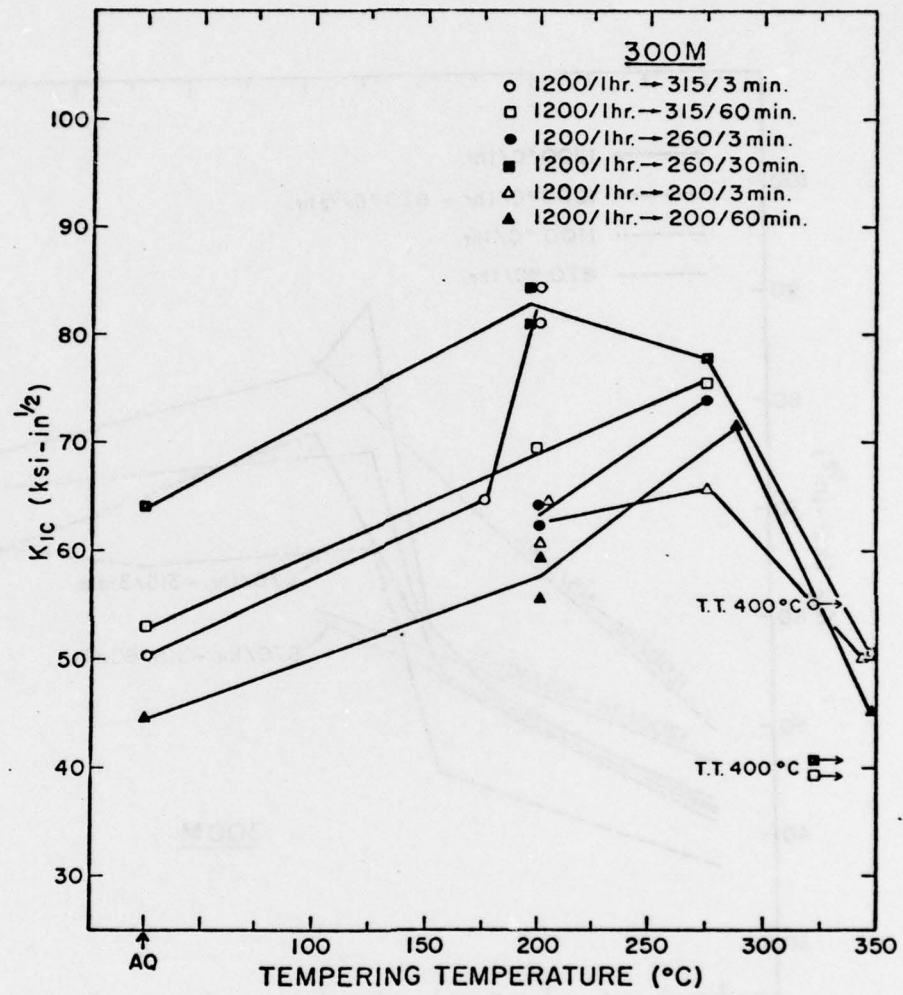


Figure 22

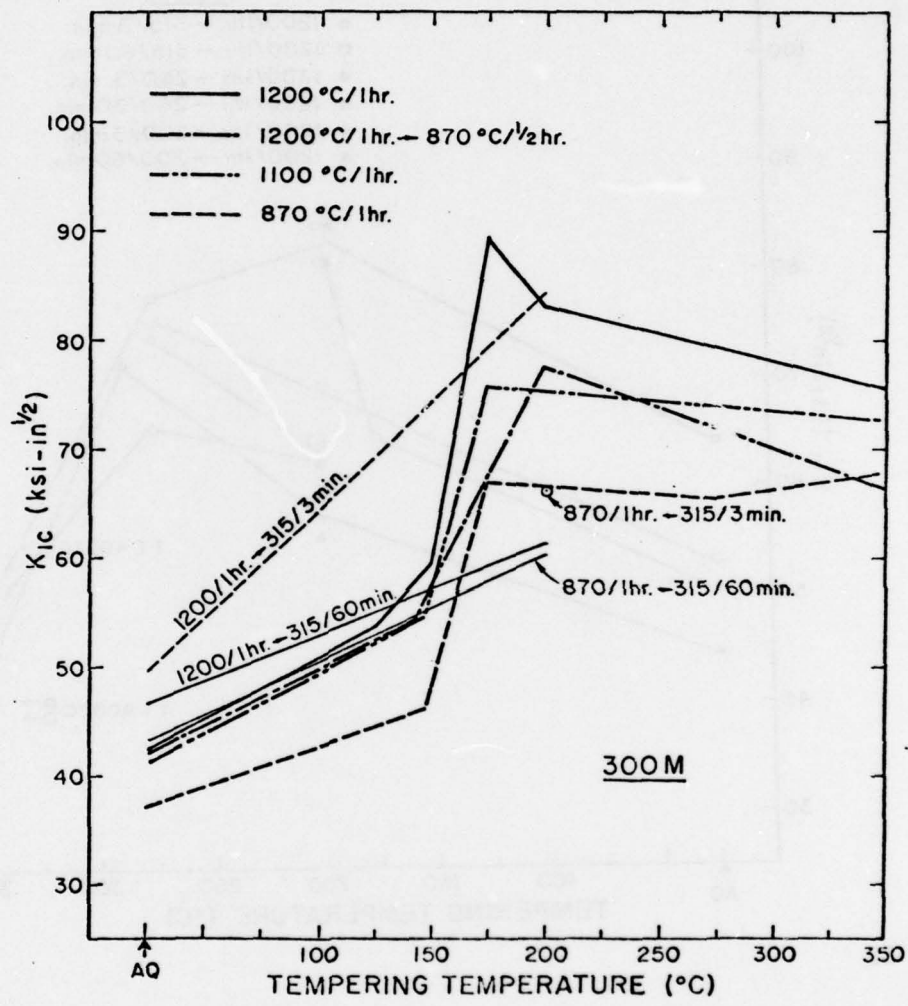


Figure 23

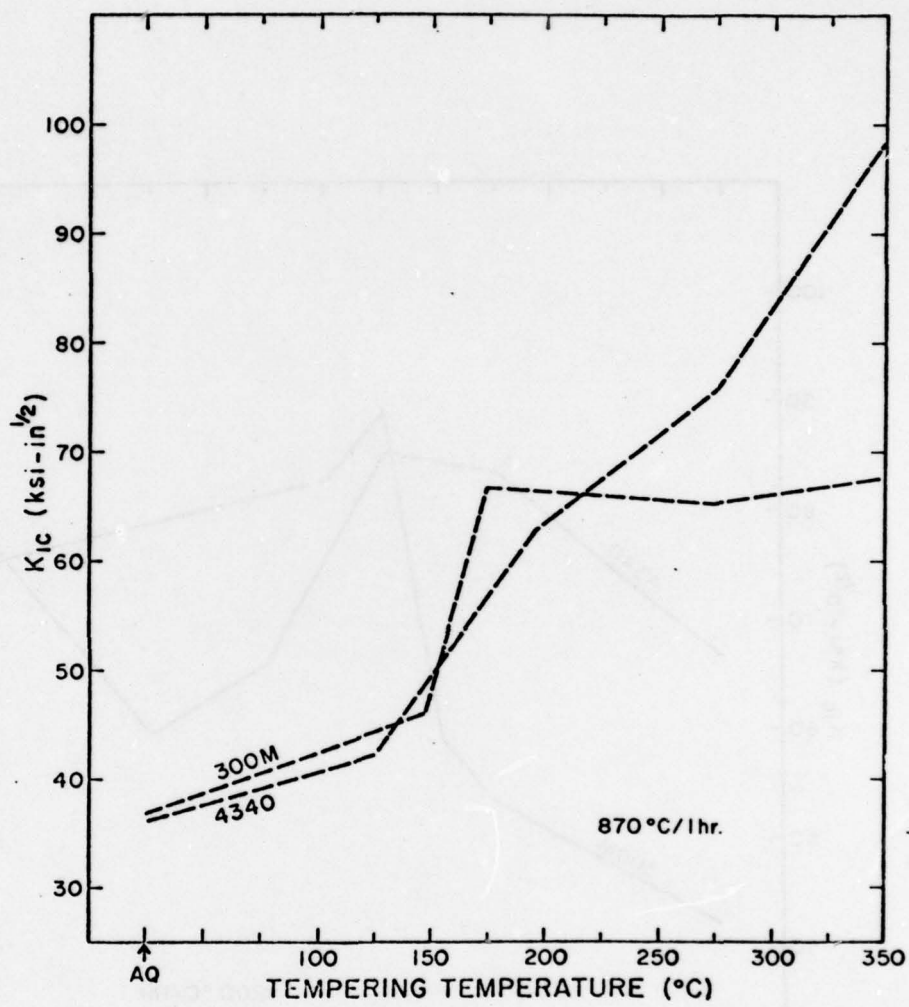


Figure 24

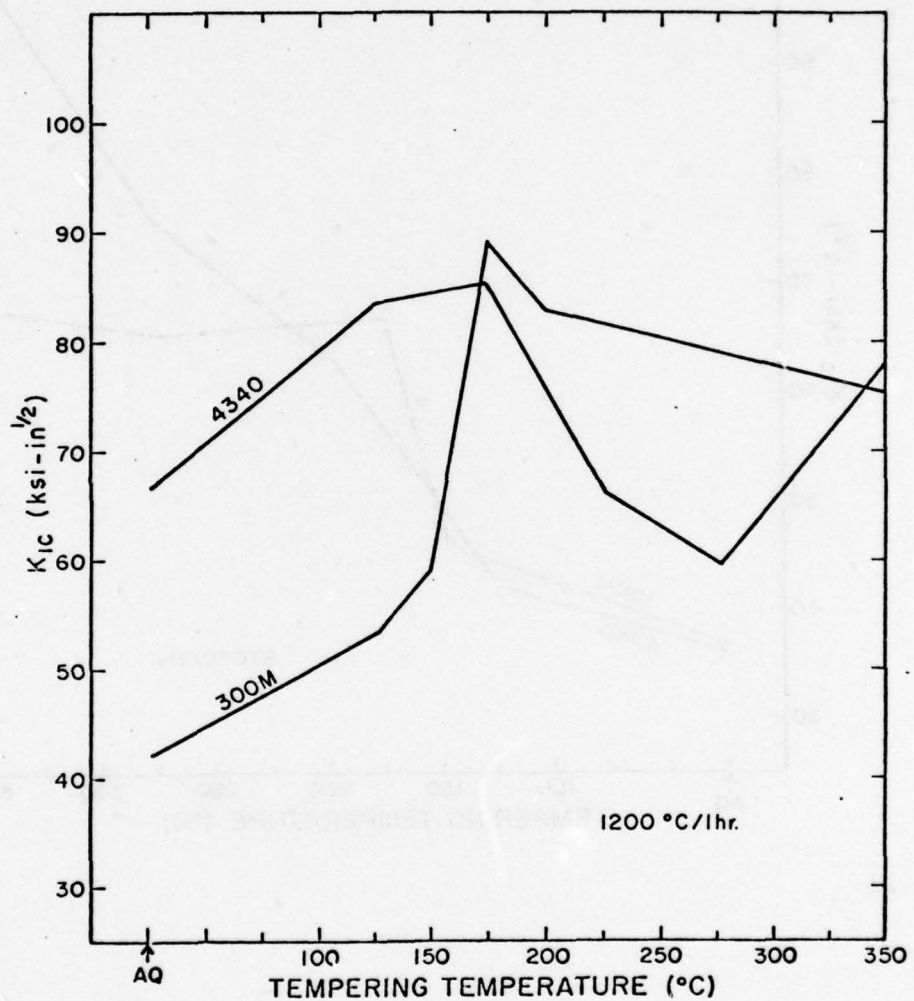


Figure 25

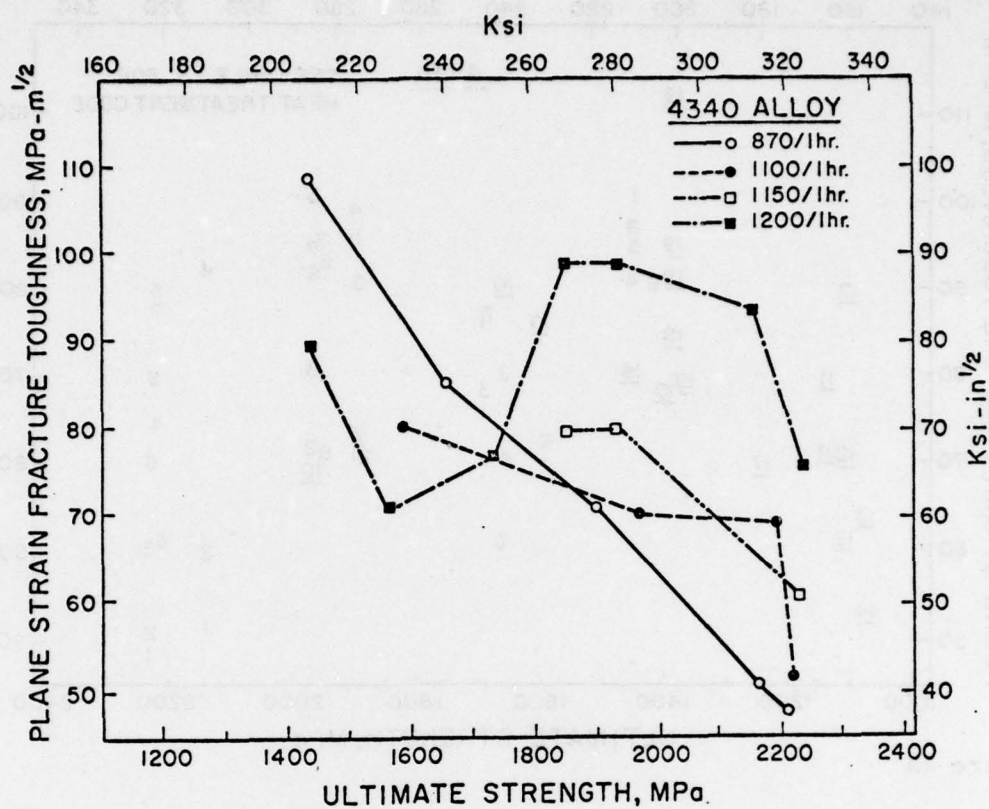


Figure 26

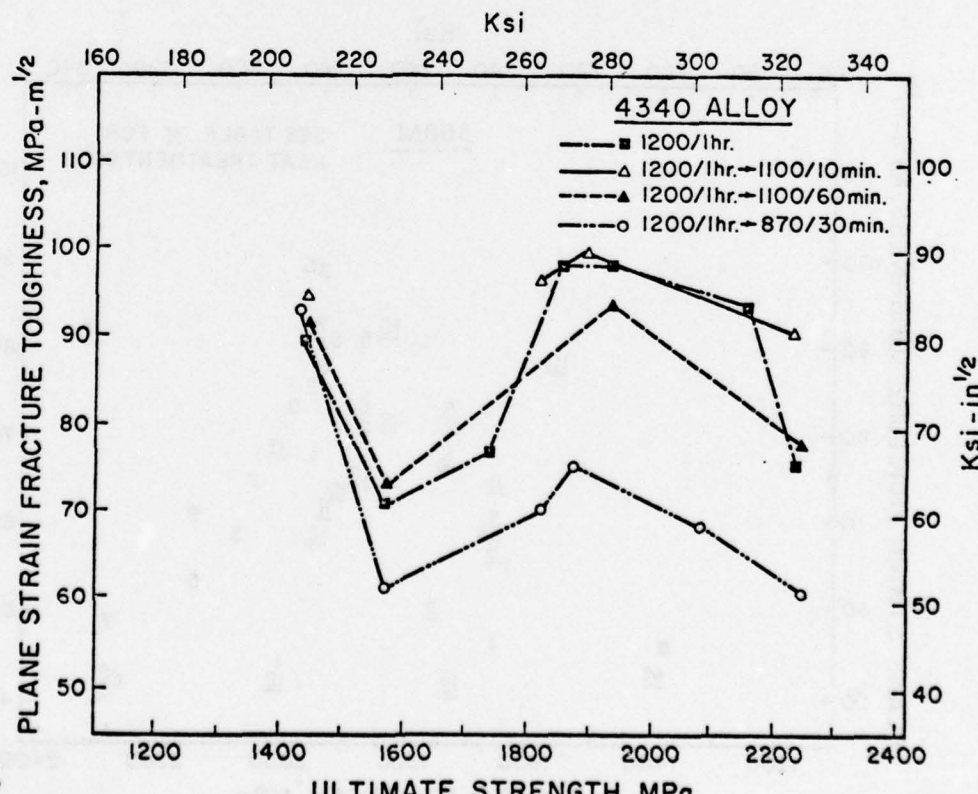


Figure 27

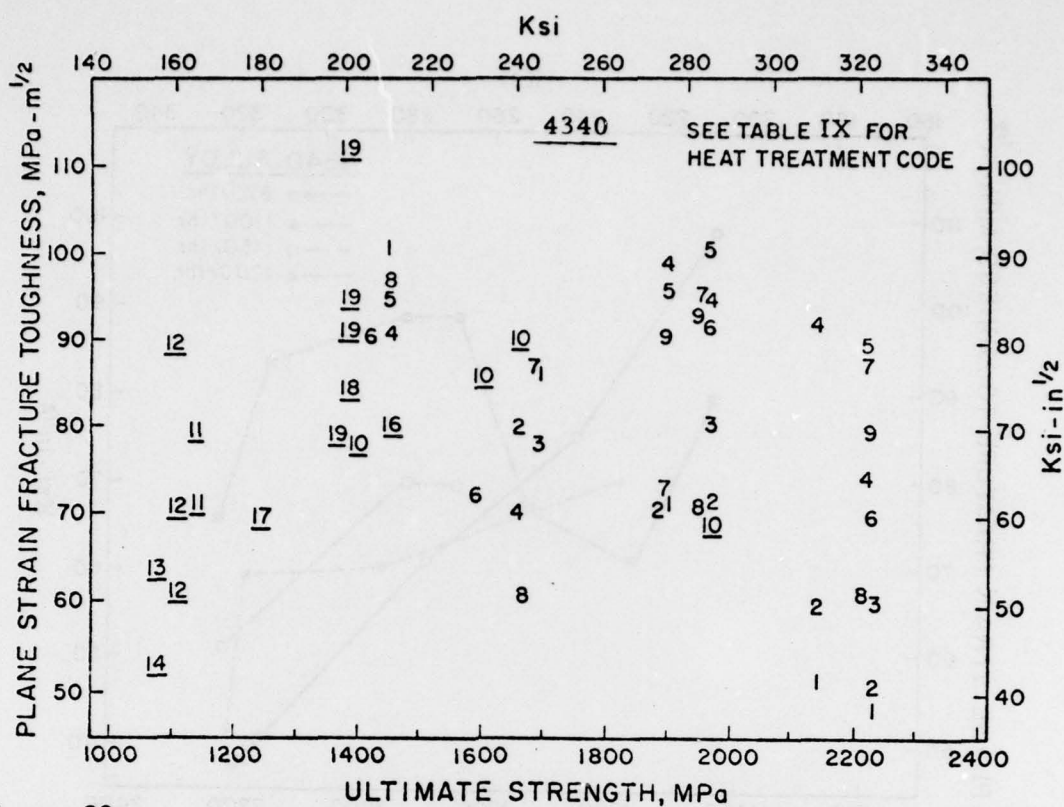


Figure 28

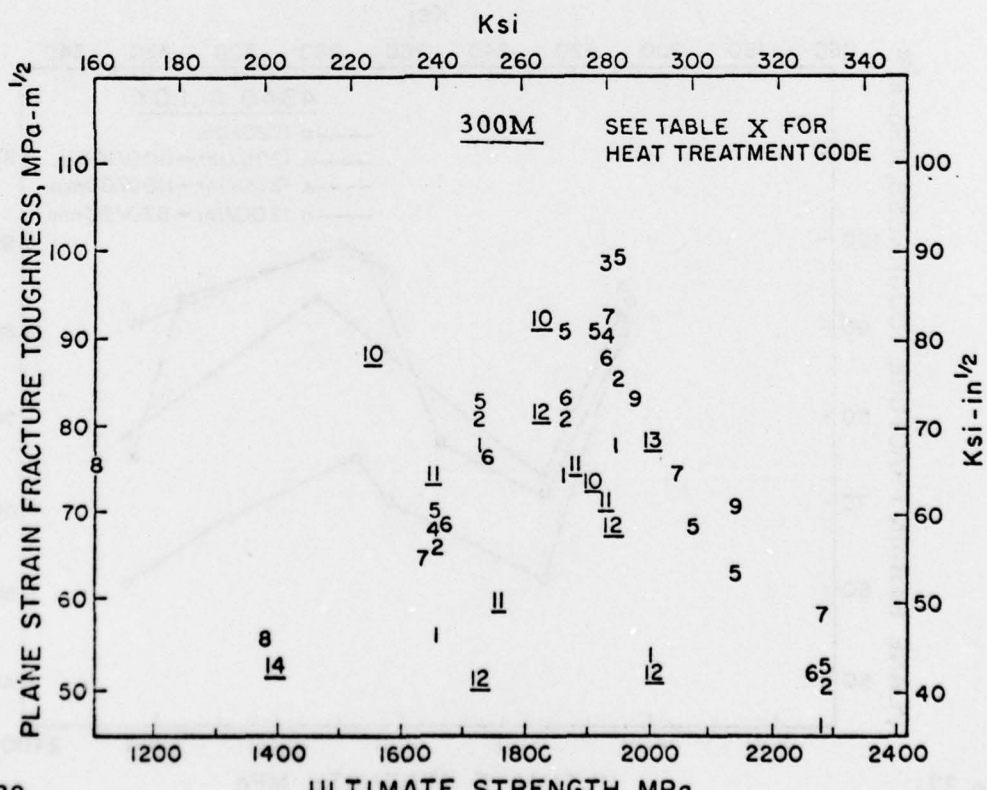


Figure 29

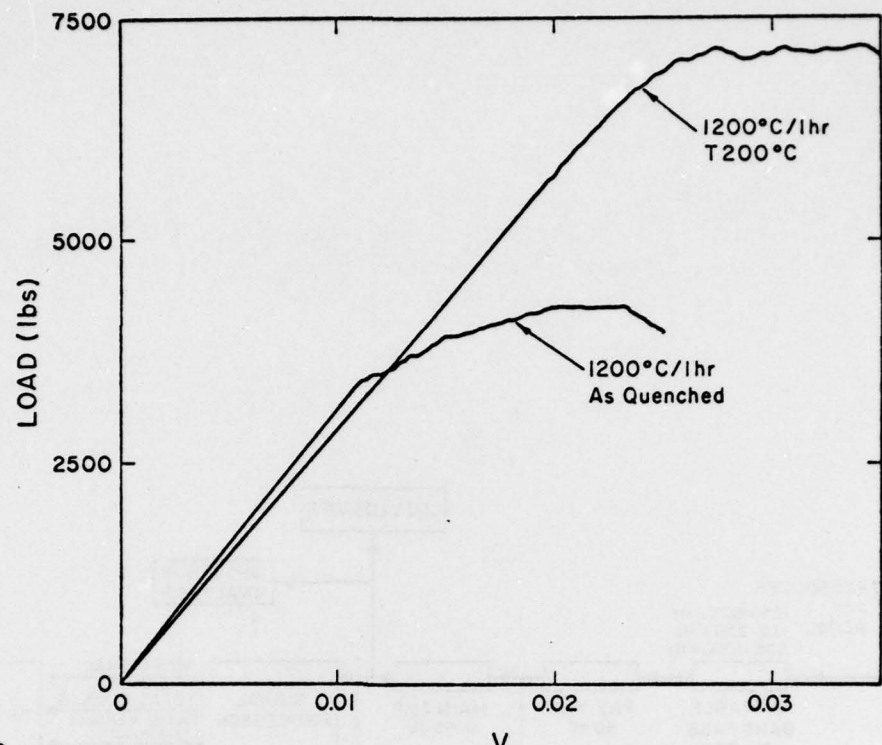


Figure 30

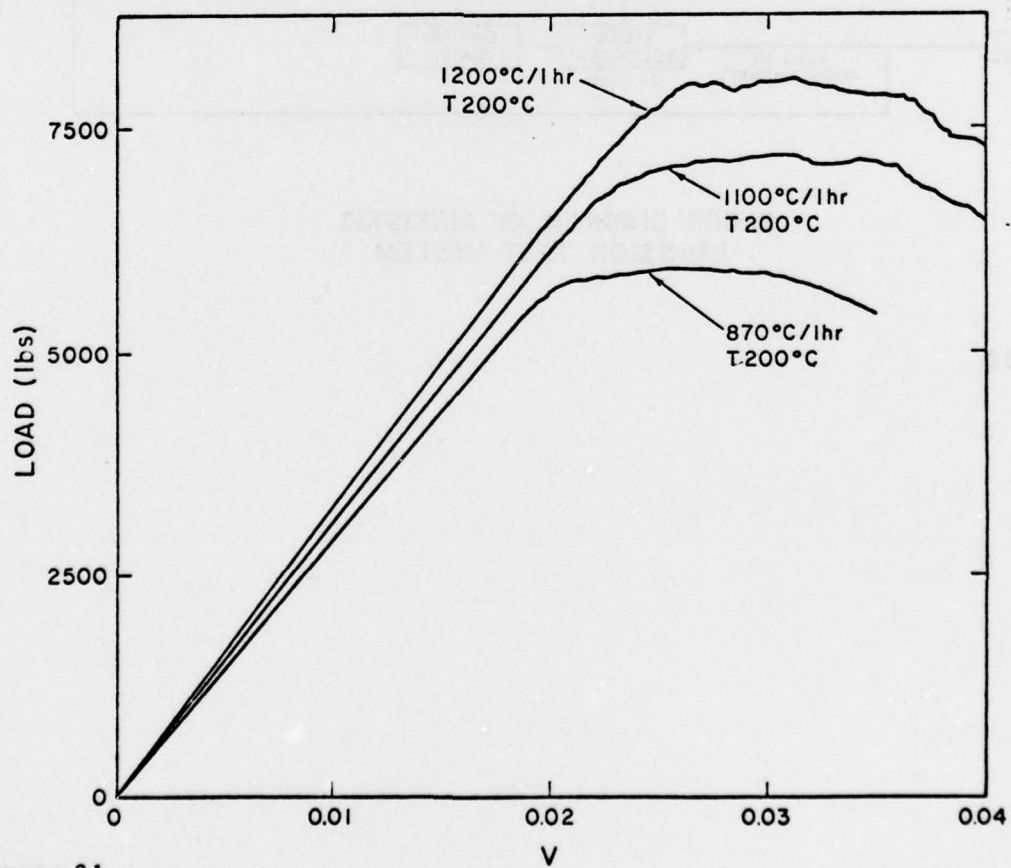
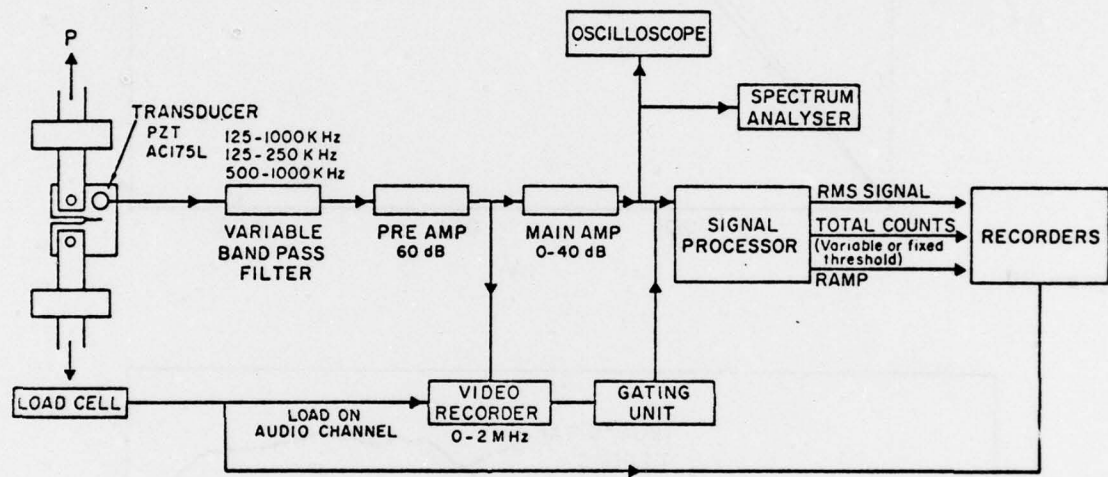


Figure 31



BLOCK DIAGRAM OF ACOUSTIC EMISSION TEST SYSTEM

Figure 32

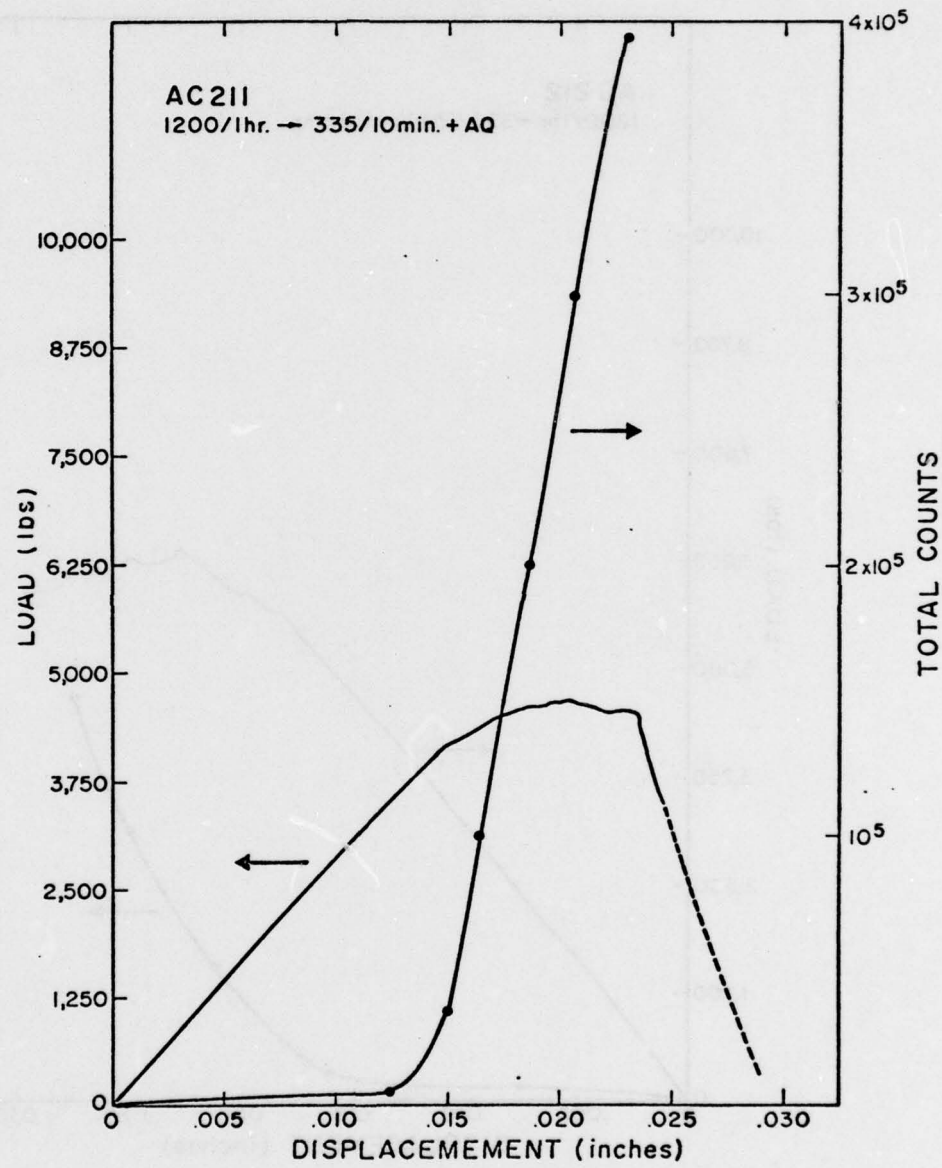


Figure 33

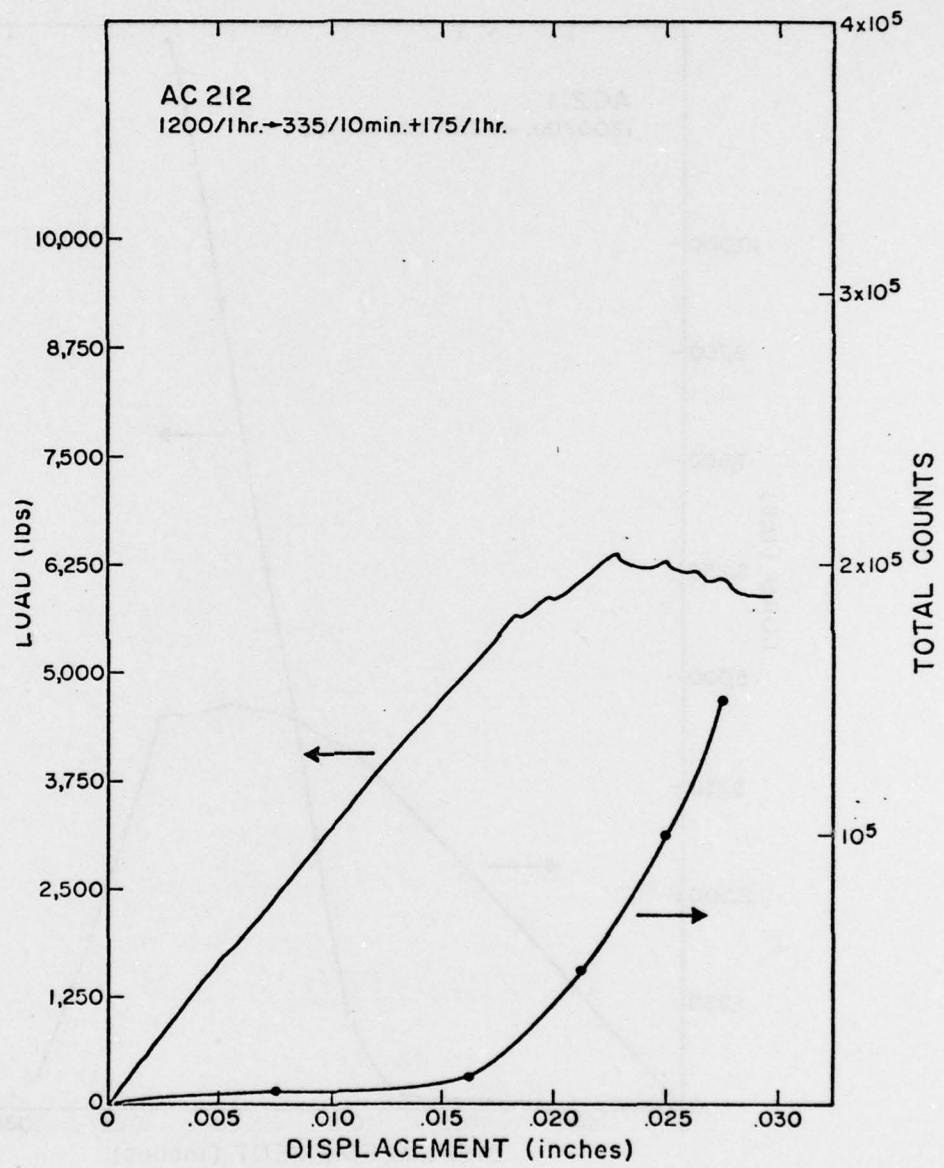


Figure 34

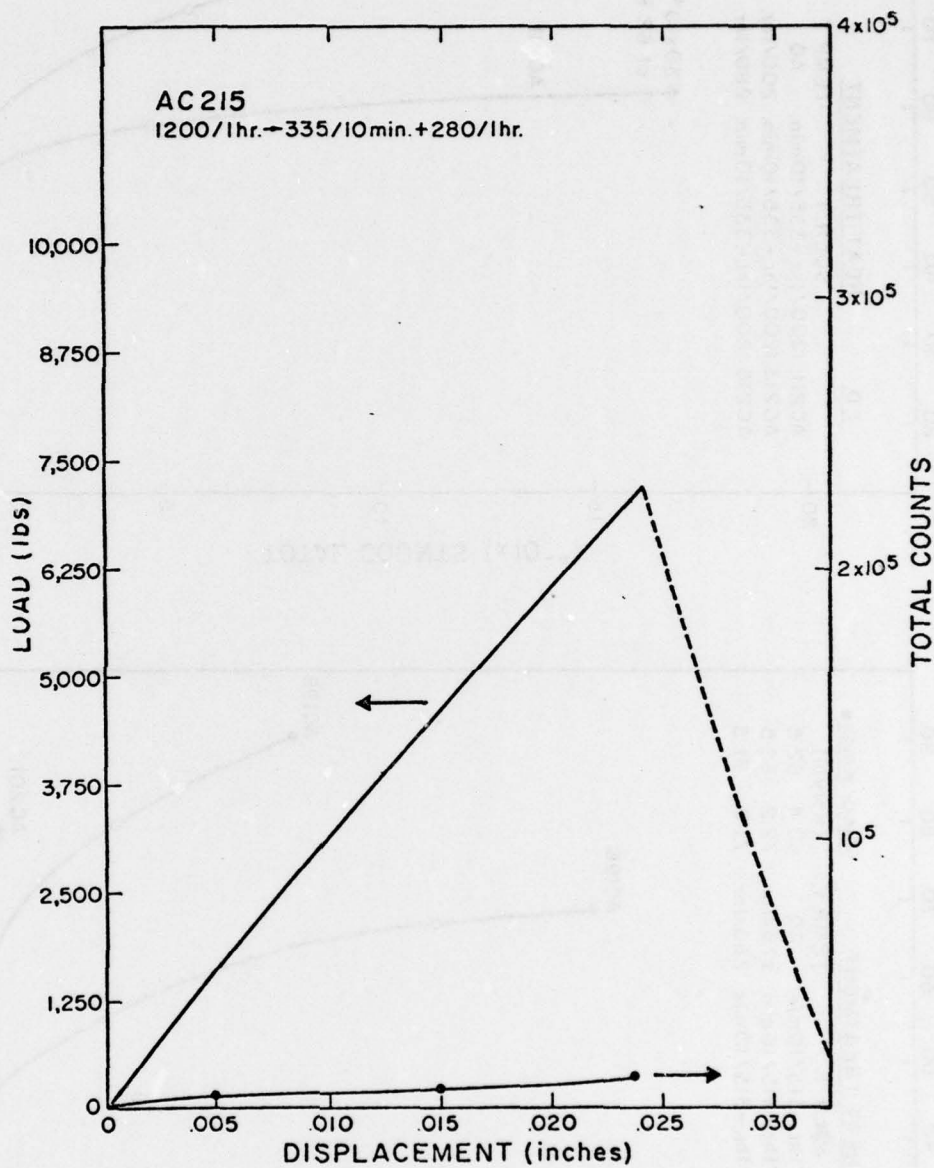
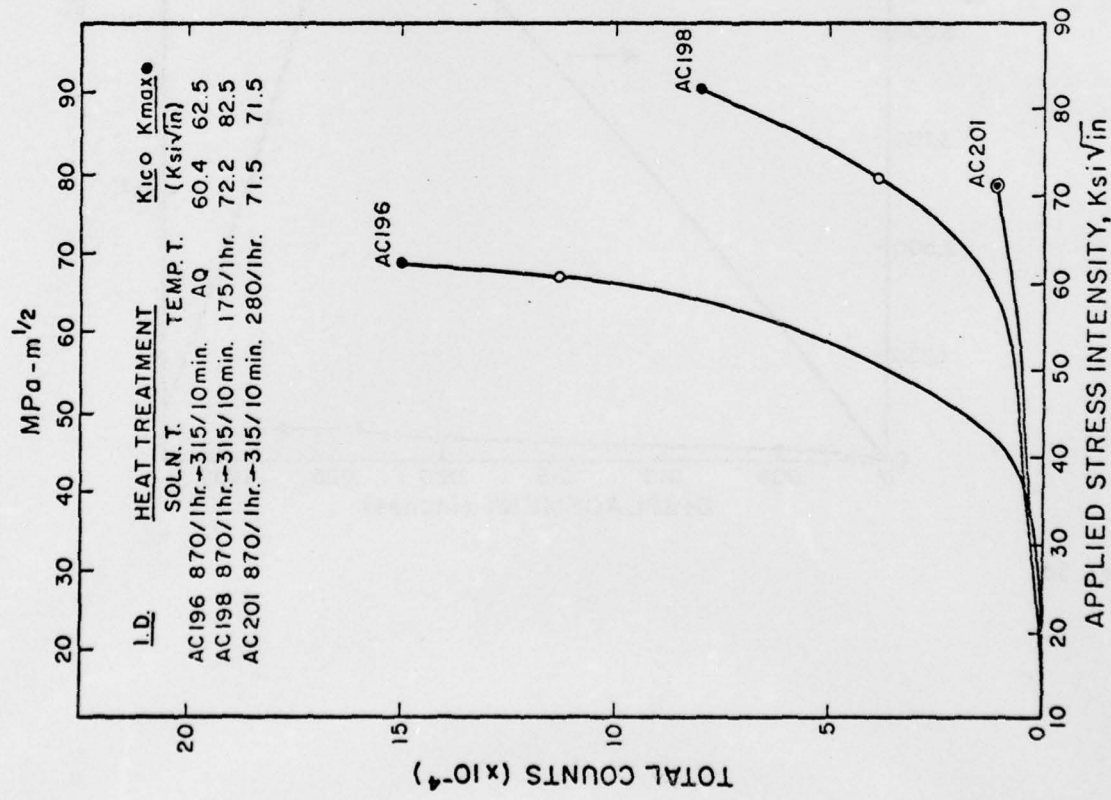
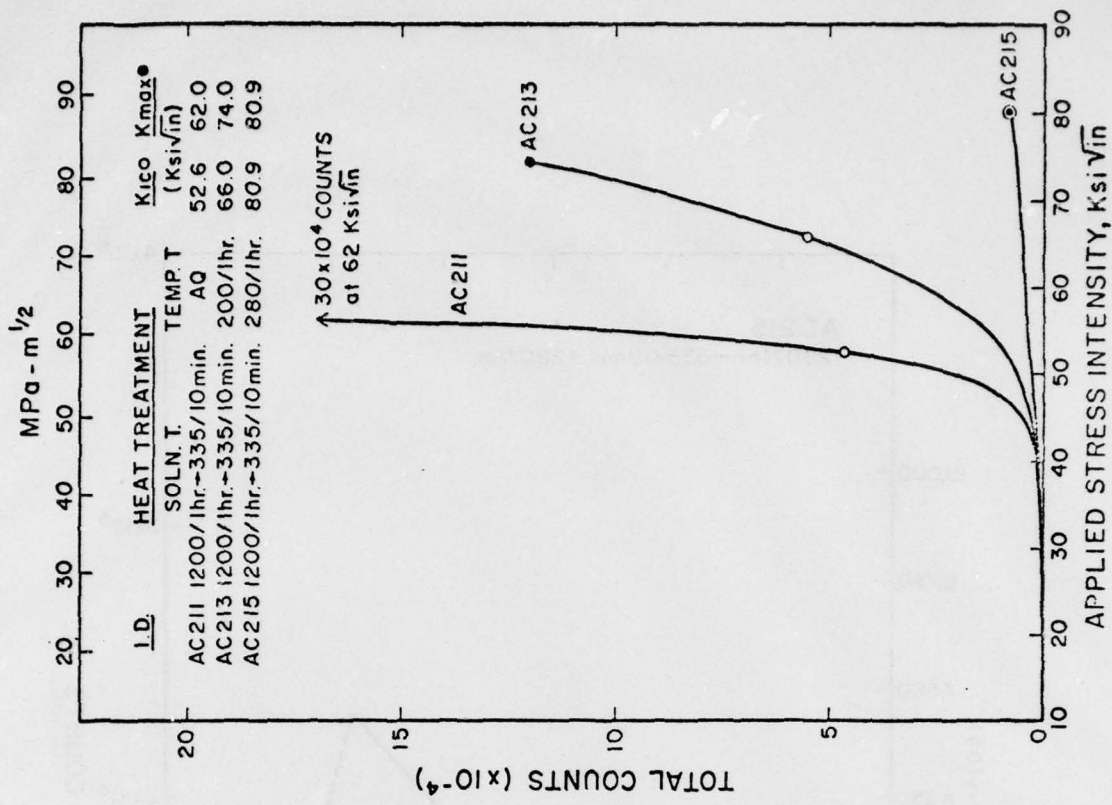


Figure 35



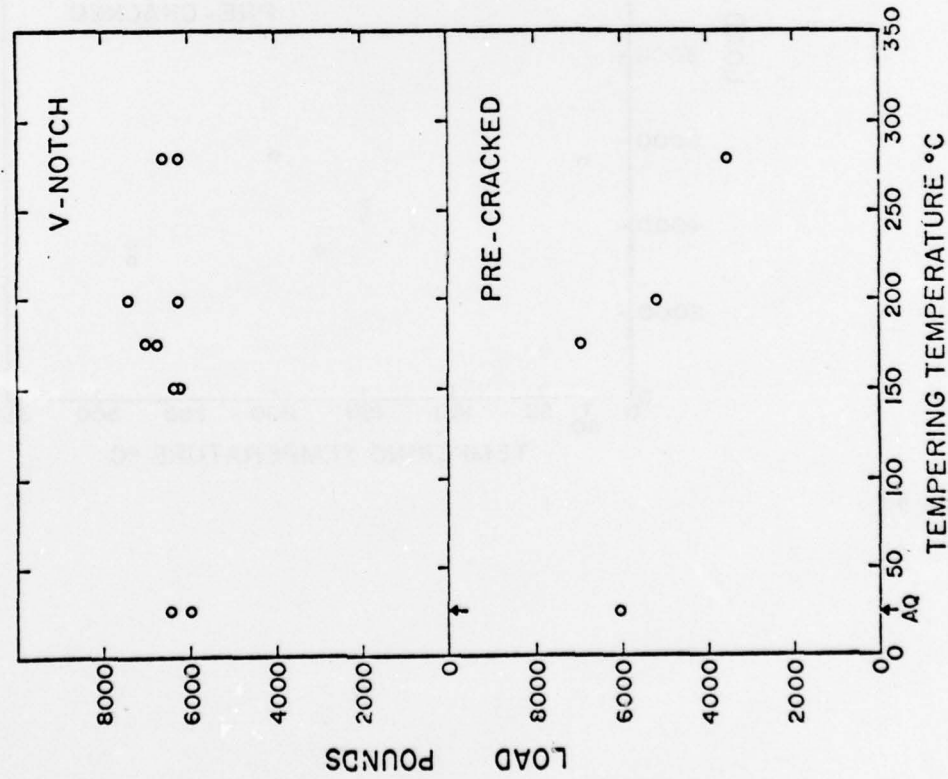
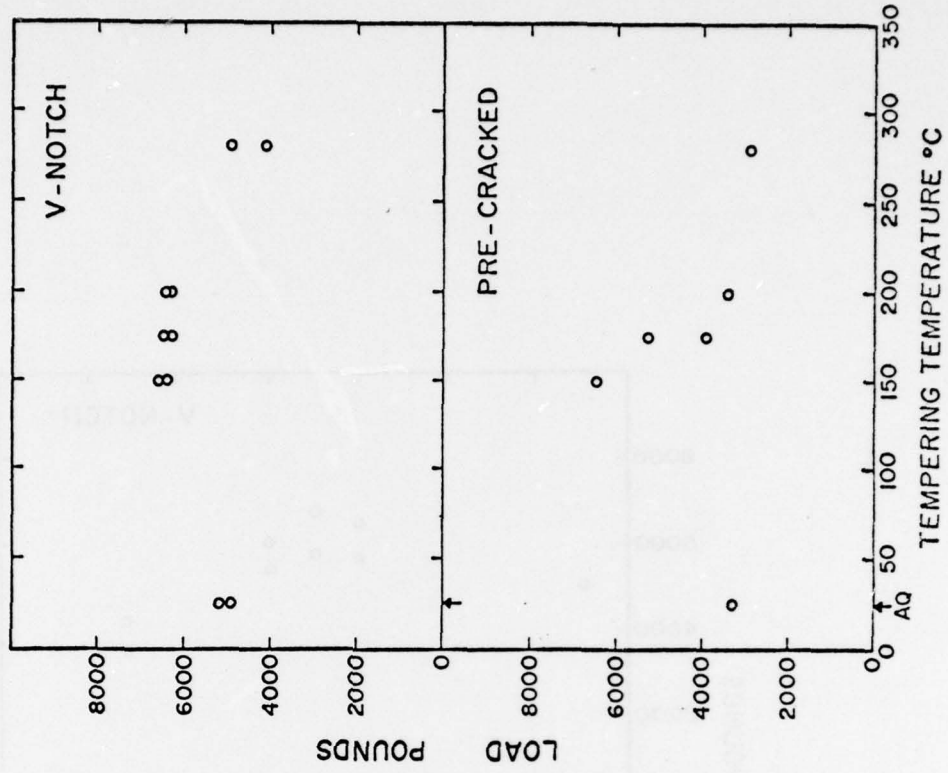


Figure 38

Figure 39

105

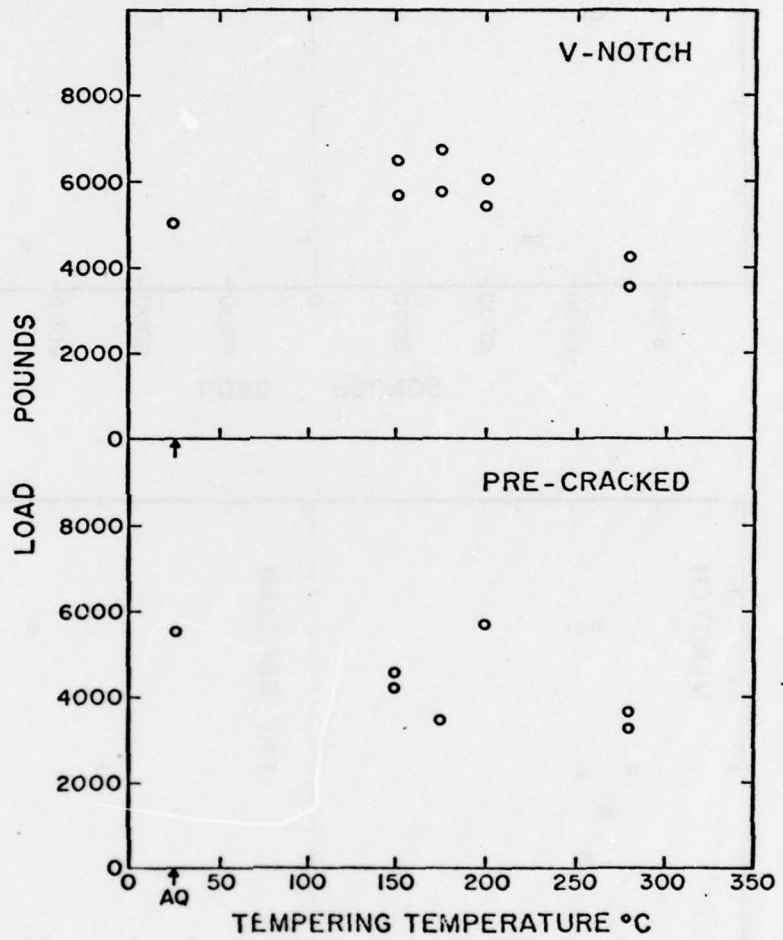


Figure 40

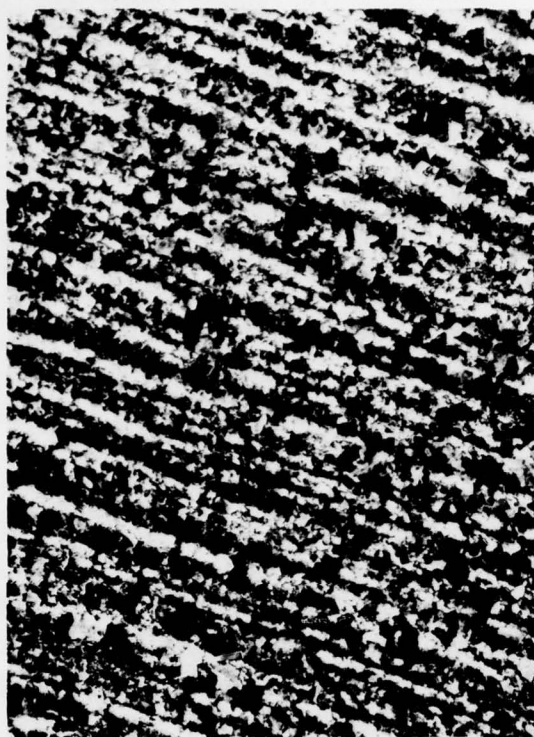


Fig. 41a

100X

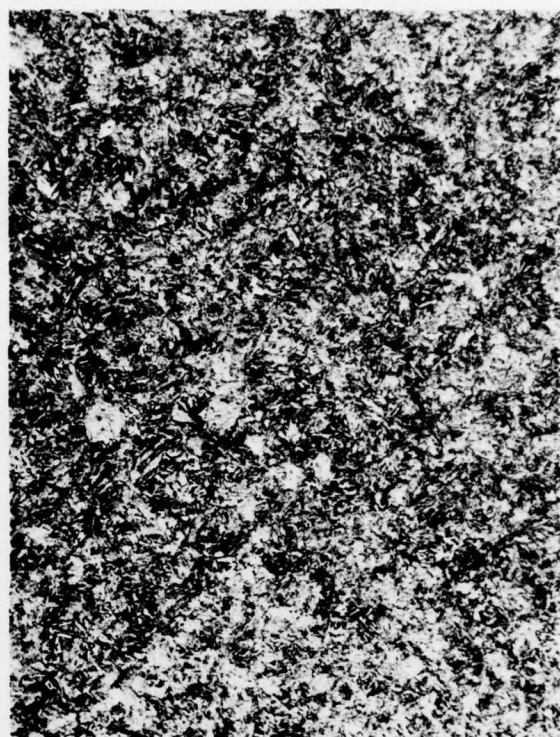


Fig. 41b

100X

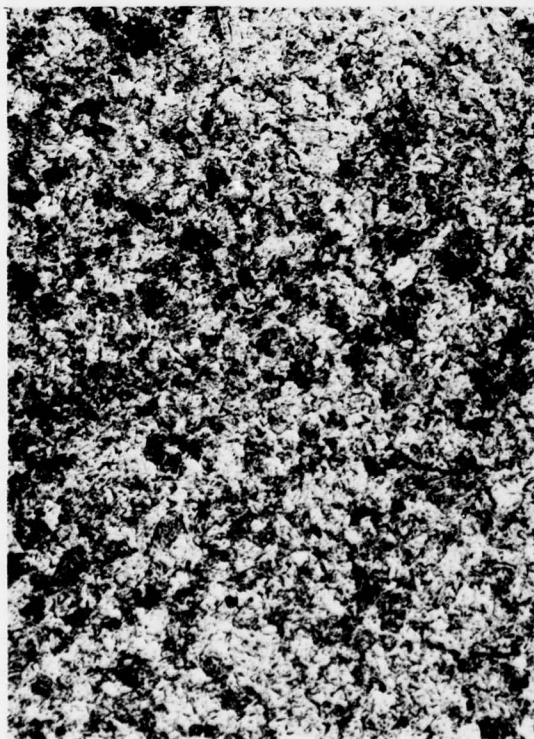


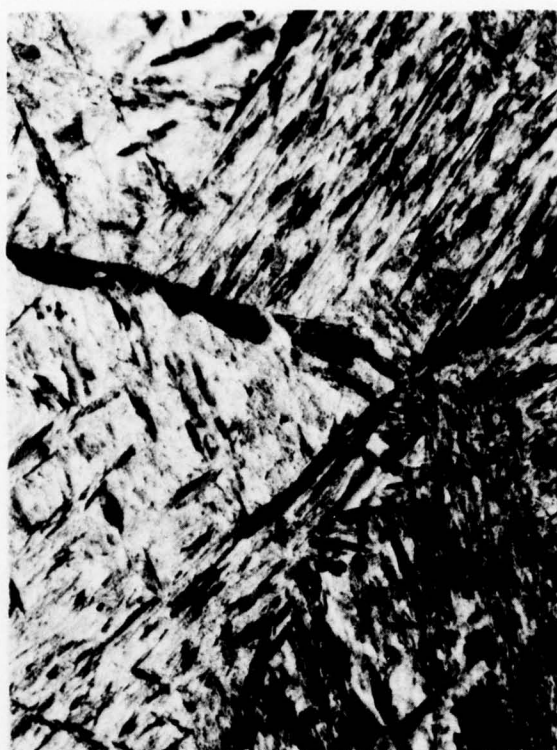
Fig. 42a

1383X



Fig. 42b

2000X



a.

1000X



b.

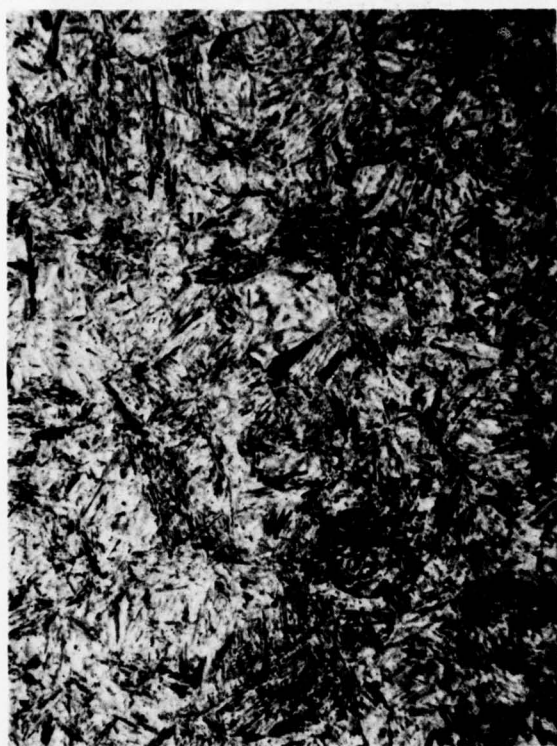
500X



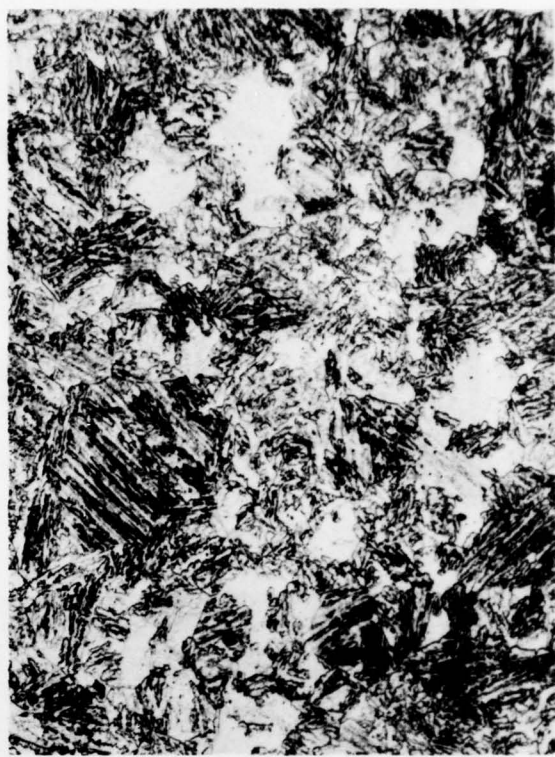
c.

1000X

Figure 43



a



b



c

100X



d

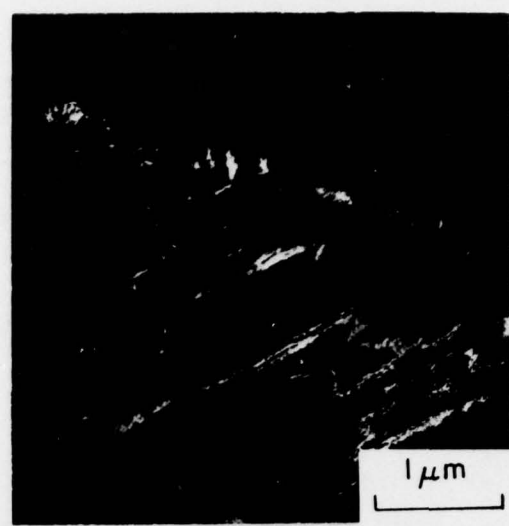
500X

109

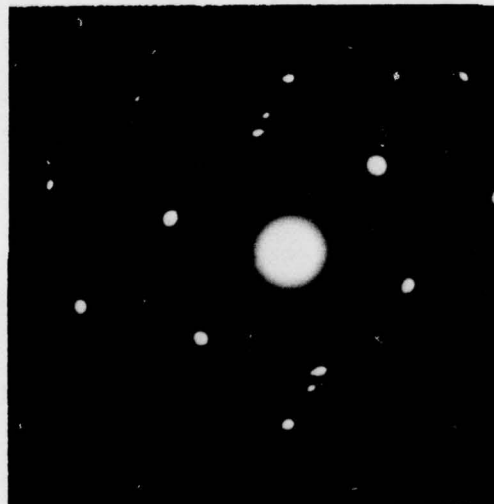
Figure 44



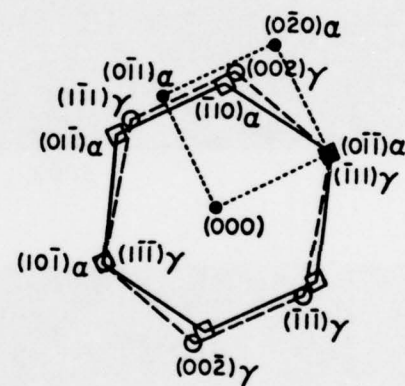
a



b



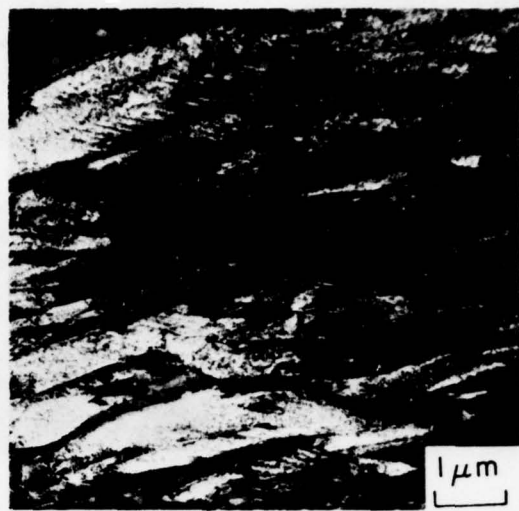
c



- - [100] MARTENSITE SPOT
- - [111] MARTENSITE SPOT
- - [110] AUSTENITE SPOT

d

Figure 45



a

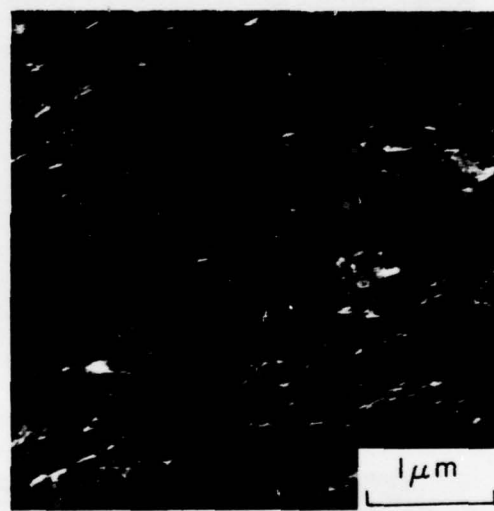


Figure 46

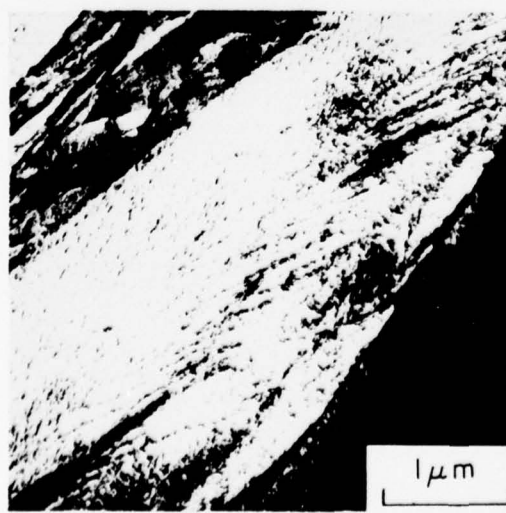
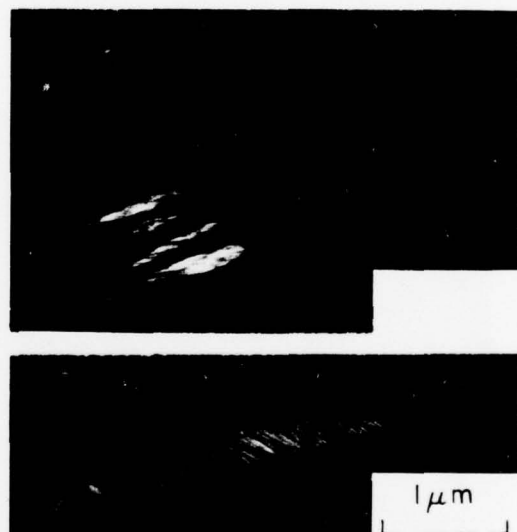
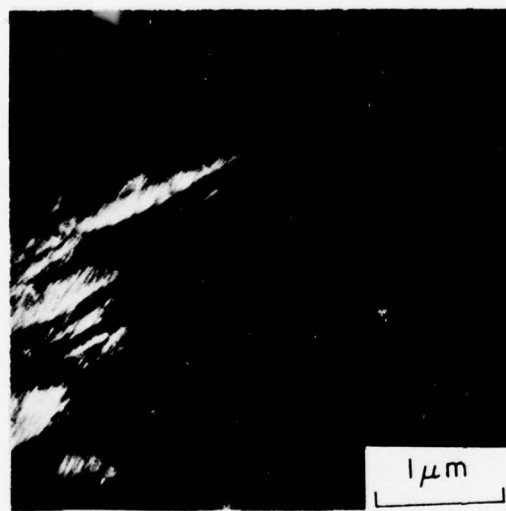
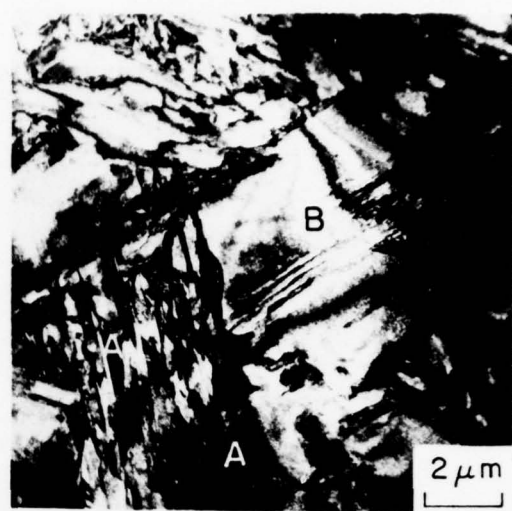
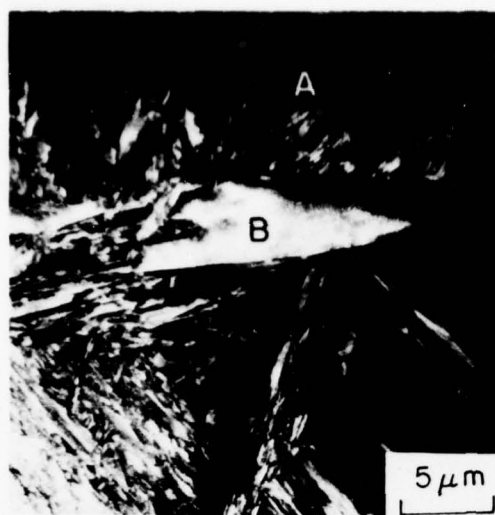


Figure 47



Figure 47 (cont'd)

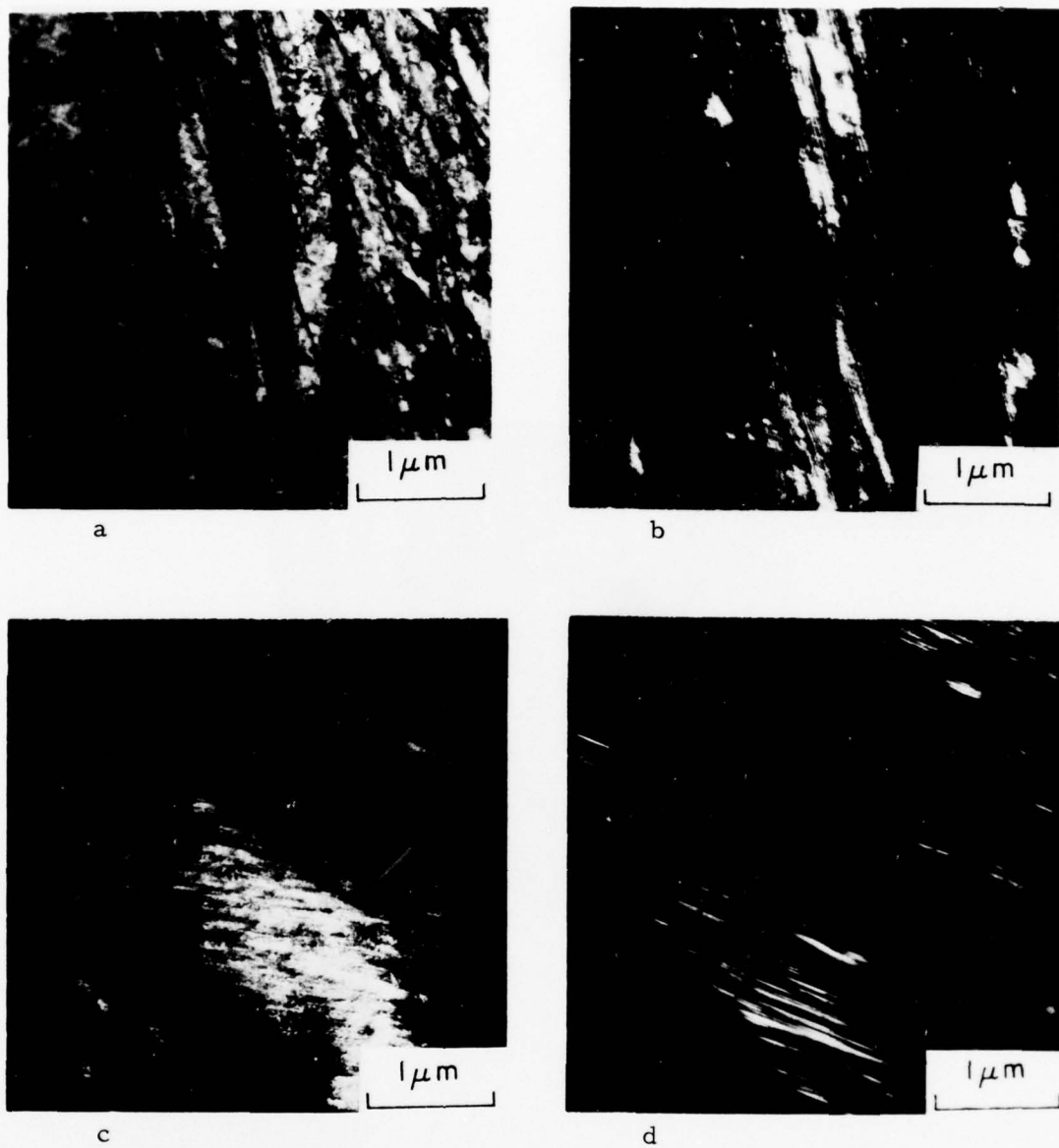


Figure 48



Figure 48-e (cont'd)

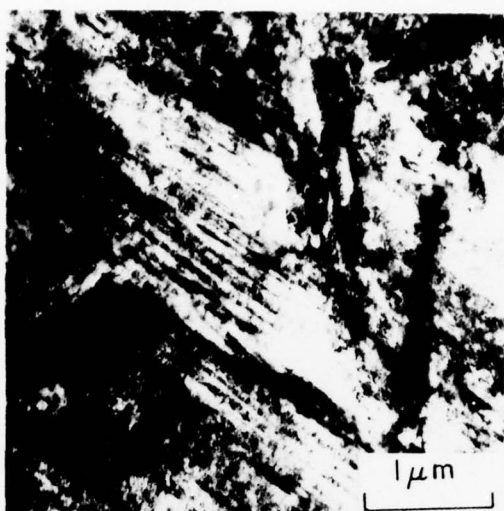


Fig. 49

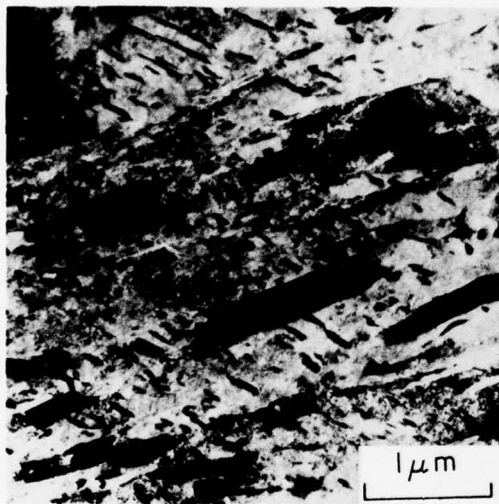


Fig. 50a

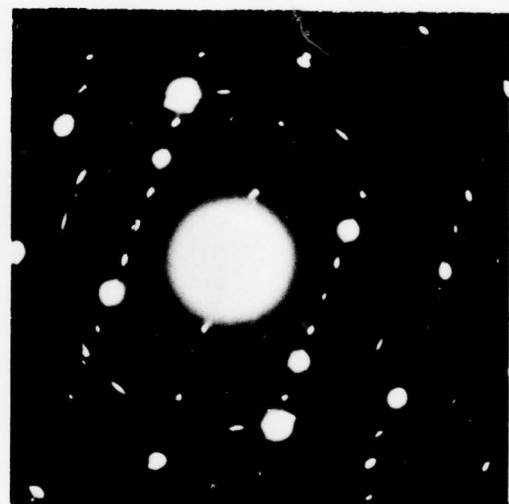


Fig. 50b



Fig. 51a

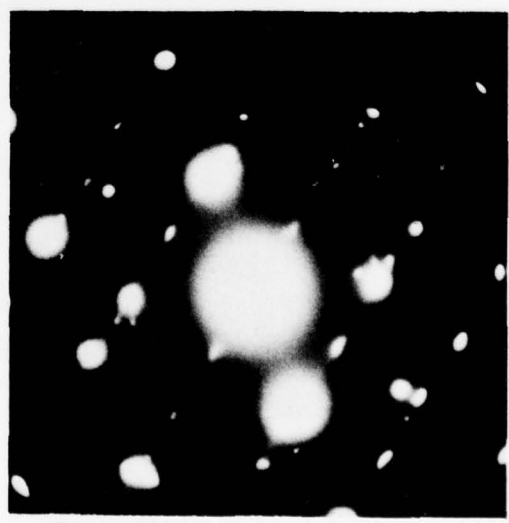
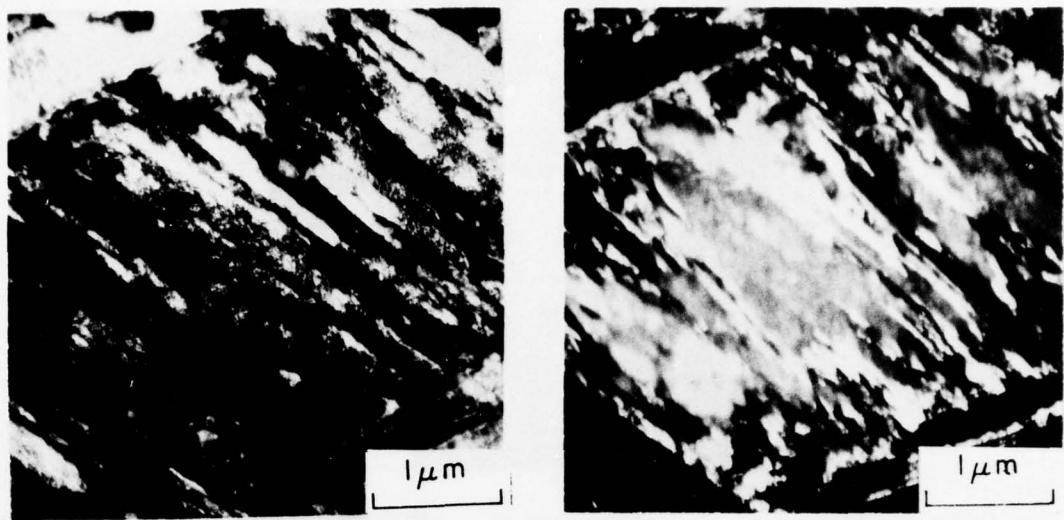
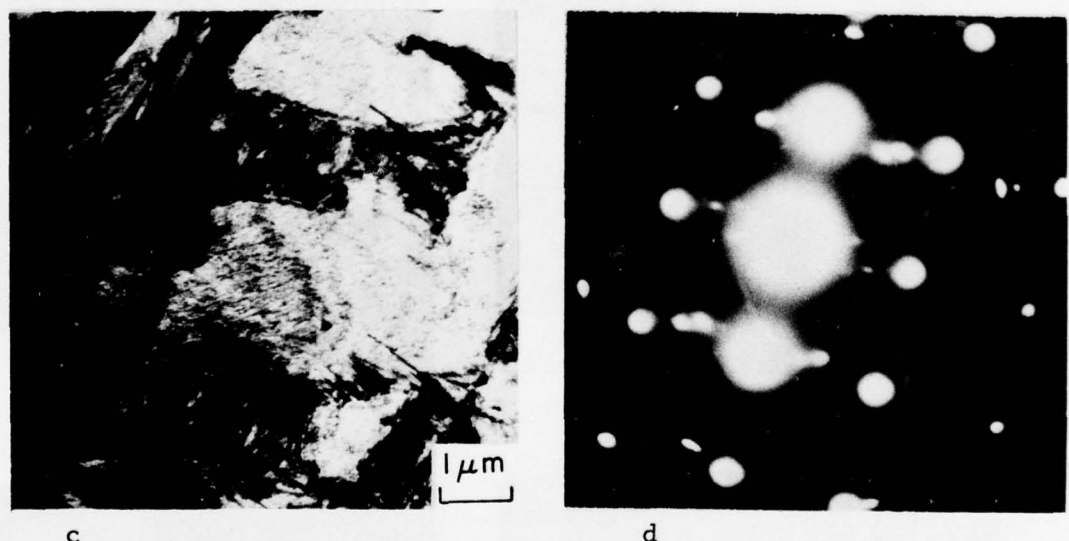


Fig. 51b



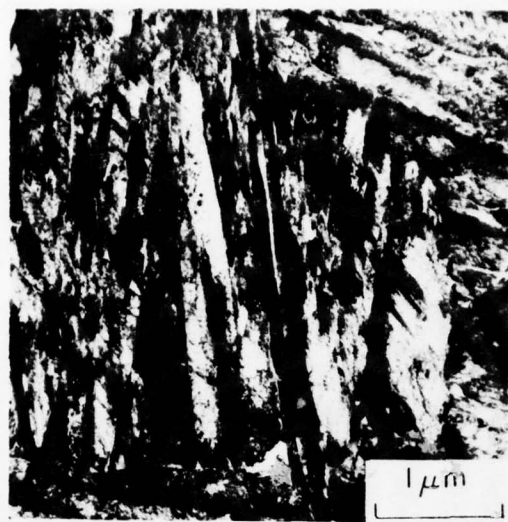
a



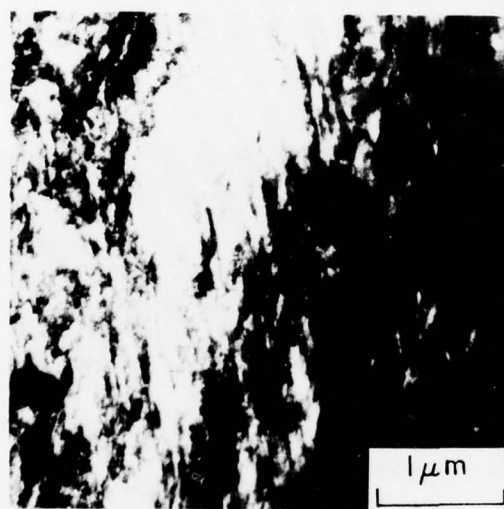
c

d

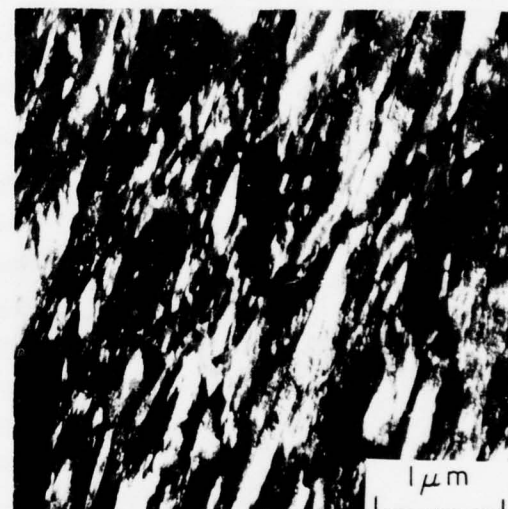
Figure 52



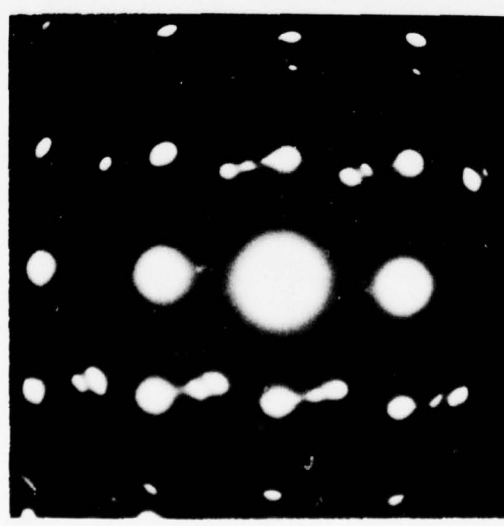
a



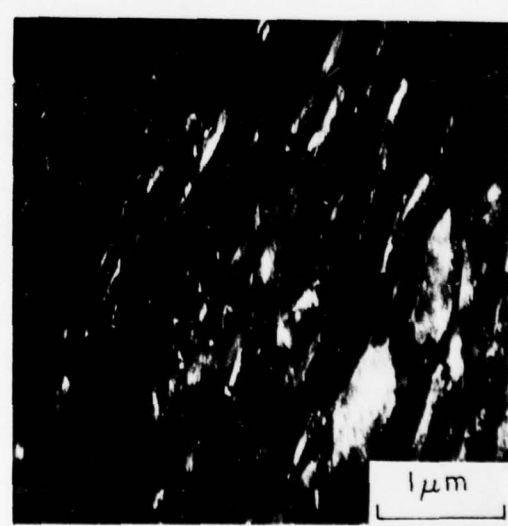
b



c



d



e

Figure 53

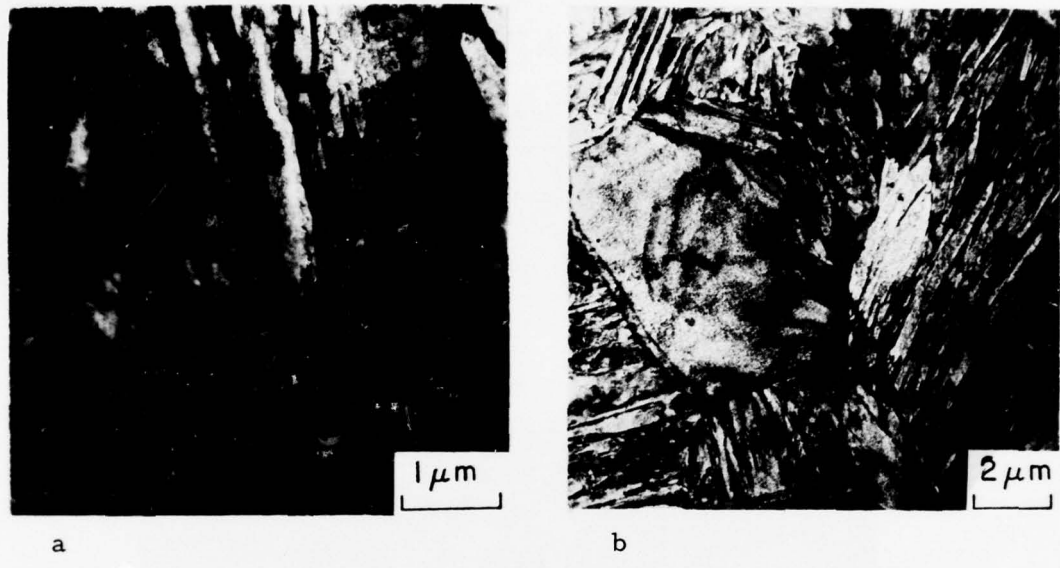
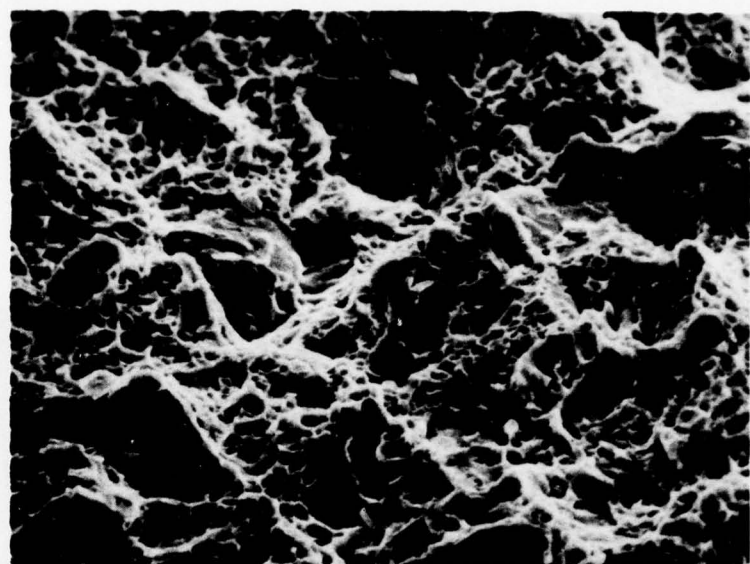
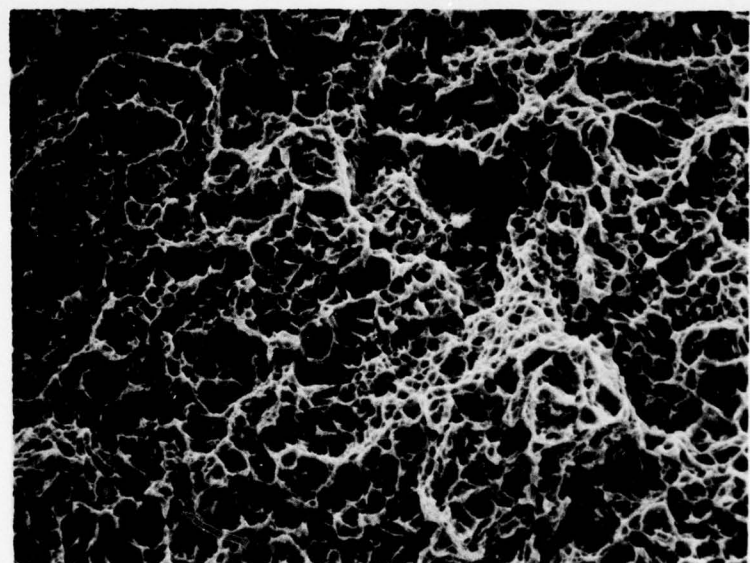


Figure 54



a

2000X



b

2000X

Figure 55

140

Figure 56

200X

100X

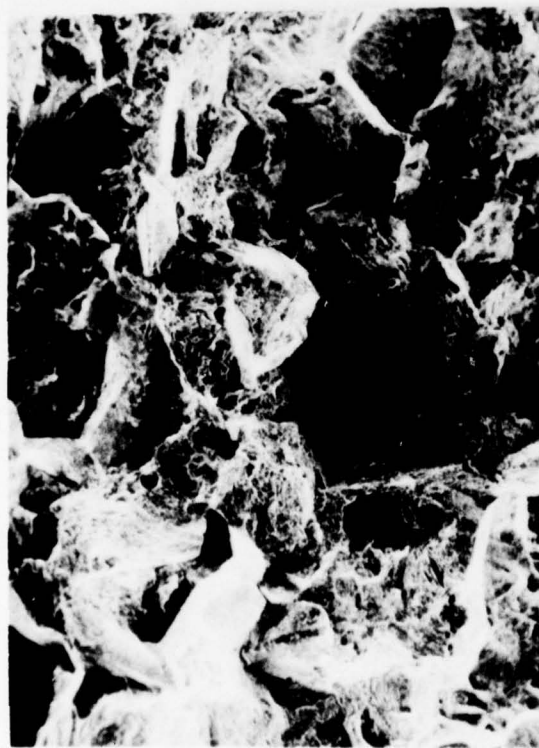
c



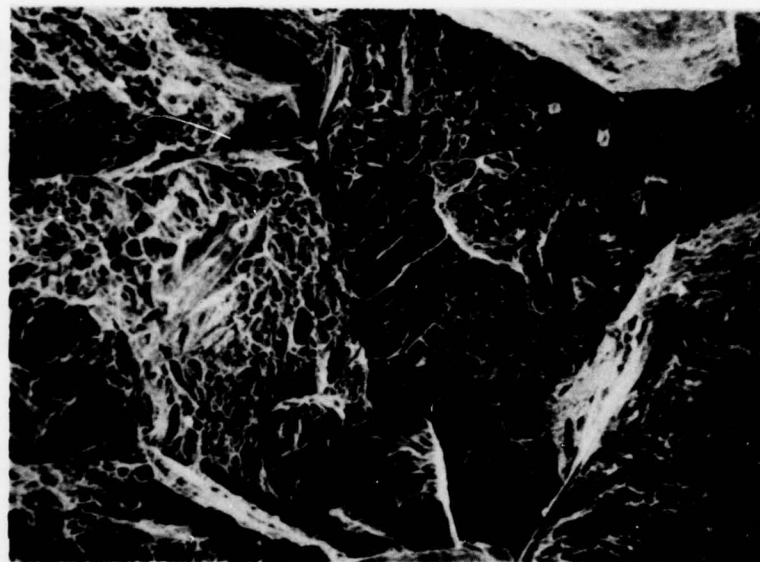
500X

100X

a



121



a

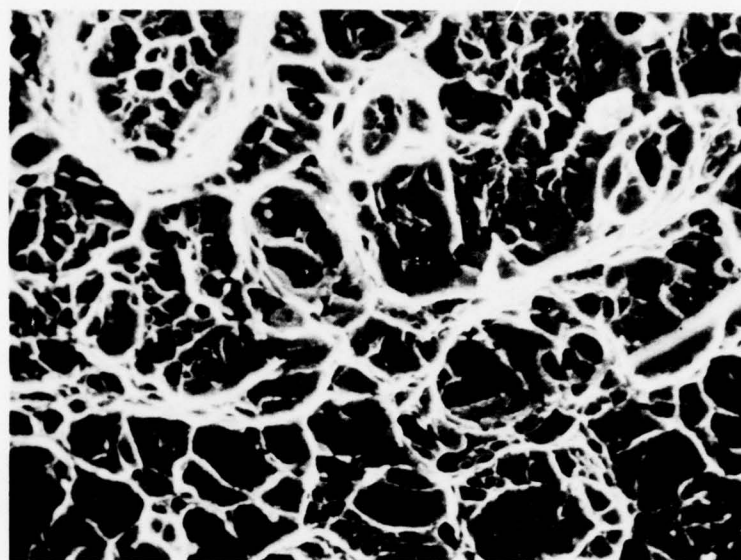
500X



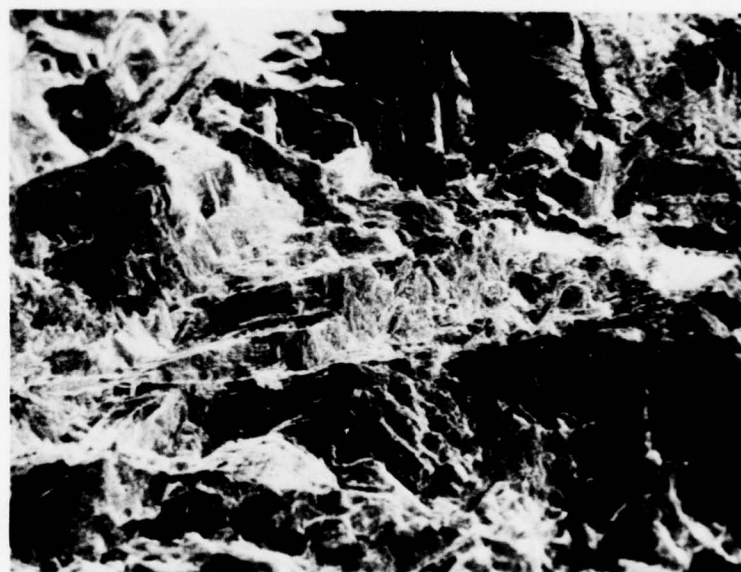
b

2000X

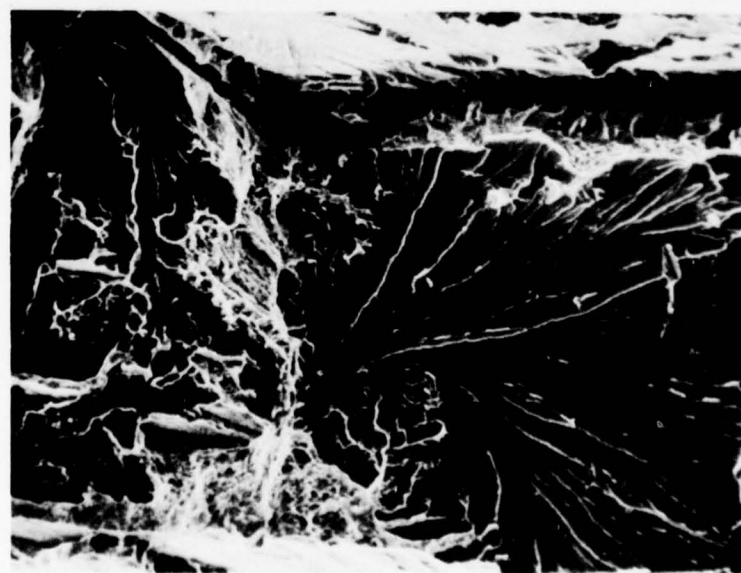
104



(a)
2000X

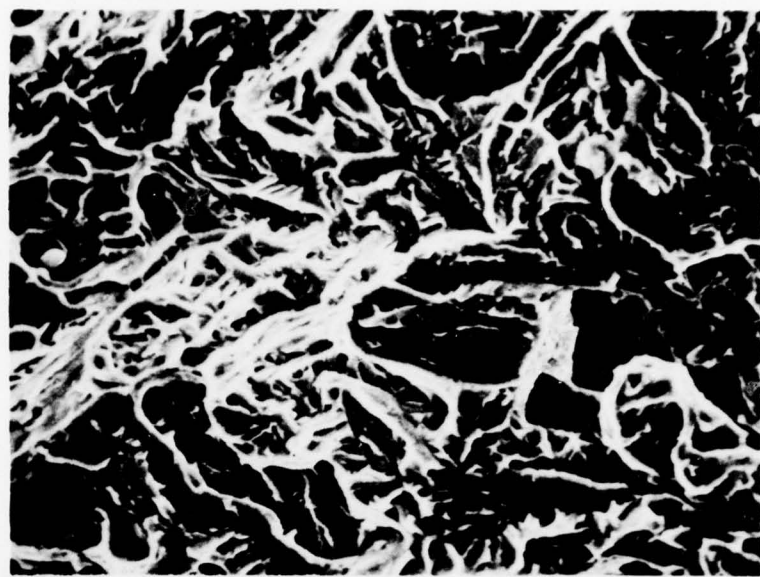


(b)
100X

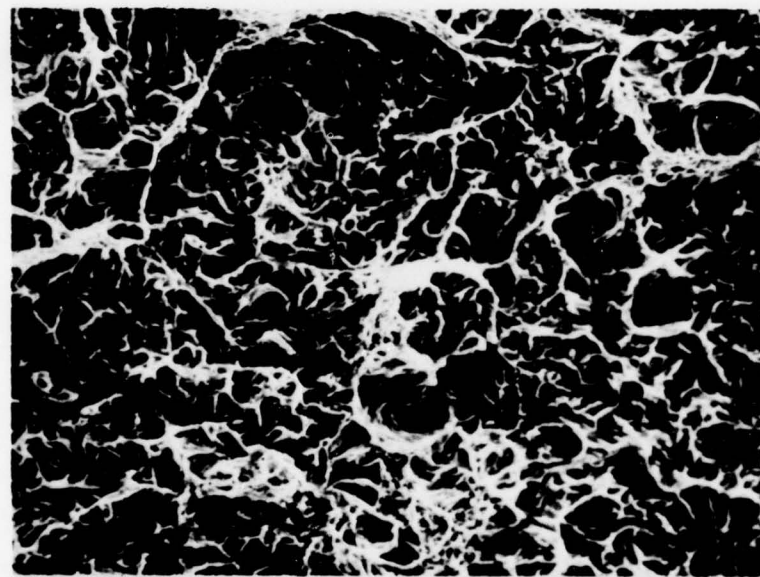


(c)
500X

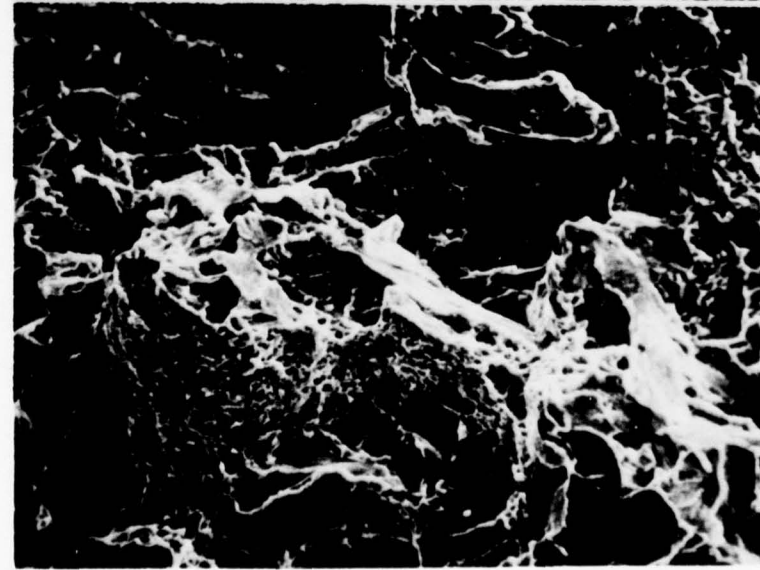
Figure 58



(a)
1000X



(b)
500X



(c)
1000X

Figure 59

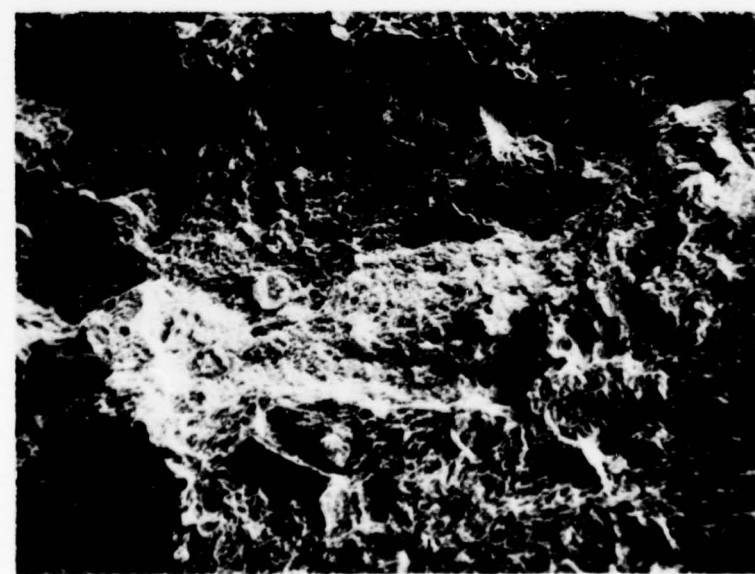
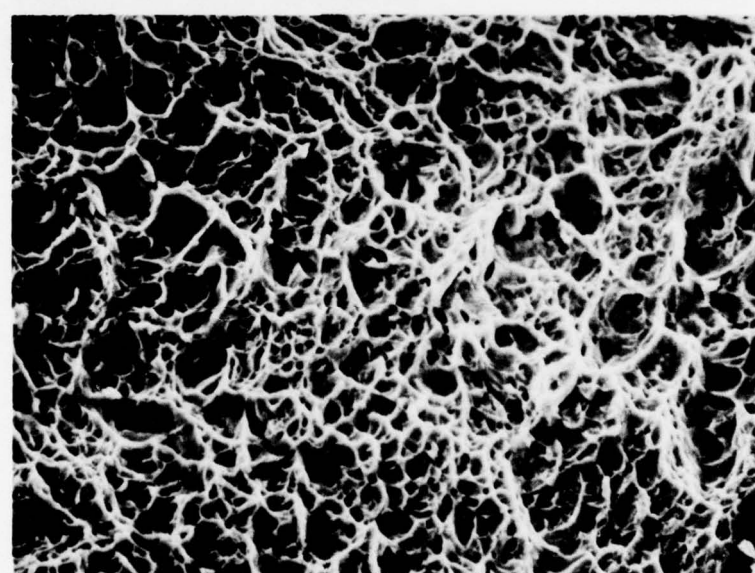
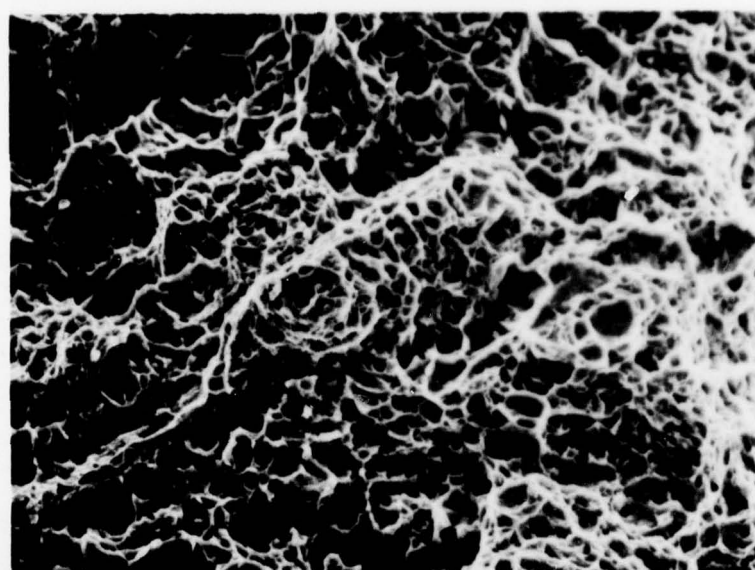
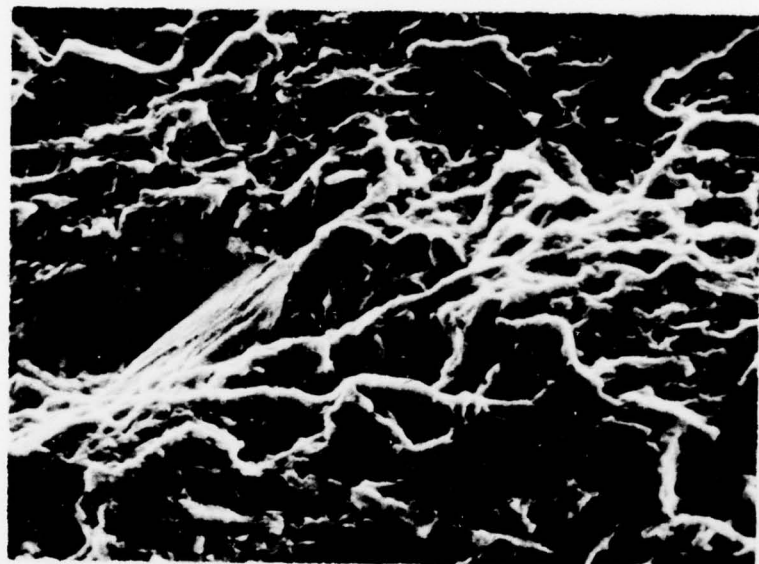


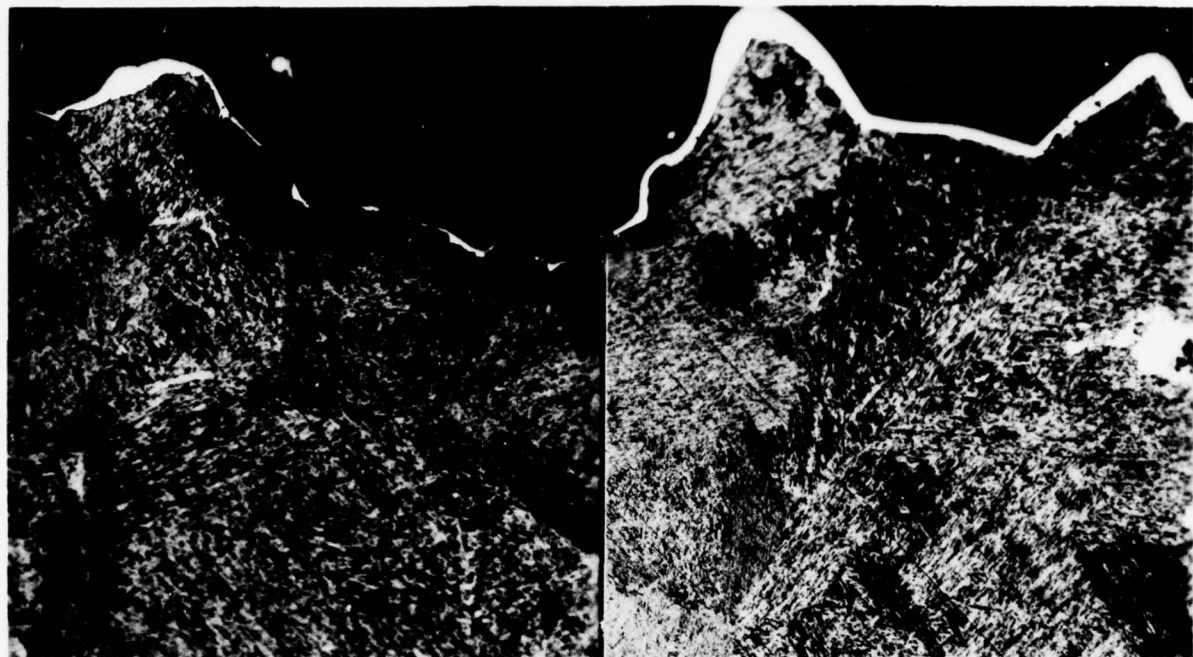
Figure 60



2000X

Figure 61

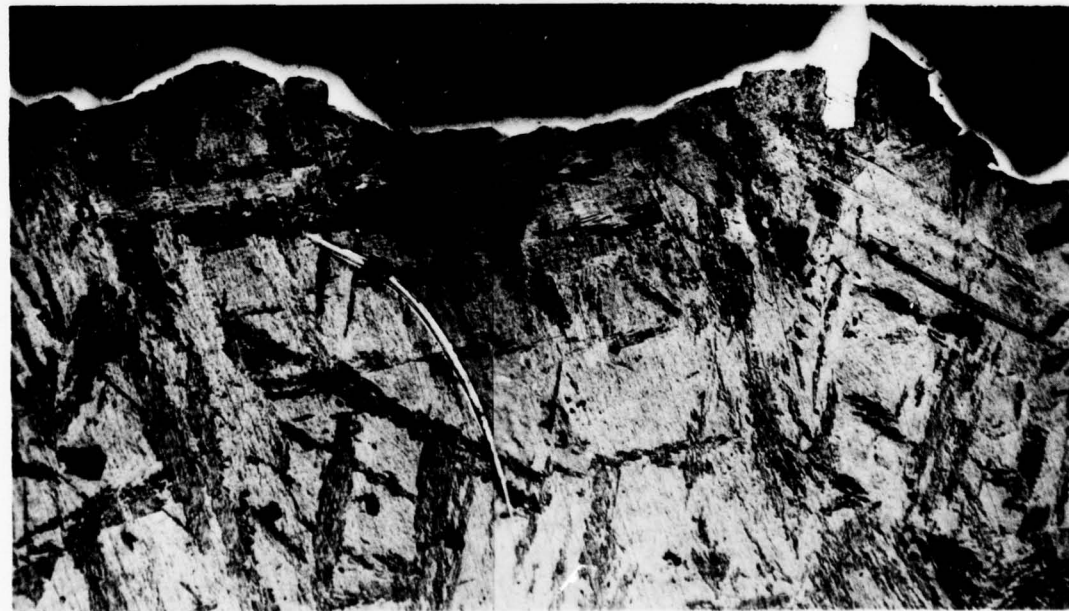
Direction of Crack Propagation ←



(a) AC72

200 X

→ Direction of Crack Propagation



(b) AC 75

200X

Figure 62

127

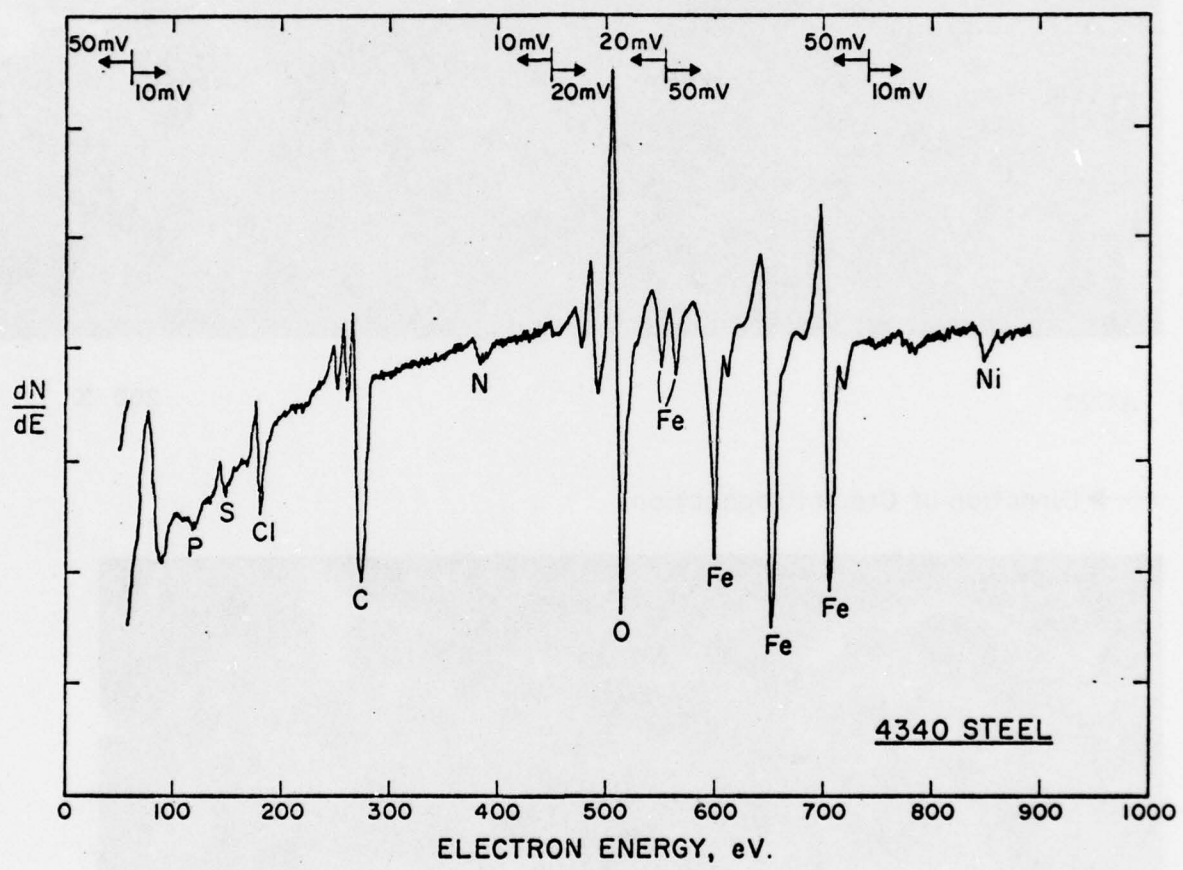


Figure 63

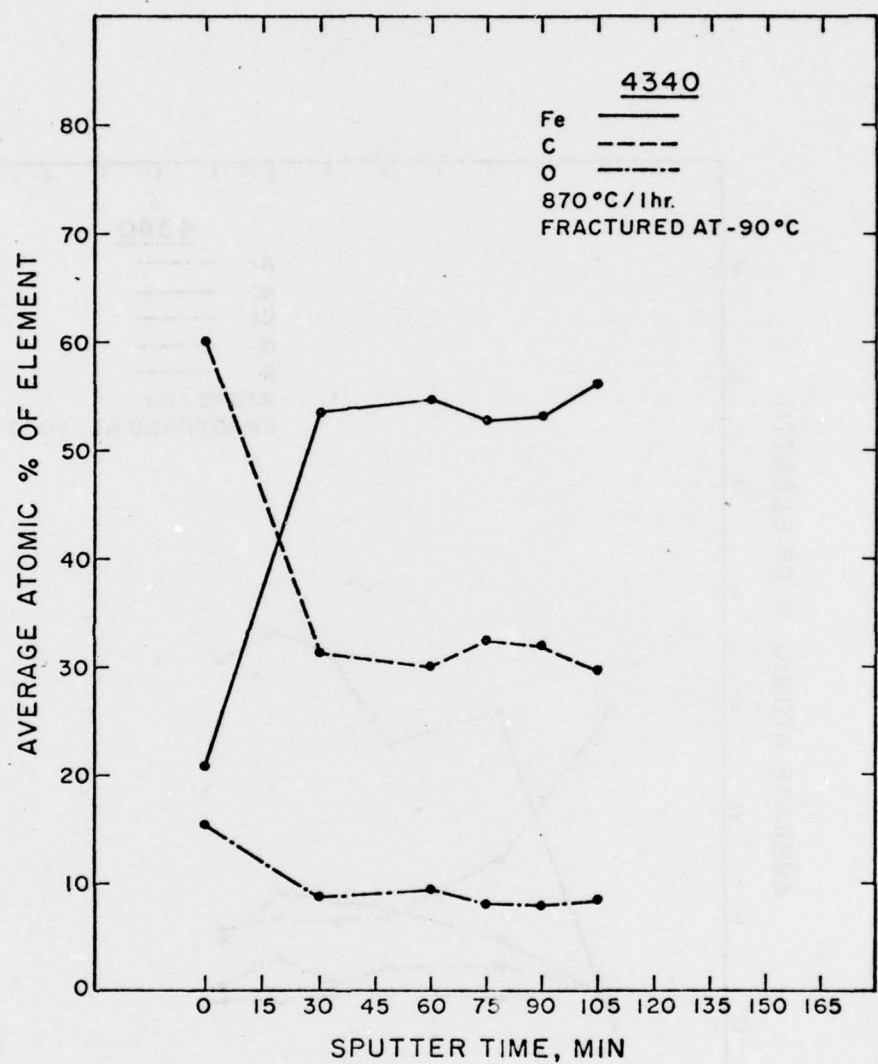


Figure 64 a

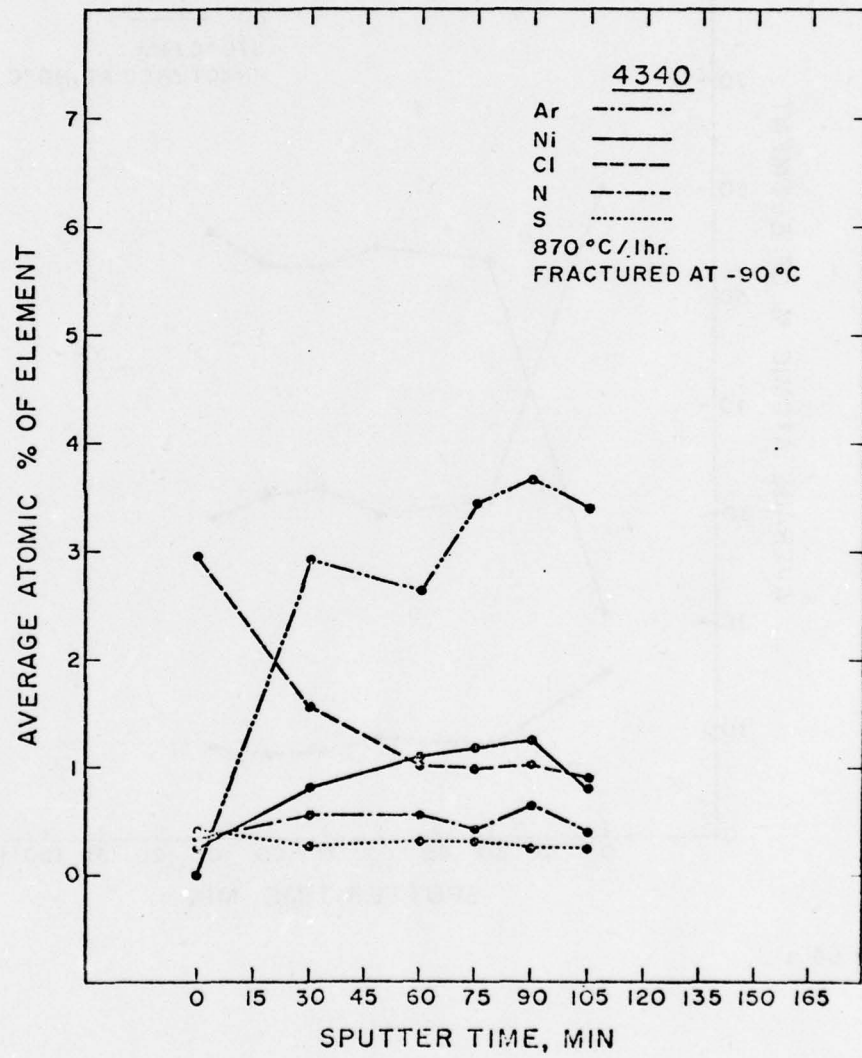


Figure 64 b

136

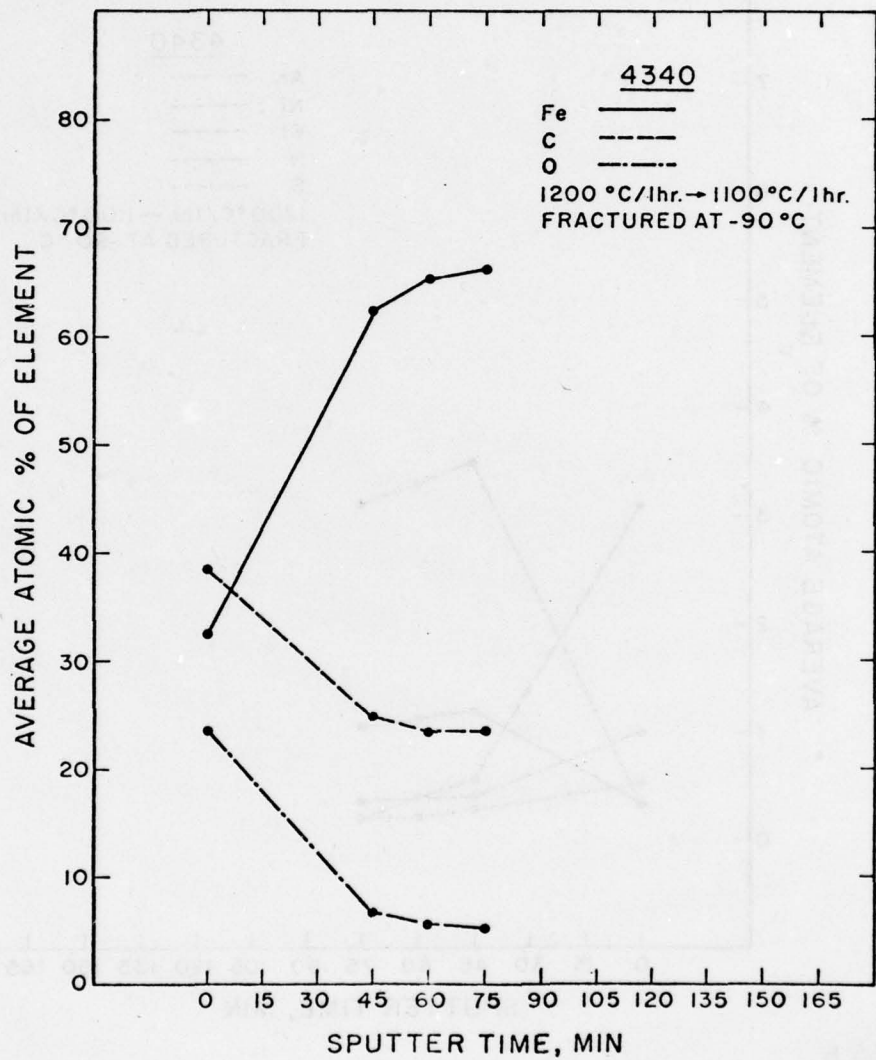


Figure 65 a

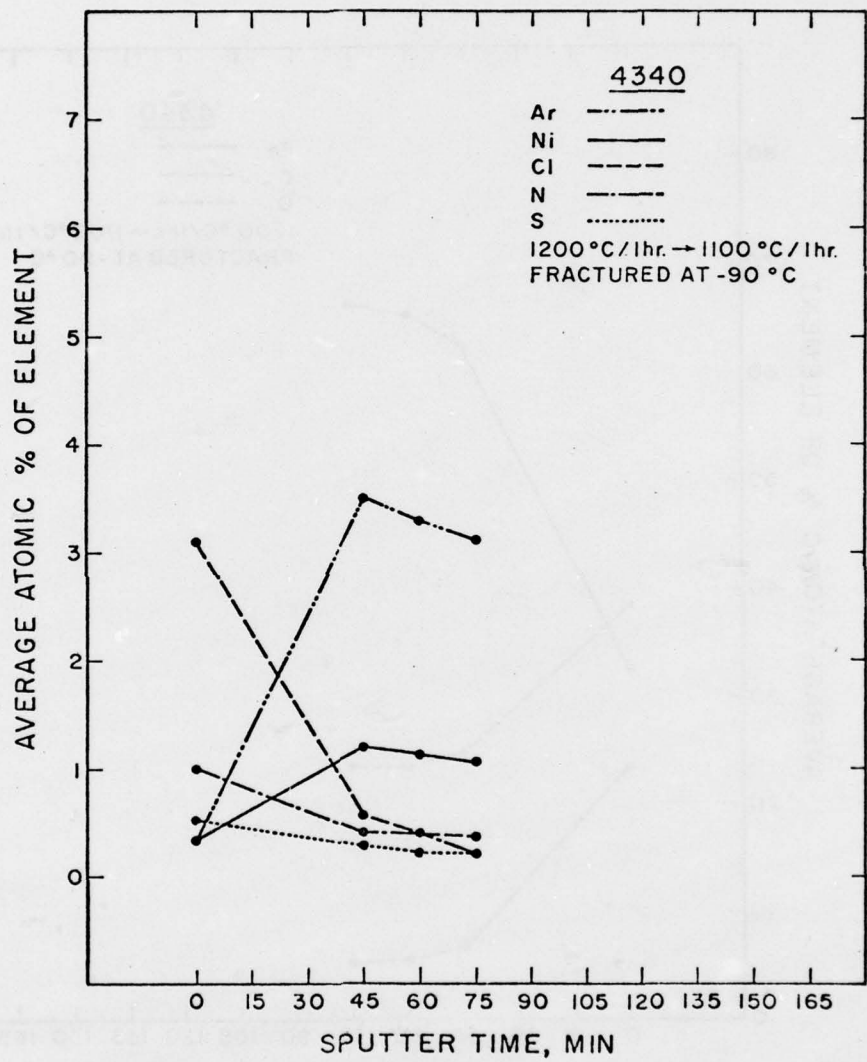


Figure 65 b

132

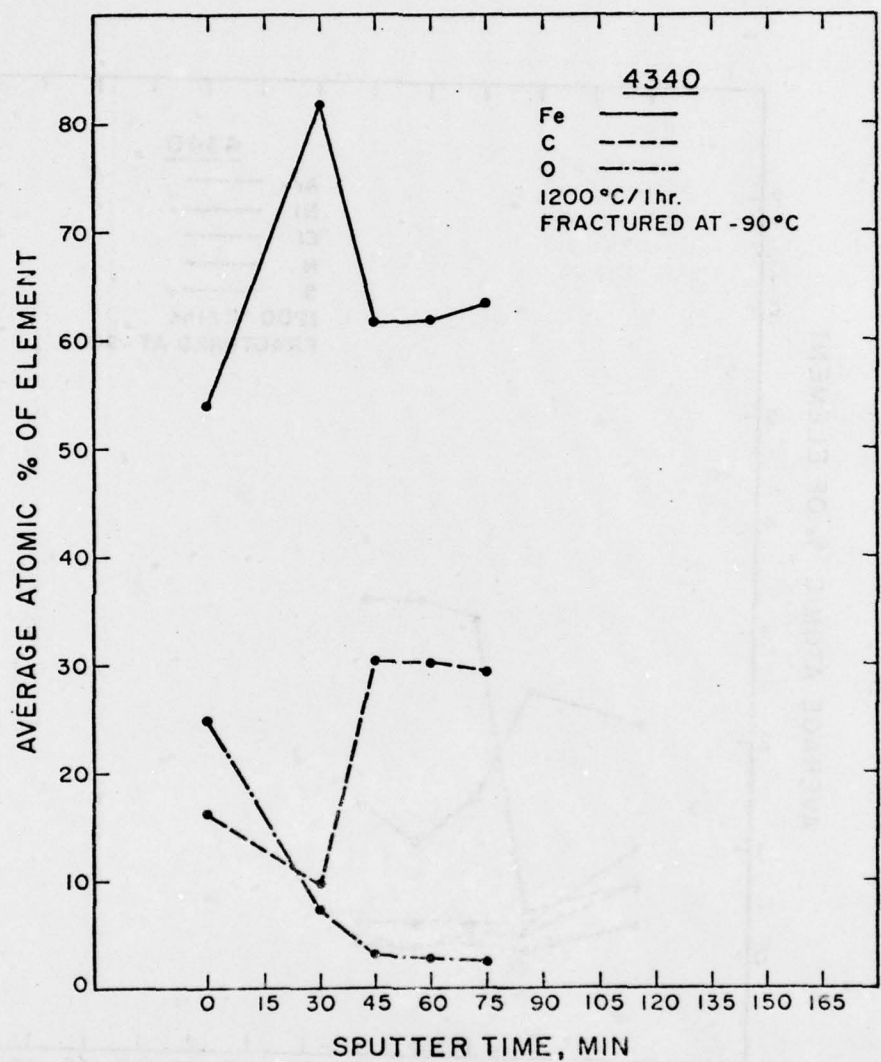


Figure 66 a

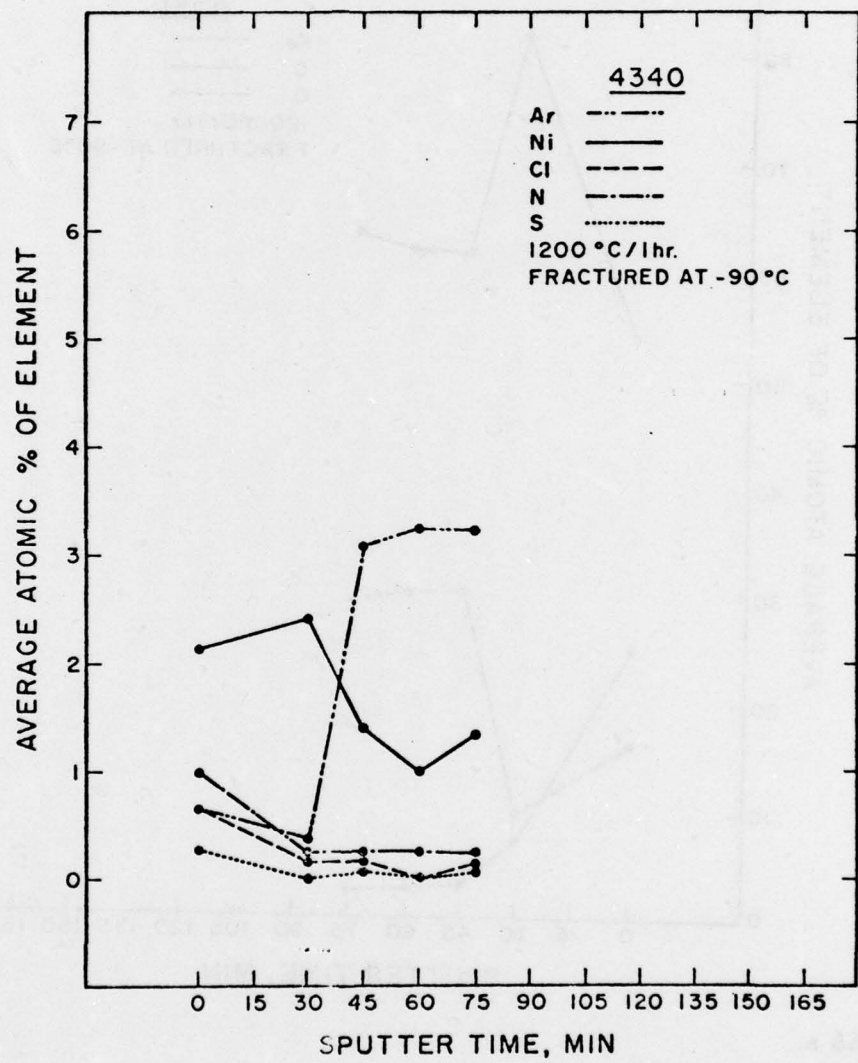


Figure 66 b

134

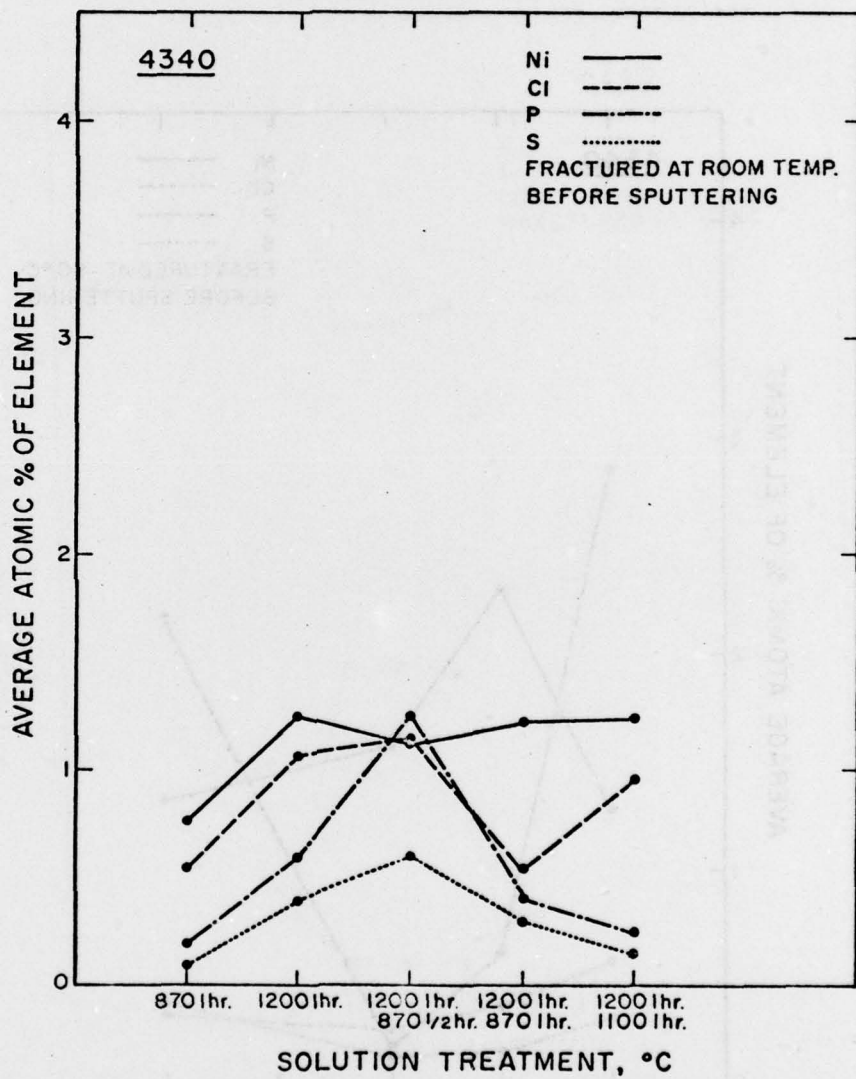


Figure 67

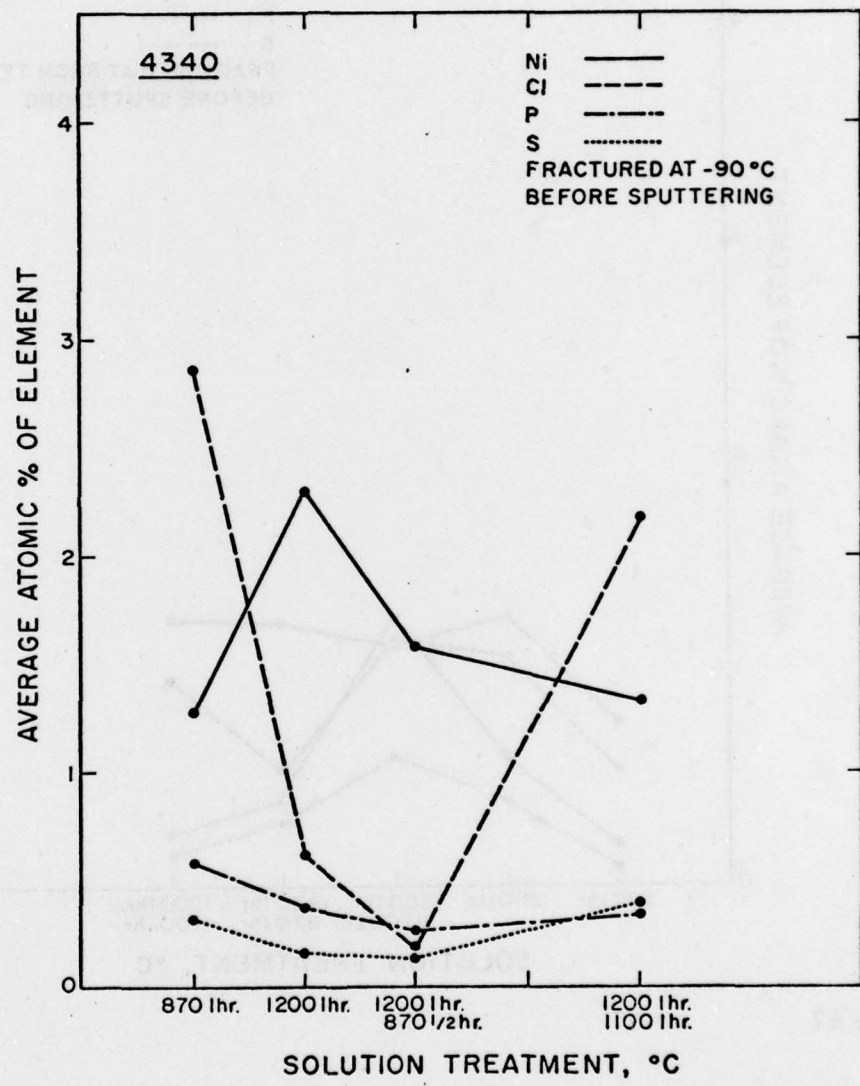


Figure 68

136

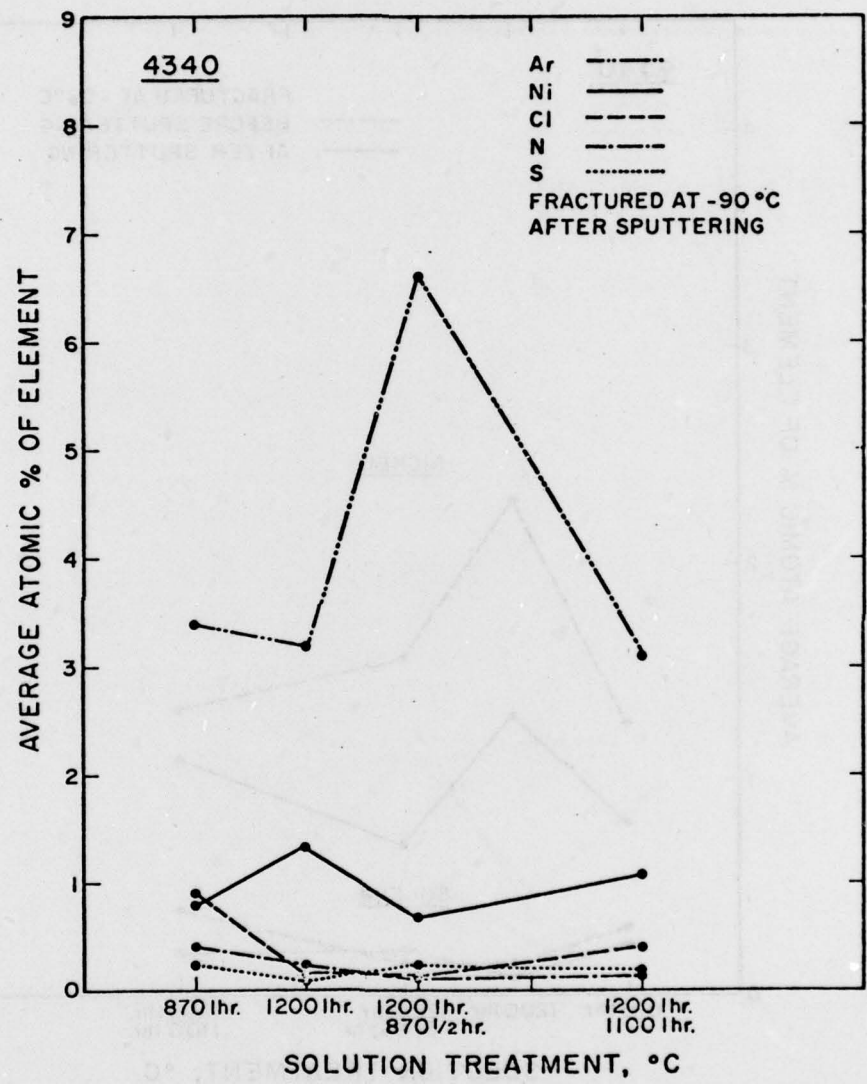


Figure 69

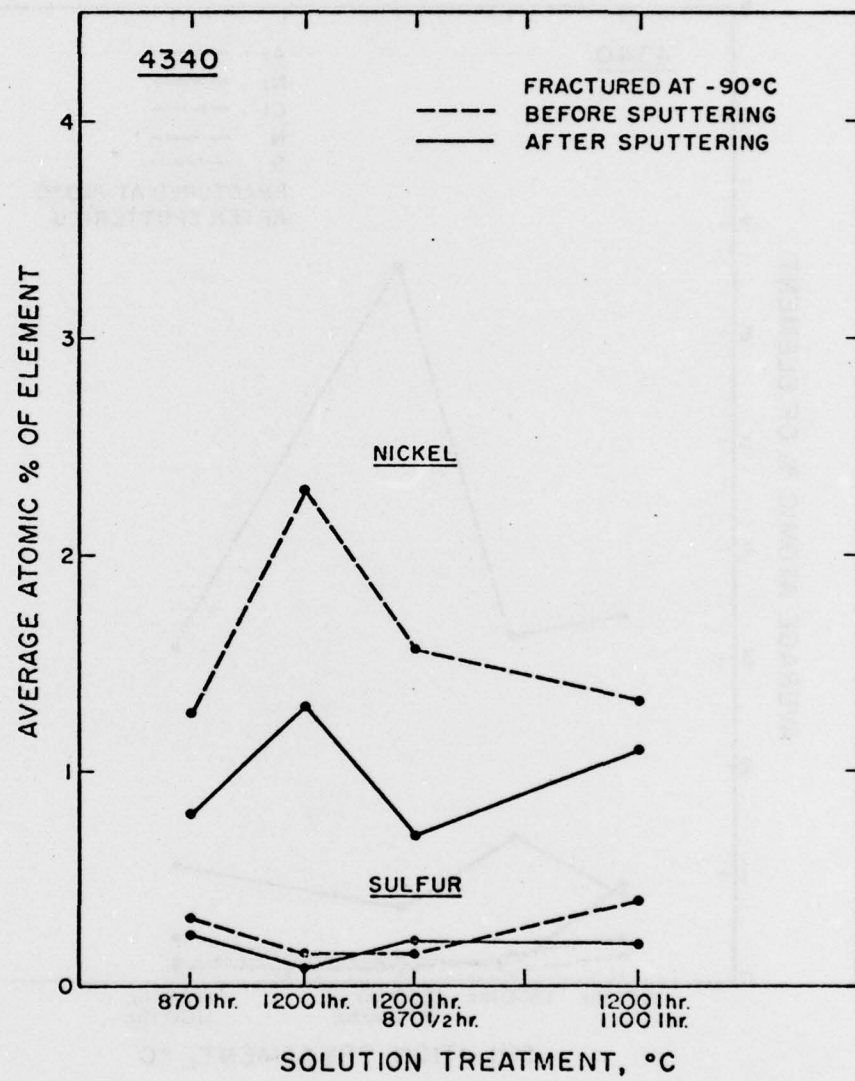


Figure 70

138

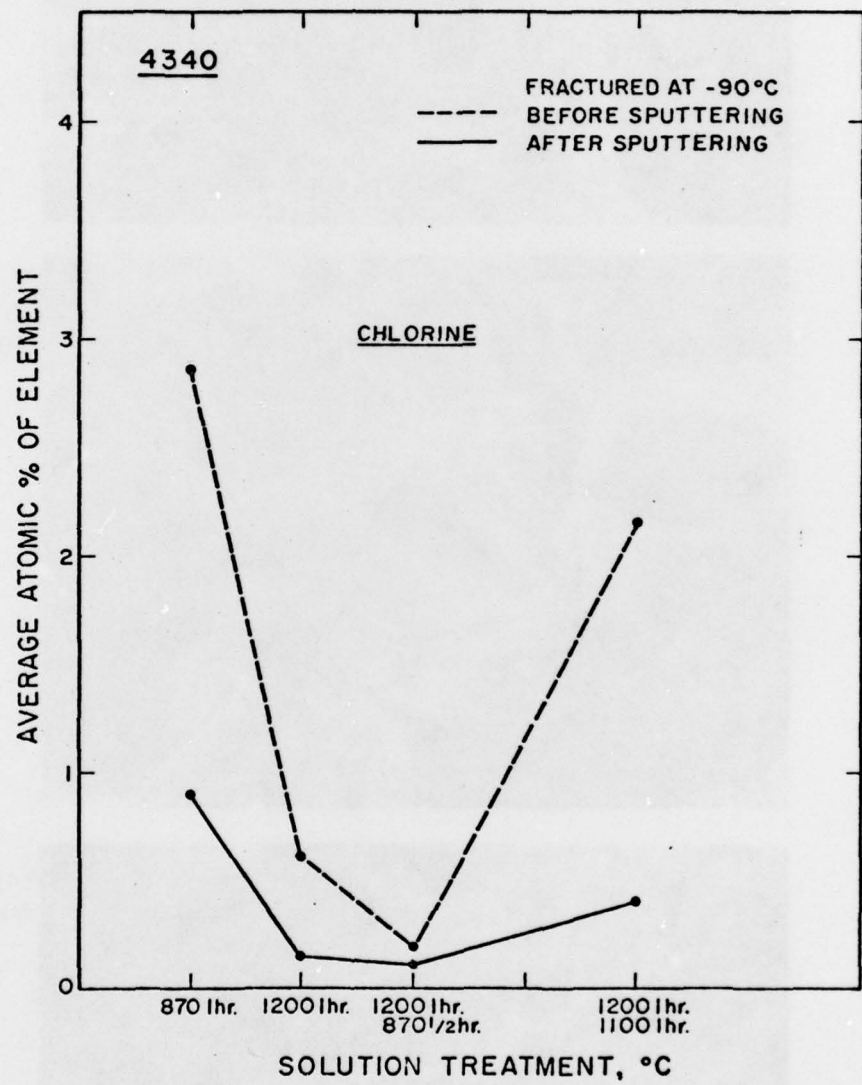
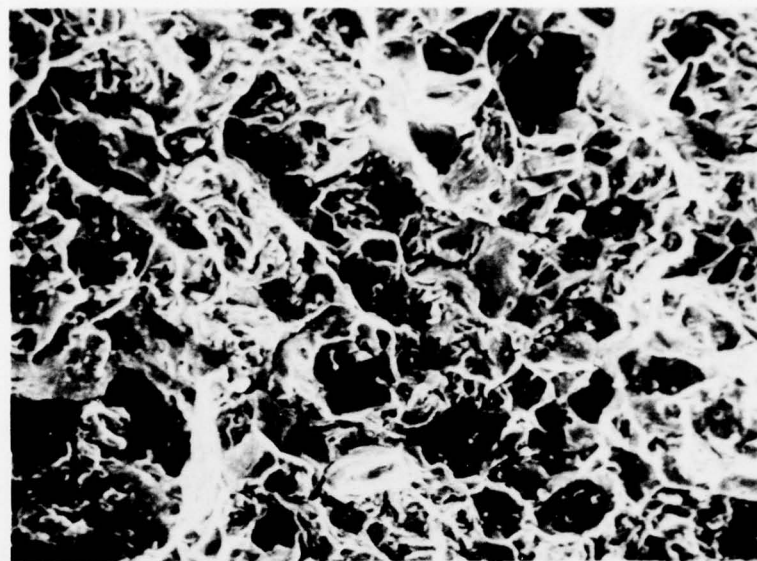


Figure 71



(a)
1000X



(b)
5000X



(c)
500X

Figure 72

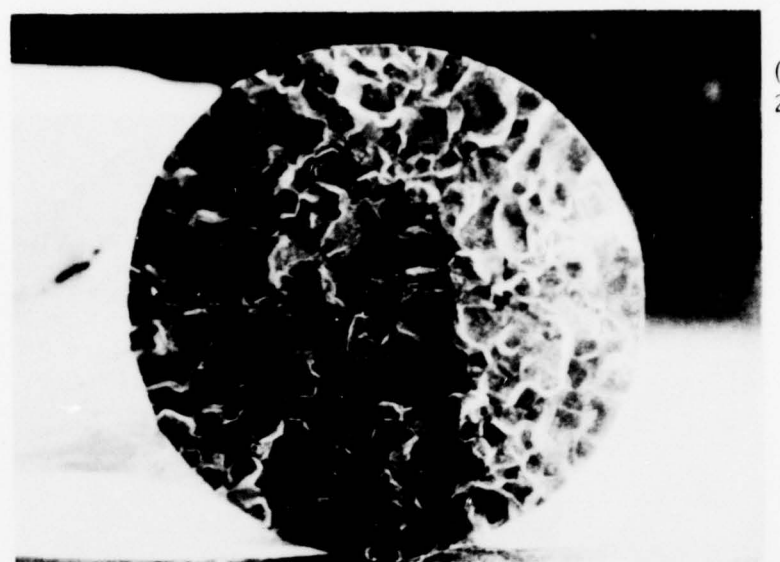
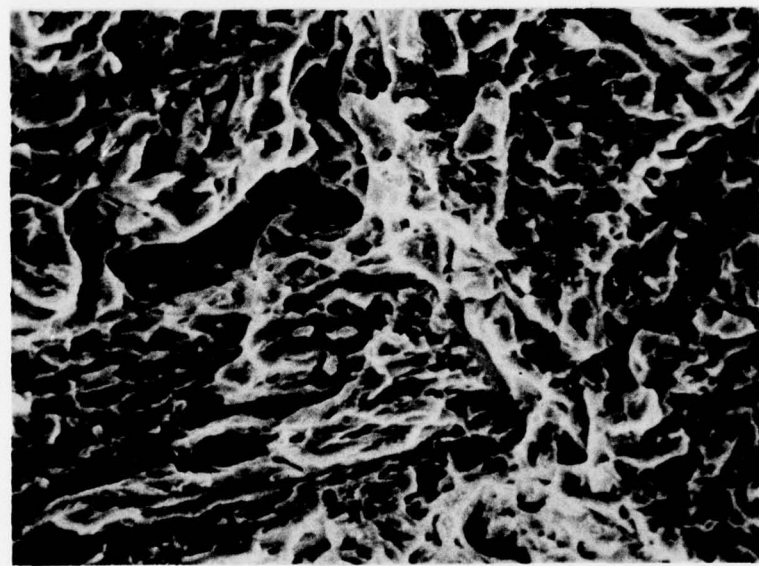


Figure 73



(d)

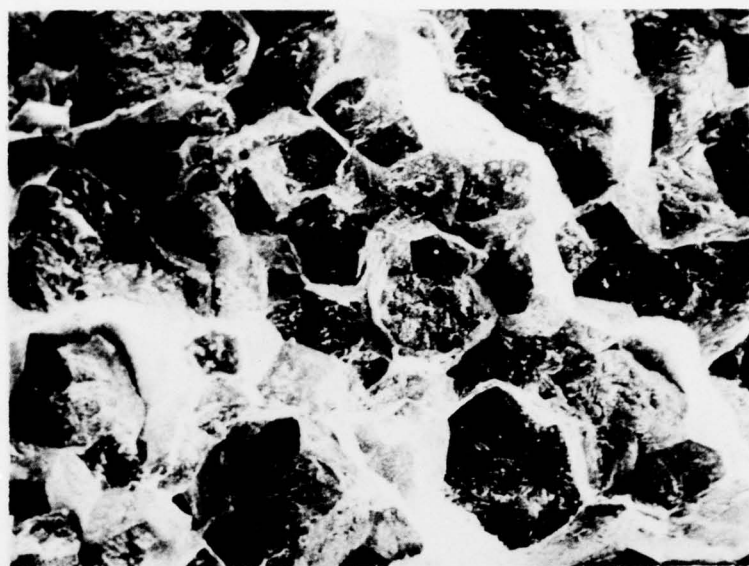
100X



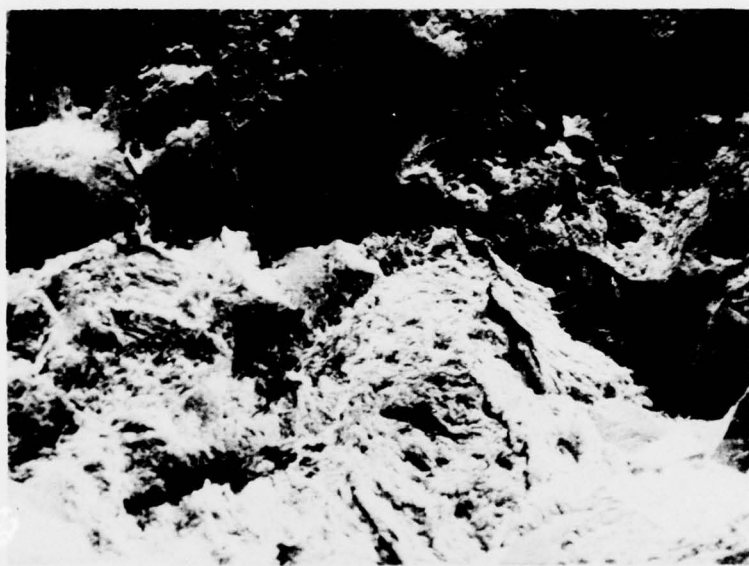
(e)

2000X

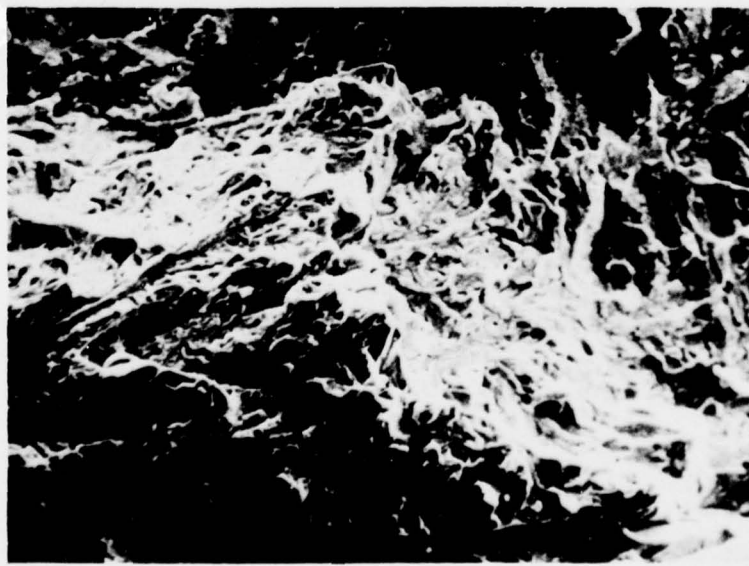
Figure 73 (cont'd)



(a)
100X

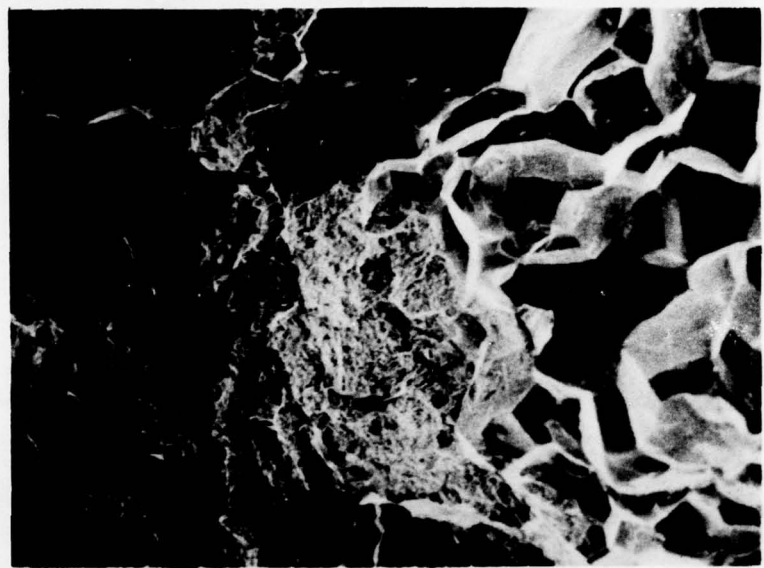


(b)
100X



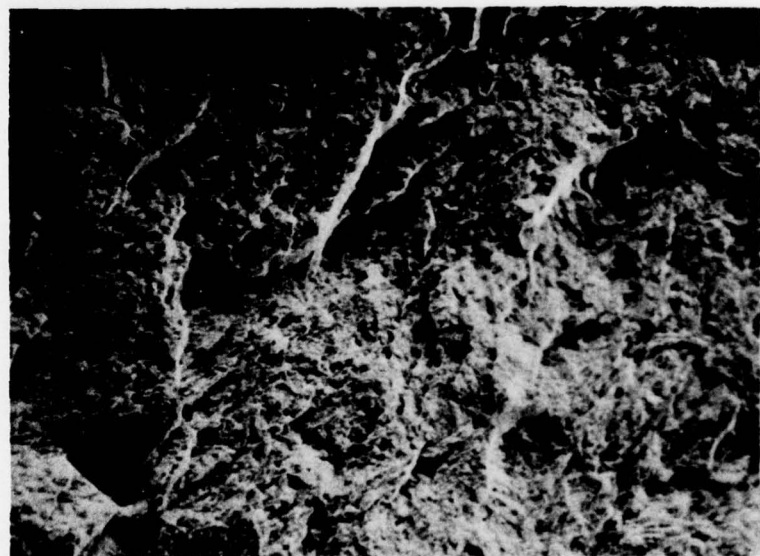
(c)
500X

Figure 74



(a)

100X



(b)

100X

Figure 75

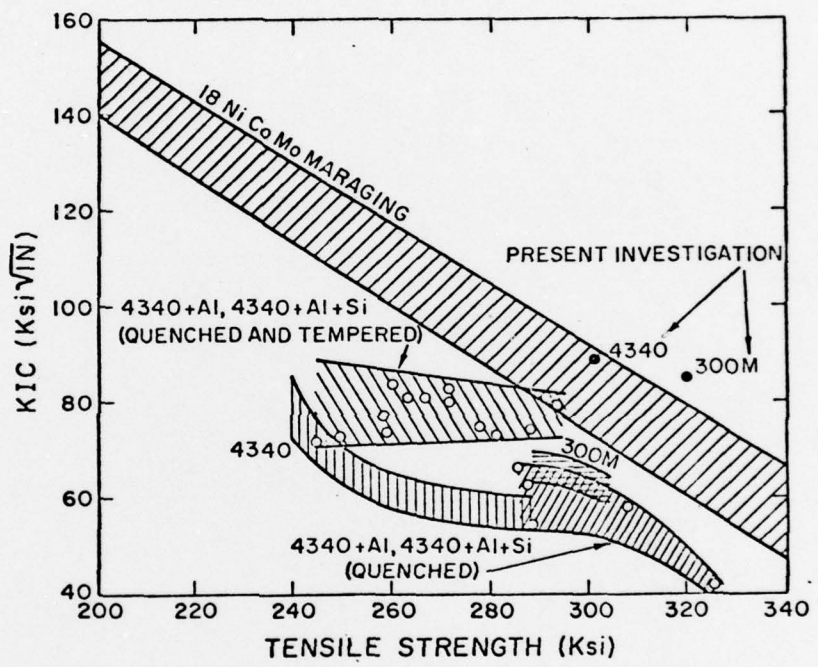


Figure 76

ED
78